GENETIC REGULATION OF GERM CELL APOPTOSIS IN *CAENORHABDITIS ELEGANS*

DISSERTATION
ZUR

ERLANGUNG DER NATURWISSENSCHAFTLICHEN DOKTORWÜRDE

(DR. SC. NAT.)

VORGELEGT DER

MATHEMATISCH-NATURWISSENSCHAFTLICHEN FAKULTÄT

DER

UNIVERSITÄT ZÜRICH

VON

GUILLAUME LETTRE

AUS

QUÉBEC, CANADA

PROMOTIONSKOMITEE

PROF. MICHAEL O. HENGARTNER (VORSITZ, LEITER DER DISSERTATION)

PROF. KONRAD BASLER

PROF. ALEX HAJNAL

PROF. SCOTT W. LOWE

ZÜRICH 2005

GENETIC REGULATION OF GERM CELL APOPTOSIS IN *CAENORHABDITIS ELEGANS*

SUBMITTED IN ACORDANCE WITH REQUIREMENTS OF
THE UNIVERSITY OF ZURICH
FOR THE DEGREE OF
DOCTOR OF PHILOSOPHY

GUILLAUME LETTRE

University of Zurich

POUR MES PARENTS DENISE ET MICHEL,
POUR MON FRÈRE HUGO ET MA SŒUR JOSIANE,
ΚΑΙ ΣΤΗ ΚΑΤΕΡΙΝΑ ΜΟΥ

‘THEY CALLED ME MAD. I CALLED THEM MAD.
AND DAMN THEM THEY OUTVOTED ME!’

-ANONYMOUS-

• ACKNOWLEDGEMENTS •

It has been a long way from Sherbrooke (Québec, Canada), where I started my career in biology, to Zurich (Switzerland), where I will obtain my doctoral degree. The road has been difficult, even painful at moment, but so rewarding at the end. It is impossible to acknowledge everybody responsible for making this trip a reality, so first I thank the people I will forget. I also would like to thank the Fonds Québécois de la Recherche sur la Nature et les Technologies for financial support.

At the Université de Sherbrooke, I want to thank my mentor Benoit Chabot and my supervisor Marco Blanchette, who introduced me to the world of molecular biology. In Cold Spring Harbor Laboratory, I am indebted to Bill Tansey, Adrian Krainer, and Winshep Herr, for teaching me how to give a presentation and how to write a scientific article. I want to acknowledge the importance of Rob Martienssen, who taught me the true beauty of genetics. During that one year in CSHL, I was privileged to be in the same class than amazingly gifted biologists: Ira Hall, Patrick Paddison, and Zach Lippman. I am grateful to Zach for his patience, enthusiasm, and scientific criticism.

The Hengartner laboratory has been my home for the past three years. I want to thank past and current members of the lab for inputs and discussions. I am especially thankful to Randy Hofmann, Ekat Kritikou, Steffi Züllig, Kelvin Wong, Clémentine Perrier, and Lukas Neukomm, who have all become dear friends. I am also grateful to members of the Basler lab, for their friendship. A special bravo goes to Michi Röthlisberger, who wrote the german version of this thesis' summary. In Zurich, I also would like to thank my climbing buddies: George, Colin, Raymond, Ekat, and Attila, who made Monday night the best night of the week… and Tuesday morning the worst morning.

I want to thank my thesis committee, Konrad Basler, Alex Hajnal, and Scott Lowe, for healthy criticism and advices throughout this project. And finally, I thank my advisor Michael O. Hengartner who taught me genetics and supported me during the last three years; from him, I learned what kind of scientist I want to become.

• ZUSAMMENFASSUNG •

Als Apoptose, oder programmierten Zelltod, bezeichnet man einen physiologischen Mechanismus, der gebraucht wird, um schädliche oder beschädigte Zellen in kontrollierter Art und Weise zu entfernen. Dies ist ein aktiver Prozess der genetisch gesteuerten Selbstzerstörung, welcher eine biologisch bedeutende homöostatische Funktion übernimmt. Durch extensive Forschung in den letzten 15 Jahren wurden die wichtigsten Komponenten apoptotischer Signalkaskaden identifiziert. Es wurde ebenfalls aufgezeigt, dass das Phänomen der Apoptose in Metazoen evolutiv hoch konserviert ist. Dennoch blieben faszinierende Fragen bezüglich des programmierten Zelltodes bislang unbeantwortet: Warum erzeugt ein Organismus Zellen, die schlussendlich Selbstmord begehen? Welches sind die Auslöser, welche eine Zelle in dieses Schicksal treiben? In dieser Dissertation präsentiere ich meine Arbeit der letzten drei Jahre über das Studium der Entscheidung über Leben und Tod von Zellen in der Keimbahn des Nematoden *Caenorhabditis elegans*.

Um neue Gene zu identifizieren, welche an der Regulation von Apoptose in der Keimbahn beteiligt sind, klonierte ich Mutationen, welche ein erhöhtes Mass an Keimbahn Apoptose bewirken (Kapitel 2). Des weiteren führte ich einen reverse genomic screen aus (Kapitel 3). Mit dem Ansatz der so genannten genomweiten RNA-Interferenz (RNAi) wurden mehr als 20 Gene identifiziert, welche Keimzellen vor Apoptose zu schützen vermögen. Darüber hinaus wurden diese Gene mittels Epistasie-Experimenten in p53-abhängige, oder -unabhängige Signalwege eingeordnet Da apoptotische Signalkaskaden evolutiv hoch konserviert sind, besteht die Möglichkeit, dass das Studium dieser neuen apoptotischen Gene in *C. elegans* Hinweise darüber liefert, wie auch in Säugetieren Genomische Stabilität, p53-Aktivierung und Fertilität kontrolliert wird.

Das p38 MAPK Gen *pmk-3* wurde im Screen identifiziert (Kapitel 4). PMK-3 fördert das Ueberleben von Keimzellen, und dessen Inaktivierung löst p53 unabhängige Apoptose aus. *pmk3* wird in der Keimbahn exprimiert und dessen Aktivität ist notwendig

um das Ueberleben von Zellen in diesem Gewebe zu sichern. Ich liefere den genetischen Nachweis, dass die MAPKKK MTK-1 und die MAPKK MKK-4 als Kinasen oberhalb von PMK-3 in der selben Signalkaskade agieren, und dass der Transkriptionsfaktor MEF-2 die überlebensfördernde Rolle von PMK-3 in der Keimbahn von *C. elegans* vermittelt.

Schliesslich führte ich einen genetischen 'modifier screen' aus, um Gene zu finden, welche in der Keimbahn Apoptose auslösen. Aufgrund des experimentellen Aufbaus des screens fand ich neue Allele von zuvor bekannten Genen, welche für die Apoptose essentiell (*ced-3*) und für das Entfernen von apoptotischen Zellen (*ced-2* und *ced-6*) verantwortlich sind. Dieser Ansatz führte auch zur Identifizierung von zwei neuen Chromosomalen Loci, *op385* und *op387*, welche die physiologische Apoptose, jedoch nicht DNA-damage induzierten Zelltod supprimieren. *op385* und *op387* konnten kleinen Abschnitten auf den Chromosomen V, resp. X zugeordnet werden. Obschon die molekulare Natur dieser Gene zur Zeit unbekannt ist, könnte deren Identifkation die der Apoptose in der Keimbahn zugrunde liegenden Geheimnisse lüften.

• SUMMARY •

Apoptosis can be defined as a physiological mechanism that removes unneeded, harmful, or damaged cells in a regulated manner. It is an active process of gene-directed cellular self-destruction that usually serves a biologically meaningful, homeostatic function. Extensive research, over the last fifteen years, has identified the key components of apoptotic cascades, and showed that apoptosis is conserved in metazoans. However, there are still fascinating questions concerning apoptosis that remain largely unanswered: Why are some cells born to eventually commit suicide? And what are the cues that determine this cell fate? In this dissertation, I present the work I carried out in the last three years to study the life-versus-death decision of cells in the germ line of the nematode *C. elegans*.

To identify new genes that regulate germ cell apoptosis, I cloned mutations that cause increased levels of germline apoptosis (Chapter 2), and performed a reverse genomic screen (Chapter 3). By using a genome-wide RNAi approach, more than 20 genes were identified that protect germ cell from undergoing apoptosis. Furthermore, epistasis analysis placed these genes in p53-dependent or -independent pathways. Because apoptotic pathways are conserved, it is possible that the study of these new apoptotic genes in *C. elegans* will shed light on the mechanisms that control genomic stability, p53 activation, and fertility in mammals.

The p38 MAPK gene *pmk-3* was identified in the RNAi screen (Chapter 4). PMK-3 promotes germ cell survival, and its inactivation causes p53-independent germ cell apoptosis. *pmk-3* is expressed in the germ line, and its activity is required in this tissue to promote cell survival. I provide genetic evidences that the MAPKKK MTK-1 and the MAPKK MKK-4 are the kinases upstream of PMK-3, and that the transcription factor MEF-2 mediates PMK-3's pro-survival role in the *C. elegans* germ line.

Finally, I performed a genetic modifier screen to discover genes that trigger germ cell apoptosis (Chapter 5). Because of the experimental setup, I recovered alleles of already

known genes essential for apoptosis (*ced-3*) and corpse removal (*ced-2* and *ced-6*). This approach also led to the identification of two new loci, *op385* and *op387*, that suppress physiological germ cell death but not DNA damage-induced apoptosis. *op385* and *op387* have been mapped to small intervals on chromosome V and X, respectively. Although the molecular natures of these genes are currently unknown, their identification could unravel the mysteries underlying *C. elegans* germline apoptosis.

• TABLE OF CONTENTS •

• FIGURES •

• TABLES •

• CHAPTER 1 •

APOPTOSIS IN *C. ELEGANS*

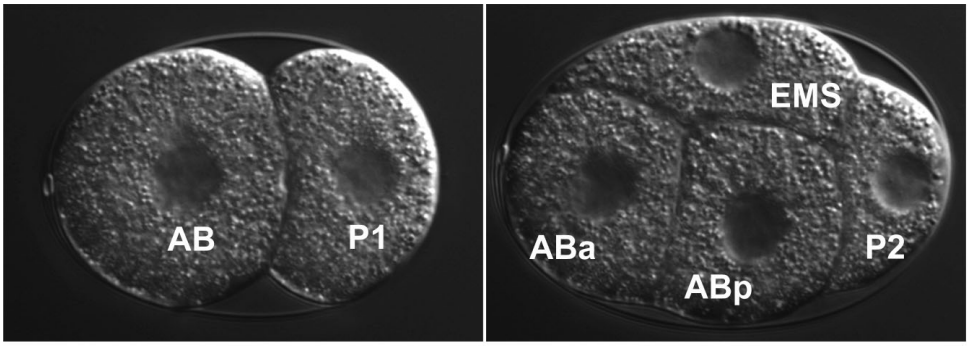

C. elegans embryos - The P lineage gives rise to the germ line

• CHAPTER 1 •

APOPTOSIS IN *C. ELEGANS*

1.1 INTRODUCTION

Apoptosis, or programmed cell death, is a complex process of gene-directed cellular self-destruction that usually serves a biologically meaningful, homeostatic function. Because of its complexity, it is not surprising that biologists have turned towards simpler, genetically tractable systems to understand the regulation and mechanistic of apoptosis. Determination of the complete cell lineage of *C. elegans* hermaphrodites by John Sulston set the basis for the study of apoptosis in the worm (Figure 1.1a) (Sulston and Horvitz, 1977; Sulston et al., 1983). It was then possible to perform genetic screens in order to identify genes involved in the regulation, execution, and termination of apoptosis (Figure 1.2). By cloning and characterizing several of these genes, the laboratory of H. Robert Horvitz played a major role in establishing *C. elegans* development as an excellent paradigm to dissect the genetics of apoptotic cell death. More importantly, the genes cloned in the Horvitz laboratory were shown to have functional mammalian homologues. These results were the first evidences that apoptosis is conserved across distantly related species, and suggested that its study in worms might shed light on how and why it occurs in higher metazoans, including humans.

In this review, we summarize our current knowledge of the regulation, execution, and termination of apoptosis in *C. elegans*. Special emphasis will be placed on new findings, which have not been discussed elsewhere. We will also try to draw a general picture of apoptosis, by highlighting similarities and differences between apoptotic death in *C. elegans* and mammals.

1.2 APOPTOSIS DURING *C. ELEGANS* EARLY DEVELOPMENT

1.2.1 The worm core apoptotic machinery

Genetic screens for mutant worms with abnormal cell death identified mutations in four genes essential for all somatic cell deaths: *ced-3*, *ced-4*, *ced-9*, and *egl-1* (*ced*, *ce*ll *d*eath abnormal; *egl*, *eg*g *l*aying-defective). Further genetic characterization revealed that *ced-3*, *ced-4*, and *egl-1* are pro-apoptotic because loss-of-function (lf) mutations in any of

these genes block most if not all apoptotic deaths in the soma (Conradt and Horvitz, 1998; Desai et al., 1988; Ellis and Horvitz, 1986). The first mutation identified in *ced-9* was a gain-of-function (gf) mutation that blocks apoptosis; the *ced-9(lf)* phenotype confirmed that this gene has anti-apoptotic activity because its inactivation results in ectopic cell deaths (Hengartner et al., 1992). Epistasis studies ordered these genes in a 'linear' genetic pathway, with *egl-1* upstream of *ced-9*, and *ced-9* upstream of *ced-4* and *ced-3* (Figures 1.2 and 1.3).

ced-3 and *ced-4* encode a caspase and an adaptor protein similar to Apaf-1, respectively (Xue and Horvitz, 1995; Xue et al., 1996; Yuan and Horvitz, 1992; Yuan et al., 1993). Similar to their mammalian homologues, CED-3 and CED-4 interact to form an apoptosome-like complex, and they are essential to all apoptotic cell deaths in the worm. The mammalian apoptosome is formed of caspase-9, Apaf-1, and the electron carrier cytochrome *c*. So far, no role has been assigned to the worm cytochrome *c* in apoptosis. In mammalian cells, mitochondrial release of cytochrome *c* allows quick response to apoptotic stimuli (e.g. genotoxic stresses). The simplicity of the worm might not require this further level of complexity, and it is apparent that regulation of transcriptional networks is sufficient to control all developmental programmed cell deaths in the *C. elegans* soma (see below).

The Bcl-2 family member CED-9 promotes survival of all cells in *C. elegans*: null mutations in *ced-9* are lethal, and this lethality can be suppressed by mutations in either *ced-3* or *ced-4* (Hengartner and Horvitz, 1994a; Hengartner and Horvitz, 1994b). In somatic cells fated to die, *ced-9* is inactivated by *egl-1*, a gene encoding a BH3-only domain protein (Conradt and Horvitz, 1998). *egl-1* was placed upstream of *ced-9* in the death pathway since a *egl-1(lf)* mutation does not suppress the lethal phenotype of *ced-9* null mutants.

A model, based on the interpretation of genetic, biochemical, and structural data, has been proposed to explain how apoptosis occurs in *C. elegans* (Yan et al., 2004). In most somatic cells, CED-9 sequesters CED-4 (and possibly CED-3) on the surface of mitochondria. However, in the 131 cells that normally undergo apoptosis, developmental cues transcriptionaly activate *egl-1*; EGL-1 binds to CED-9, thus disrupting the interaction between CED-9 and CED-4 (del Peso et al., 1998). This releases the CED-

4/CED-3 death complex, leading to the activation of the caspase CED-3 and the initiation of apoptosis (Chen et al., 2000).

1.2.2 Transcriptional regulation of egl-1 expression

In the *C. elegans* soma, a cell's decision to live or die is determined by whether *egl-1* is expressed or not (Figure 1.3). Interestingly, we know really few regulators of *egl-1* transcription, and those known can only explain a small subset of the cell deaths observed during normal development. The two sister cells of the serotonergic NSM neurons undergo apoptosis in wild-type worms; these deaths depend on the worm core apoptotic machinery (*egl-1*, *ced-9*, *ced-4*, *ced-3*), but also two other genes: *ces-1* and *ces-2* (*ces*, *ce*ll death *s*pecification abnormal). Mutations that cause a gain of *ces-1* function, or a loss of *ces-2* function, promote survival of the NSM sister cells, without affecting most other cell deaths (Ellis and Horvitz, 1991). *ces-1* and *ces-2* encode a member of the Snail family of zinc-finger transcription factor and a basic region leucine-zipper (bZIP) transcription factor, respectively (Metzstein et al., 1996; Metzstein and Horvitz, 1999). Epistasis analysis showed that *ces-2* acts upstream of *ces-1*: in *ces-1(lf) ces-2(lf)* double mutants, the NSM sister cells die, suggesting that *ces-2* causes NSM sister cells death by inhibiting the cell death protective effect of *ces-1*.

Recently, elegant genetic and biochemical experiments from Conradt and co-workers established the molecular link between the *ces* genes and *egl-1* transcription (Thellmann et al., 2003). The authors identified two new basic helix-loop-helix (bHLH) transcription factor genes, *hlh*-2 and *hlh*-3, which are expressed in the NSM sister cells and required for their death. In the NSM sister cells of wild-type animals, HLH-2/HLH-3 heterodimers activate *egl-1* transcription by binding a regulatory sequence, called region B, in the *egl-1* promoter. Interestingly, the same study showed that CES-1 can also bind region B, suggesting a competition model between HLH-2/HLH-3 and CES-1 for region B of the *egl-1* locus. According to this scenario, increased *ces-1* activity, such as in *ces-1(gf)* or *ces-2(lf)* mutants, prevents the death of the NSM sister cells because CES-1 can successfully compete with HLH-2/HLH-3 for region B, and therefore block *egl-1* transcription (Figure 1.3)

The fate of the hermaphrodite-specific neurons (HSNs) is also a good model to study cell-specific apoptotic death in *C. elegans*. These neurons are required for egg-laying in the hermaphrodite; they are useless in males and therefore normally undergo apoptosis. The original dominant gain-of-function mutation in *egl-1* was identified because it specifically induces the death of the HSNs in hermaphrodites, thus giving the egg-laying defect (Egl) phenotype. The mutation was found to affect a binding site in the *egl-1* locus for the transcriptional repressor TRA-1A, hence causing ectopic *egl-1* expression and HSN death (Conradt and Horvitz, 1999). To identify positive regulators of *egl-1* expression in the HSN, Hoeppner and colleagues screened for suppressors of the Egl phenotype of *egl-1(gf)* mutant worms (Hoeppner et al., 2004). They found mutations in two genes, *eor-1* and *eor-2* (*eor*, *egl-1* suppressor/*D*iO uptake defective/*r*af enhancer), that only block apoptosis in the HSNs: EOR-1 is a putative transcription factor, and EOR-2 is a new, but evolutionarily conserved, protein. Further characterization of the *eor* revealed that these genes are likely implicated in neuronal cell fate determination in the *C. elegans* nervous system in general, and specifically in the apoptotic cell fate of the male HSNs. However, it remains unclear how *eor-1*/*eor-2* function to promote apoptosis in the male HSNs (Figure 1.3)

How many different transcriptional cascades, such as the ones described above, are required to explain all the 131 somatic cell deaths that occur during *C. elegans* hermaphrodite development? We still ignore the answer to this question, but it seems reasonable to think that cells emerging from different lineages will induce *egl-1* expression using different transcription factors. This possibility highlights the complexity to study the regulation of developmental apoptosis, even in simple system like the worm *C. elegans*.

1.2.3 Inhibition of apoptosis: a new player

Contrary to the situation in flies and mammals, no inhibitor of apoptosis protein (IAP) has been identified so far in *C. elegans*. The *C. elegans* genome contains two genes, *bir-1* and *bir-2*, that encode proteins with BIR domains (BIR domains are often found in IAPs; they are thought to fit into the catalytic site of caspases and inactivate their protease activity). However, inactivation of *bir-1* by RNA interference (RNAi) revealed that this

gene, like its mammalian homologue survivin, is involved in cytokinesis, but does not play any role in suppressing apoptosis in *C. elegans* (Fraser et al., 1999, Speliotes et al., 2000). There is no known function for *bir-2*.

icd-1(*i*nhibitor of *c*ell *d*eath-1) was recently found in a screen for genes implicated in *C. elegans* early embryogenesis (Bloss et al., 2003). The authors discovered that reducing ICD-1 activity by RNAi results in one of two possible phenotypes: either early arrest during embryogenesis, or increased programmed cell death in embryos that developed past the first embryonic stages. Further characterization of *icd-1(RNAi)* animals demonstrated that various cell types, but especially neurons, undergo ectopic apoptosis, and that, importantly, *icd-1* over-expression can block apoptosis. The most unexpected finding of the new study came when Bloss et al. performed epistasis analysis to determine whether the worm core apoptotic machinery is required for *icd-1(RNAi)*-induced programmed cell death. They found that in older embryos and in larvae, loss of *ced-4* function, but not loss of *ced-3* function, could suppress the increased number of dying cells in *icd-1(RNAi)* animals. This result suggests that ICD-1 suppresses a CED-4-dependent, CED-3-independent apoptotic program, thus conferring a pro-apoptotic function for CED-4 above its ability to activate CED-3. ICD-1 is similar to the β subunit of the nascent-polypeptide associated complex (NAC), which might regulates protein localization during translation (Rospert et al., 2002). Like βNAC, ICD-1 localizes to the mitochondria.

What triggers apoptosis in *ced-3(lf); icd-1(RNAi)* mutants? Unfortunately, the authors did not perform any experiment to answer this important question. Also, the possibility that ICD-1, like the human βNAC, is involved in some aspects of mitchondrial functions raises some concerns regarding the specificity of the *icd-1(RNAi)* phenotype. After all, CED-9 normally localizes to the mitochondrial membrane, and it is possible that the absence of ICD-1 at the mitochondrion interferes with CED-9's survival function. Clearly, more experiments are needed to better understand the anti-apoptotic activity of ICD-1.

1.2.4 pvl-5 protects hypodermal cells from apoptosis

In wild-type hermaphrodites at the larval stage L2, there are 11 P*n.p* hypodermal cells in the ventral midline arrayed along the anterior-posterior axis. Joshi and Eisenmann found that recessive mutations in the gene *pvl-5* (*pvl*, *p*rotruding *v*u*l*va) causes some of these hypodermal cells to undergo apoptosis; these deaths required CED-3, but surprinsingly not CED-4 (Joshi and Eisenmann, 2004). One possible model to explain this phenotype could be that *pvl-5* normally suppresses transcription of *ced-3* in the P*n.p* cells, such that in the absence of *pvl-5*, CED-3 accumulates. Indeed, it is known that *ced-3* over-expression can bypass a requirement for *ced-4* function (Shaham and Horvitz, 1996). However, the epistasis with *ced-9(gf)* refutes this hypothesis: *pvl-5; ced-9(gf)* double mutants have ~11 P*n.p* hypodermal cells, thus placing *pvl-5* upstream of *ced-9*. Also intriguing is the fact that *egl-1(lf)* does not suppress the extra P*n.p* deaths in *pvl-5*; this result was unexpected because it is believed that the gain-of-function mutation in *ced-9* 'mimics' the *egl-1(lf)* mutation (del Peso et al., 1998). Molecular identification and characterization of *pvl-5* are obviously the next logical steps to understand how this gene regulates the core apoptotic machinery in the *C. elegans* P*n.p* hypodermal cells.

1.3 GERM CELL APOPTOSIS IN *C. ELEGANS* HERMAPHRODITE

1.3.1 Oocyte apoptosis in mammals

In the mammalian female ovaries, apoptosis occurs throughout fetal and postnatal life to claim up to 99.9% of the potential germ cells (Kim and Tilly, 2004). Although most germ cell deaths take place prior to birth, apoptosis continues to decimate the number of oocytes through a process called follicular atresia during juvenile and adult life. Once the supply of oocytes has been exhausted through apoptosis and ovulation, the ovaries senesce, leading to infertility and, in humans, to the menopause.

Molecular studies have found that pro- and anti-apoptotic members of the Bcl-2 family play major roles in regulating oocyte apoptosis in the mouse (Kim and Tilly, 2004). For instance, ovaries of mice knocked out for the pro-apoptotic gene *bax* have a marked accumulation of follicules (that is, oocytes enclosed in specialized somatic cells), whereas elimination of the anti-apoptotic genes *bcl-2* or *bcl-x* produces mice with fewer oocytes.

It remains unclear why so many oocytes undergo apoptosis in the mammalian female gonad. Three models have been proposed to explain this process (Tilly, 2001): germ cells die (1) due to a limited supply of growth/survival factors, (2) due to quality-control checkpoint pathways that eliminate 'unhealthy' cells, or (3) to provide nutrients for other developing oocytes, as it is seen with nurse cells apoptosis during *Drosophila* oogenesis (McCall, 2004). These models are certainly not exclusive, but hard to test in a complex organ such as the mammalian female gonad. In the next section of this review, we introduce the *C. elegans* hermaphrodite germ line as a powerful genetic model tissue to understand oocyte apoptosis, and other stimuli-induced apoptotic events.

1.3.2 Physiological germ cell death in C. elegans

C. elegans hermaphrodites have two U-shaped gonads connected at a common uterus (Figure 1.4). At the distal end of each gonad, a growth factor produced by the somatic distal tip cell (DTC) promotes the mitotic proliferation of a small population of stem cells. In the distal arm, germ cell nuclei are not completely enclosed by membrane, and thus form a large syncytium. Once germ cells escape the influence of the DTC, they enter meiosis (transition zone) and progress into the pachytene stage of meiosis I. Upon activation of the RAS/MAPK pathway, germ cells exit pachytene arrest (Figure 1.4a) (Hubbard and Greenstein, 2000). Then, they can choose one of two possible cell fates: either to cellularize and develop into mature oocytes, or to undergo apoptosis (Figure 1.1b).

Physiological germ cell death occurs only during oogenesis; no cell death is observed in male gonads or in hermaphrodite gonads that are making sperm. It increases with the age of the animals, claiming on average approximately 50% of the developing oocytes and, contrary to somatic apoptosis in worms, it is apparently stochastic (Figure 1.1b) (Gumienny et al., 1999). Like developmental cell death, physiological germline apoptosis requires CED-4 and CED-3, and is blocked by CED-9. However, it is not regulated via transcriptional activation of *egl-1* since loss of *egl-1* function does not abolish physiological germ cell death (Figure 1.3). We hypothesized that other genes, called *g*erm*l*ine *a*poptosis (*gla*) genes, form a novel regulatory pathway that controls physiological germ cell death, and we are currently trying to identify these *gla* genes

through genetic screens. The reason why so many apparently healthy germ cells succumb to apoptosis is as mysterious in *C. elegans* as it is in mammals. Our laboratory has proposed that germline apoptosis plays an homeostatic function, by eliminating excess germ cells that act as nurse cells to provide nutrients to maturing oocytes (Gumienny et al., 1999).

Few genes are known to specifically regulate physiological germ cell death. *cgh-1* (*C. elegans g*ermline *h*elicase-1) encodes a conserved DEAD-box type RNA helicase involved in gametogenesis in worms: *cgh-1(RNAi)* animals are sterile and have elevated level of germline apoptosis (Navarro et al., 2001). Because these germ cell deaths are not dependent on the DNA damage pathway (see below), it is tempting to speculate that CGH-1 might control physiological germ cell death through an as yet unknown mechanism. *daz-1* (*D*eleted in *Az*oospermia-1) is another candidate gene that might play a regulatory role in physiological germline apoptosis in *C. elegans*. It encodes a RNA binding protein similar to the mammalian *DAZ* proteins, which are, in mammals, implicated in the production of gametes in both sexes. Mutations in *daz-1* cause sterility in hermaphrodites due to defects during meiosis progression, and also lead to increased germ cell apoptosis compared to wild-type worms (Karashima et al., 2000). The phenotypes of *cgh-1(RNAi)* and *daz-1(lf)* mutants suggest that physiological germ cell death is intrinsically linked to proper oocyte development.

1.3.3 DNA damage-induced apoptosis in C. elegans

Germ cell apoptosis can be ectopically triggered by genotoxic treatment (e.g. γ-irradiation, X-rays, UV, alkylating agents) (Gartner et al., 2000). Interestingly, it was found that these DNA damage-induced apoptotic deaths required a battery of conserved checkpoint genes (e.g. *hus-1*, *rad-5*, *mrt-2*), the worm homologue of the tumor suppressor gene p53, *cep-1*, as well as the pro-apoptotic gene *egl-1* (Figure 1.3) (Ahmed et al., 2001; Ahmed and Hodgkin, 2000; Derry et al., 2001; Hofmann et al., 2002; Schumacher et al., 2001). The current model proposes that upon DNA damage in germ cells, checkpoint components of the pathway activate CEP-1, which in turn transcriptionally induces *egl-1*. If this model holds true, it suggests that the situation in *C. elegans* germ cells is very similar to the (over-simplified) scenario that occurs in mammalian cells after DNA

damage, where p53 promotes transcription of the pro-apoptotic BH3-only domain protein genes PUMA and Noxa (Nakano and Vousden, 2001; Oda et al., 2000). Among interesting questions that have yet to be addressed regarding the DNA damage-induced germ cell apoptosis pathway in *C. elegans*, we need to identify the direct activators of CEP-1, and to determine if CEP-1 directly binds any regulatory sequences in the *egl-1* locus.

In humans, it is recognized that mutations in genes that control apoptotic responses upon DNA damage are associated with cancer development (Hanahan and Weinberg, 2000). Interestingly, *C. elegans* has functional homologues of many of these genes, as was recently shown with the characterization of the worm counterparts of human BRCA1 (Boulton et al., 2004) and c-Abl (Deng et al., 2004). The worm, by its simplicity and powerful genetics, will be a valuable model organism to study pathways implicated in the maintenance of genome integrity, pathways often too complex and redundant to be genetically dissected in higher metazoans. Furthermore, genetic screens in *C. elegans* should lead to the identification of novel and conserved genes involved in genomic stability and apoptotic responses.

1.3.4 Innate immunity and germ cell death

Salmonella typhimurium kills *C. elegans* over the course of several days by a mechanism that involves the establishment of persistent infection in the worm intestine. Aballay and Ausubel found that mutations that block apoptosis render *C. elegans* hyper-susceptible to Salmonella infections: *ced-3* or *ced-4* mutants die twice as fast as wild-type animals when fed on *Salmonella*. The authors also found that *Salmonella* infections trigger germ cell apoptosis in a *egl-1*-, *ced-3*-, and *ced-4*-dependent manner (Aballay and Ausubel, 2001). Furthermore, identification of other mutants hyper-sensitive to infections revealed that a conserved p38 MAPK pathway is required for the worm immune response, and *Salmonella*-induced germ cell death (Aballay et al., 2003; Kim et al., 2002). In an effort to develop *C. elegans* as a system to study host-pathogen interactions, Aballay and co-workers performed a screen for *Salmonella* mutant strains unable to infect worms, and identified several *Salmonella* virulence factors required to elicit germ cell apoptosis in *C. elegans* (Tenor et al., 2004). It is currently unknown how these

virulence factors activate a p38 MAPK in worms, and how this kinase triggers the apoptotic cascade. Even more importantly, we still ignore how and why programmed cell death protects *C. elegans* against pathogen infections.

1.3.5 Genome-wide RNAi screen for germline apoptosis genes

In order to identify new regulators of germ cell apoptosis, we performed a genome-wide RNAi screen for genes that promote germ cell survival (Lettre et al., 2004). Using a RNAi feeding library that targets 86% of the predicted *C. elegans* protein-coding genes (Fraser et al., 2000; Kamath et al., 2003), we knocked down 16 757 genes and found several dozen candidates that protect germ cells from undergoing apoptosis. Further genetic epistasis studies revealed that most of the RNAi knockdowns identified in the screen required the checkpoint protein HUS-1 and the p53 homologue CEP-1 to trigger apoptosis. This suggests that RNAi inactivation of these genes indirectly induces apoptosis, through the activation of quality control checkpoint pathways. Among the genes that fall in the p53-dependent class, we found known genes involved in DNA repair and meiotic recombination (e.g. *rad-50*, *rad-51*), but also a score of novel genes. Characterization of these genes in *C. elegans* should provide several new hints concerning the different mechanisms that control genomic stability and p53 activation in mammals.

We also identified four genes which do not require *hus-1* or *cep-1* to induce apoptosis upon RNAi knockdown (Lettre et al., 2004). These genes – two putative RNA binding proteins, a p38 MAPK, and a RING finger protein – are under investigation in our laboratory as they are prominent candidate regulators of the physiological germ cell death pathway.

1.4 ENGULFMENT OF APOPTOTIC CELLS IN *C. ELEGANS*

1.4.1 Significance of apoptotic corpse clearance

In vivo, apoptotic cells are normally observed within other cells (Kerr et al., 1972; Wyllie et al., 1980). This process, where a motile professional eater (e.g. macrophage) or a static neighboring cell swallows a dying cell is termed phagocytosis or engulfment (Grimsley and Ravichandran, 2003; Savill and Fadok, 2000). Engulfment of apoptotic

cells prevents the release of cellular debris, which could result in inflammation and auto-immunity if spilled into the surrounding environment. In its simplest form, phagocytosis is a two-steps process: first, the engulfing cell recognizes the dying cell; second, cytoskeletal rearrangements within the engulfing cell allow it to surround and eventually swallow the apoptotic corpse. Genetic studies of *C. elegans* mutants impaired in the removal of apoptotic cells have been instrumental in improving our understanding of the mechanisms that underlie phagocytosis in mammals (Reddien and Horvitz, 2004). In the next section, new findings in the field of apoptotic cell engulfment in worms are discussed.

1.4.2 Genetics of engulfment in C. elegans

Seven genes (*ced-1*, *-2*, *-5*, *-6*, *-7*, *-10*, and *-12*) functioning in two parallel genetic pathways are known to control engulfment of apoptotic cells in *C. elegans* (Figures 1.2 and 1.5). These genes are important, but not essential for engulfment: in these mutants, engulfment is much less efficient than in wild-type animals, but still occurs to some extent. To date, there is no mutation (or mutant background) that completely blocks engulfment in worms. Double mutant analyses placed these genes into two partially redundant pathways (Figure 1.5), with *ced-1*, *-6*, and *-7* on one hand, and *ced-2*, *-5*, *-10*, and *-12* on the other hand: double mutants carrying mutations in the same group do not show a significant increase in the engulfment defect, but double mutants with one mutation in each group show a strong additive effect (Ellis et al., 1991; Gumienny et al., 2001; Wu et al., 2001; Zhou et al., 2001a). Also, mutations in *ced-2*, *-5*, *-10*, or *-12* are characterized by a second phenotype, which is mis-migration of the somatic DTC of the gonad. This is a further indication that these four genes belong to the same epistatic group.

1.4.3 The C. elegans CED-1, -6, and -7 engulfment pathway

ced-1 encodes a large (>1000 amino acids) transmembrane protein with an extracellular amino-terminal domain that contains several EGF-like repeats, a single transmembrane domain, and an intracellular carboxy-terminal adaptor motif (Zhou et al., 2001b). The mammalian orthologue of CED-1 has yet to be identified. One good

candidate is CD91/LRP: CD91 has a C-terminus end similar to CED-1, and it interacts with GULP, the mammalian homologue of the *C. elegans ced-6* gene product (Su et al., 2002). CED-6 is an adaptor protein with a PTB domain, a central leucine zipper domain that mediates homodimerization, and a proline-rich region that contains several putative SH3-binding sites (Liu and Hengartner, 1998). The functional mammalian homologue of CED-6 is GULP, as over-expression of GULP in *ced-6* mutant worms rescues the engulfment phenotype (Liu and Hengartner, 1999). CED-7 is an ABC transporter similar to the mammalian ABCA1 subfamily (Wu and Horvitz, 1998a). ABC transporters use ATP to translocate various molecules across cell membranes (e.g. lipids, ions, sugars, vitamins). ABCA1 is highly expressed in macrophages engaged in engulfment, and macrophages deficient for ABCA1 are defective in apoptotic cell clearance (Hamon et al., 2000; Luciani and Chimini, 1996). Contrary to all other engulfment genes, which are normally required only in the engulfing cell, *ced-7* function is needed in both the engulfing and the engulfed cell.

It is still unclear how cells orchestrate the activity of CED-1, -6, and -7 to promote engulfment of apoptotic cells. A CED-1::GFP fusion protein expressed in worms localizes to cell membranes and clusters around neighboring cell corpses, supporting the view that CED-1 might be a receptor important for phagocytosis (Zhou et al., 2001b). In *ced-7* mutants, but not in *ced-6* mutants, CED-1::GFP fails to cluster around apoptotic corpses, suggesting that the ABC transporter CED-7 cooperates with CED-1 in the recognition process of dying cells (Zhou et al., 2001b). Because over-expression of *ced-6* rescues the engulfment defect of *ced-1* and *ced-7* mutants, it was proposed that *ced-6* acts downstream of these two genes (Liu and Hengartner, 1998). This view is supported by biochemical studies that have shown that CED-1 and CED-6, as well as their mammalian homologues, physically interact (Su et al., 2002). What are the CED-1 ligands? How does CED-7 control CED-1 localization? What proteins act downstream of CED-6? These are all interesting, but largely unanswered, questions.

1.4.4 CED-2, -5, -10, and -12 control cytoskeletal rearrangements during engulfment

The second engulfment pathway in *C. elegans* is better understood. It culminates in the activation of a small Rac1-like GTPase (CED-10) and the subsequent cytoskeletal

reorganization required for phagocytosis and cell migration. CED-5 is a huge bridging protein (1781 amino acids) similar to mammalian DOCK180: CED-5 contains a Docker domain that specifically binds nucleotide-free Rac, and CED-5 physically interacts with CED-2 and CED-12 (Gumienny et al., 2001; Wu and Horvitz, 1998b). *ced-2* encodes an adaptor protein with a SH2-domain and two SH3-binding sites, and is similar to the mammalian protein CrkII (Reddien and Horvitz, 2000). CrkII can regulate cell shape and motility, and is also known to directly bind DOCK180 (Klemke et al., 1998). However, the mechanism by which CED-2/CrkII promotes engulfment, and the significance of the CED-2/CrkII-CED-5/DOCK180 interaction, remains to be determined. The last engulfment gene that was cloned in *C. elegans* is *ced-12*. CED-12, and its mammalian homologue ELMO, has a PH domain and interacts with CED-5/DOCK180 (Gumienny et al., 2001; Wu et al., 2001; Zhou et al., 2001a). CED-2-CED-5-CED-12 forms a ternary complex that activates a signaling cascade important for cell migration and phagocytosis of apoptotic cells (Gumienny et al., 2001).

CED-10 is similar to Rac1, a small GTPase that controls cell morphology by regulating the cytoskeleton (Reddien and Horvitz, 2000). Genetically, *ced-10* acts downstream of *ced-2*, *-5*, and *-12* because its over-expression rescues the engulfment phenotype of these different mutant strains. However, recent over-expression studies from our laboratory indicate that *ced-10* migth also act downstream of the *ced-1*, *-6*, and *-7* pathway (J.M. Kinchen and M.O. Hengartner, in press). GTPases are molecular switches that can be found in an inactive GDP-bound state and an active GTP-bound state; GTPase activating proteins (GAPs) promote inactivation of the enzymes, whereas GTP exchange factors (GEFs) activate them. In mammalian cells, biochemical experiments revealed that DOCK180 and ELMO function as a bipartite Rac-GEF, able to promote phagocytosis and cell migration through Rac1 activation (Brugnera et al., 2002; Grimsley et al., 2004). Assuming that the CED-5/CED-12 complex has similar activity in worms, one can propose a model where signals emanating from the dying cell activate the GEF activity of CED-5/CED-12 (maybe through CED-2?), leading to CED-10 activation and reorganization of the actin cytoskeleton (Figure 1.5).

1.4.5 Phosphatidylserine recognition in C. elegans

Phosphatidylserine (PS) is a phospholipid normally present in the inner leaflet of the plasma membrane bilayer. However, during apoptosis, PS accumulates on the outer leaflet of the cell's plasma membrane and is thought to be one of the primary 'eat-me' signals recognize by phagocytes. In mammals, the phosphatidylserine receptor (PSR) is expressed in most cells able to engulf apoptotic cells, and shows specific binding activity towards PS *in vitro* (Fadok et al., 2000). However, disruption of PSR in the mouse gave contradicting results: whereas one group reported an engulfment defect in *psr*$^{-/-}$ mice, with apoptotic cells accumulating in the lung, liver, and thymus (Li et al., 2003), another independent study did not observe any defect in apoptotic corpse removal in their PSR knockout mice (Bose et al., 2004). Both laboratories reported essential functions for PSR during embryogenesis. Even more complicated is the fact that PSR contains several nuclear localization signals sufficient to promote nuclear localization of a GFP fusion protein (Cui et al., 2004). It is currently undetermined how a nuclear protein could act as a 'eat-me' signal receptor in phagocytes.

C. elegans has one PSR homologue, *psr-1*. A mutation in the *psr-1* locus was reported to cause a subtle engulfment defect in worms, and epistasis analysis placed *psr-1* upstream of the *ced-2*, *-5*, *-10*, and *-12* pathway (Wang et al., 2003). In this study, over-expression of human PSR in *psr-1* mutant worms could partially suppress the engulfment defect, suggesting conservation of function. Therefore, it is possible that PSR-1 plays a minor role in the recognition of apoptotic cells in *C. elegans*, but it is clearly not the main receptor that recognizes apoptotic cells because the engulfment phenotype of *psr-1(lf)* worms is much weaker than the phenotype of any of the other worm engulfment genes. In contradiction with the published data, our laboratory has obtained two deletion alleles of *psr-1* (including the allele characterized by Wang et al.) and has not been able to observe an engulfment defect (S. Züllig and M.O. Hengartner, unpublished observations).

Annexin I is an intracellular protein that translocates from the cytosol to the outer leaflet of the plasma membrane during apoptosis, and has been proposed to be the bridging molecule between PS on the dying cell and PSR on the phagocyte (Arur et al., 2003). Annexin I colocalizes with PS, and is required for PSR clustering around apoptotic cells. RNAi knockdown of *nex-1*, the *C. elegans* orthologue of mammalian annexin I, has been reported to lead to a moderate, but significant, engulfment defect

(Arur et al., 2003). However, a *nex-1* mutant does not have an observable engulfment phenotype (L. Neukomm and M.O. Hengartner, unpublished observations). It is possible that RNAi against *nex-1* also cross-inactivate the three remaining genes in the *C. elegans* genome that encode annexin-like proteins, and that knockdown of these four genes is required to observe a defect in apoptotic corpse clearance. In any case, mutations in these *nex* genes are desired to definitely determine the role of annexins in the phagocytosis of apoptotic cells in *C. elegans*, and also to find out how they interact with the other *ced* engulfment genes.

1.4.6 Engulfment promotes apoptosis

Figure 1.2 presents programmed cell death in *C. elegans* as a linear process, where a cell first dies, after which point it is recognized by a neighboring cell and removed. However, elegant genetic studies have shown that the apoptotic pathway is not strictly linear, and that engulfment promotes apoptosis (Hoeppner et al., 2001; Reddien et al., 2001). Screening for mutations that enhanced the defect in programmed cell death of a weak *ced-3* mutation, Reddien and co-workers unexpectedly isolated mutations in engulfment genes (Reddien et al., 2001). Hoeppner et al. used four-dimensional microscopy to study the kinetics of death and engulfment, and showed that blocking engulfment enhances cell survival in animals with a weak *ced-3(lf)* mutation (Hoeppner et al., 2001). These two groups proposed that phagocytosis actively promotes apoptosis to make sure that once a cell has decided to commit suicide, there is no possible 'turning back'. Future work should aim at identifying the molecular mechanisms by which engulfment cooperates with the death machinery.

1.5 THE FINAL STEP: APOPTOTIC DNA FRAGMENTATION

Chromosomal DNA degradation into a ladder is one of the best described hallmarks of apoptotic cell death (Wyllie, 1980). In mammals, the nuclease CAD/DFF40 becomes activated and degrades genomic DNA when its inhibiting binding partner, ICAD/DFF45, gets cleaved by caspases (Nagata, 2000). In *C. elegans*, the Dnase II protein NUC-1 is the main nuclease responsible for degrading the DNA of cells undergoing apoptosis: a loss-of-function mutation in *nuc-1* results in accumulation of TUNEL-positive nuclei in

mutant embryos (Wu et al., 2000). Although not essential for apoptosis, DNA fragmentation is thought to occur in dying cells as a further way to kill it (destruction of the genetic code), to prevent DNA transformation, or to get rid of a potent auto-antigen (DNA) that could trigger an immune response (Nagata, 2000).

Work from Ding Xue's laboratory has led to the identification of several other genes involved in apoptotic DNA degradation in *C. elegans*. This group found that CPS-6 (*cps*, *C*ED-3 *p*rotease *s*uppressor), the worm orthologue of mitochondrial endonuclease G (EndoG), a protein normally involved in mitochondrial DNA replication, also participates in apoptotic DNA degradation in *C. elegans* (Parrish et al., 2001). This finding is supported by biochemical experiments in mammalian cells that have shown that upon apoptotic stimuli, EndoG is released from mitochondria, translocates to the nucleus, and cleaves chromosomal DNA (Li et al., 2001). Xue and colleagues also demonstrated that the worm mitochodrial oxidoreductase apoptotis-inducing factor (AIF) WAH-1 (*wah*, *w*orm *A*IF *h*omologue) promotes DNA degradation and apoptosis in worms by cooperating with CPS-6/EndoG (Wang et al., 2002). Finally, Parrish and Xue used RNAi to inactivate 77 proteins that could be implicated in apoptotic DNA degradation because they have a nuclease domain (Parrish and Xue, 2003). They identified seven new nucleases, and characterized one of them further, CRN-1 (*crn*, *c*ell death-*r*elated *n*uclease), the *C. elegans* homologue of human flap endonuclease-1 (FEN-1). They showed that CRN-1 cooperates with CPS-6/EndoG to promote fragmentation of genomic DNA in apoptotic cells (Parrish et al., 2003). How these different nucleases interact in worms, and why does the worm needs so many proteins for a non-essential process – apoptotic DNA degradation – are interesting questions that should find answers in the near future.

1.6 PERSPECTIVES

Since the introduction of *C. elegans* as a model organism to genetically dissect programmed cell death, the study of apoptosis in worms has been prolific and is responsible for several breakthroughs in the field of apoptosis research. There is no doubt that further characterization of the new worm apoptotic genes, briefly reviewed here, will help to understand apoptosis in other species, including humans.

But what is next? We have reached a point where we understand relatively well the death machinery of the worm. Our attention must now be focused on what lies upstream and downstream of the CED-9 —| CED-4 → CED-3 pathway. The identification and characterization of novel genes that control the life-versus-death decision of cells, or that interact with the known engulfment genes is certainly the next big challenge for 'apoptologists' working with *C. elegans*. To find these genes, new strategies, involving modifier genetic screens in sensitized backgrounds, will need to be undertaken. These screens are likely not to be trivial, but at the end should produce quite rewarding results. In this post-genomic era, other methods, such as the determination of expression profiles of apoptosis mutants or the establishment of interaction maps with the proteins involved in apoptosis through large-scale yeast-two-hybrid screens, should provide complementing information to the more traditional genetic approaches. We have learned a lot by studying programmed cell death in worms, yet it is obvious that *C. elegans* still have plenty to teach us on how and why apoptosis occurs. Not bad, not bad at all for a simple worm…

1.7 REFERENCES

Aballay, A., and Ausubel, F. M. (2001). Programmed cell death mediated by *ced-3* and *ced-4* protects *Caenorhabditis elegans* from *Salmonella typhimurium*-mediated killing. Proc Natl Acad Sci U S A *98*, 2735-2739.

Aballay, A., Drenkard, E., Hilbun, L. R., and Ausubel, F. M. (2003). *Caenorhabditis elegans* Innate Immune Response Triggered by *Salmonella enterica* Requires Intact LPS and Is Mediated by a MAPK Signaling Pathway. Curr Biol *13*, 47-52.

Ahmed, S., Alpi, A., Hengartner, M. O., and Gartner, A. (2001). *C. elegans* RAD-5/CLK-2 defines a new DNA damage checkpoint protein. Curr Biol *11*, 1934-1944.

Ahmed, S., and Hodgkin, J. (2000). MRT-2 checkpoint protein is required for germline immortality and telomere replication in *C. elegans*. Nature *403*, 159-164.

Arur, S., Uche, U. E., Rezaul, K., Fong, M., Scranton, V., Cowan, A. E., Mohler, W., and Han, D. K. (2003). Annexin I is an endogenous ligand that mediates apoptotic cell engulfment. Dev Cell *4*, 587-598.

Bloss, T. A., Witze, E. S., and Rothman, J. H. (2003). Suppression of CED-3-independent apoptosis by mitochondrial betaNAC in *Caenorhabditis elegans*. Nature *424*, 1066-1071.

Bose, J., Gruber, A. D., Helming, L., Schiebe, S., Wegener, I., Hafner, M., Beales, M., Kontgen, F., and Lengeling, A. (2004). The phosphatidylserine receptor has essential functions during embryogenesis but not in apoptotic cell removal. J Biol *3*, 15.

Boulton, S. J., Martin, J. S., Polanowska, J., Hill, D. E., Gartner, A., and Vidal, M. (2004). BRCA1/BARD1 orthologs required for DNA repair in *Caenorhabditis elegans*. Curr Biol *14*, 33-39.

Brugnera, E., Haney, L., Grimsley, C., Lu, M., Walk, S. F., Tosello-Trampont, A. C., Macara, I. G., Madhani, H., Fink, G. R., and Ravichandran, K. S. (2002). Unconventional Rac-GEF activity is mediated through the Dock180-ELMO complex. Nat Cell Biol *4*, 574-582.

Chen, F., Hersh, B. M., Conradt, B., Zhou, Z., Riemer, D., Gruenbaum, Y., and Horvitz, H. R. (2000). Translocation of *C. elegans* CED-4 to nuclear membranes during programmed cell death. Science *287*, 1485-1489.

Conradt, B., and Horvitz, H. R. (1998). The *C. elegans* protein EGL-1 is required for programmed cell death and interacts with the Bcl-2-like protein CED-9. Cell *93*, 519-529.

Conradt, B., and Horvitz, H. R. (1999). The TRA-1A sex determination protein of *C. elegans* regulates sexually dimorphic cell deaths by repressing the *egl-1* cell death activator gene. Cell *98*, 317-327.

Cui, P., Qin, B., Liu, N., Pan, G., and Pei, D. (2004). Nuclear localization of the phosphatidylserine receptor protein via multiple nuclear localization signals. Exp Cell Res *293*, 154-163.

del Peso, L., Gonzalez, V. M., and Nunez, G. (1998). *Caenorhabditis elegans* EGL-1 disrupts the interaction of CED-9 with CED-4 and promotes CED-3 activation. J Biol Chem *273*, 33495-33500.

Deng, X., Hofmann, E. R., Villanueva, A., Hobert, O., Capodieci, P., Veach, D. R., Yin, X., Campodonico, L., Glekas, A., Cordon-Cardo, C.*, et al.* (2004). *Caenorhabditis elegans* ABL-1 antagonizes p53-mediated germline apoptosis after ionizing irradiation. Nat Genet *36*, 906-912.

Derry, W. B., Putzke, A. P., and Rothman, J. H. (2001). *Caenorhabditis elegans* p53: role in apoptosis, meiosis, and stress resistance. Science *294*, 591-595.

Desai, C., Garriga, G., McIntire, S. L., and Horvitz, H. R. (1988). A genetic pathway for the development of the *Caenorhabditis elegans* HSN motor neurons. Nature *336*, 638-646.

Ellis, H. M., and Horvitz, H. R. (1986). Genetic control of programmed cell death in the nematode *C. elegans*. Cell *44*, 817-829.

Ellis, R. E., and Horvitz, H. R. (1991). Two *C. elegans* genes control the programmed deaths of specific cells in the pharynx. Development *112*, 591-603.

Ellis, R. E., Jacobson, D. M., and Horvitz, H. R. (1991). Genes required for the engulfment of cell corpses during programmed cell death in *Caenorhabditis elegans*. Genetics *129*, 79-94.

Fadok, V. A., Bratton, D. L., Rose, D. M., Pearson, A., Ezekewitz, R. A., and Henson, P. M. (2000). A receptor for phosphatidylserine-specific clearance of apoptotic cells. Nature *405*, 85-90.

Fraser, A. G., James, C., Evan, G. I., and Hengartner, M. O. (1999). *Caenorhabditis elegans* inhibitor of apoptosis protein (IAP) homologue BIR-1 plays a conserved role in cytokinesis. Curr Biol *9*, 292-301.

Fraser, A. G., Kamath, R. S., Zipperlen, P., Martinez-Campos, M., Sohrmann, M., and Ahringer, J. (2000). Functional genomic analysis of *C. elegans* chromosome I by systematic RNA interference. Nature *408*, 325-330.

Gartner, A., Milstein, S., Ahmed, S., Hodgkin, J., and Hengartner, M. O. (2000). A conserved checkpoint pathway mediates DNA damage-induced apoptosis and cell cycle arrest in *C. elegans*. Mol Cell *5*, 435-443.

Grimsley, C., and Ravichandran, K. S. (2003). Cues for apoptotic cell engulfment: eat-me, don't eat-me and come-get-me signals. Trends Cell Biol *13*, 648-656.

Grimsley, C. M., Kinchen, J. M., Tosello-Trampont, A. C., Brugnera, E., Haney, L. B., Lu, M., Chen, Q., Klingele, D., Hengartner, M. O., and Ravichandran, K. S. (2004). Dock180 and ELMO1 proteins cooperate to promote evolutionarily conserved Rac-dependent cell migration. J Biol Chem *279*, 6087-6097.

Gumienny, T. L., Brugnera, E., Tosello-Trampont, A. C., Kinchen, J. M., Haney, L. B., Nishiwaki, K., Walk, S. F., Nemergut, M. E., Macara, I. G., Francis, R., *et al.* (2001). CED-12/ELMO, a novel member of the CrkII/Dock180/Rac pathway, is required for phagocytosis and cell migration. Cell *107*, 27-41.

Gumienny, T. L., Lambie, E., Hartwieg, E., Horvitz, H. R., and Hengartner, M. O. (1999). Genetic control of programmed cell death in the *Caenorhabditis elegans* hermaphrodite germline. Development *126*, 1011-1022.

Hamon, Y., Broccardo, C., Chambenoit, O., Luciani, M. F., Toti, F., Chaslin, S., Freyssinet, J. M., Devaux, P. F., McNeish, J., Marguet, D., and Chimini, G. (2000). ABC1 promotes engulfment of apoptotic cells and transbilayer redistribution of phosphatidylserine. Nat Cell Biol *2*, 399-406.

Hanahan, D., and Weinberg, R. A. (2000). The hallmarks of cancer. Cell *100*, 57-70.

Hengartner, M. O. (1997). Cell death. in *C elegans II (*eds Riddle, DL, Blumenthal, T, Meyer, BJ & Priess, JR), 383-415.

Hengartner, M. O., Ellis, R. E., and Horvitz, H. R. (1992). *Caenorhabditis elegans* gene *ced-9* protects cells from programmed cell death. Nature *356*, 494-499.

Hengartner, M. O., and Horvitz, H. R. (1994a). Activation of *C. elegans* cell death protein CED-9 by an amino-acid substitution in a domain conserved in Bcl-2. Nature *369*, 318-320.

Hengartner, M. O., and Horvitz, H. R. (1994b). *C. elegans* cell survival gene *ced-9* encodes a functional homolog of the mammalian proto-oncogene bcl-2. Cell *76*, 665-676.

Hoeppner, D. J., Hengartner, M. O., and Schnabel, R. (2001). Engulfment genes cooperate with *ced-3* to promote cell death in *Caenorhabditis elegans*. Nature *412*, 202-206.

Hoeppner, D. J., Spector, M. S., Ratliff, T. M., Kinchen, J. M., Granat, S., Lin, S. C., Bhusri, S. S., Conradt, B., Herman, M. A., and Hengartner, M. O. (2004). *eor-1* and *eor-2* are required for cell-specific apoptotic death in *C. elegans*. Dev Biol *274*, 125-138.

Hofmann, E. R., Milstein, S., Boulton, S. J., Ye, M., Hofmann, J. J., Stergiou, L., Gartner, A., Vidal, M., and Hengartner, M. O. (2002). *Caenorhabditis elegans* HUS-1 is a DNA damage checkpoint protein required for genome stability and EGL-1-mediated apoptosis. Curr Biol *12*, 1908-1918.

Hubbard, E. J., and Greenstein, D. (2000). The *Caenorhabditis elegans* gonad: a test tube for cell and developmental biology. Dev Dyn *218*, 2-22.

Joshi, P., and Eisenmann, D. M. (2004). The *Caenorhabditis elegans pvl-5* gene protects hypodermal cells from *ced-3*-dependent, *ced-4*-independent cell death. Genetics *167*, 673-685.

Kamath, R. S., Fraser, A. G., Dong, Y., Poulin, G., Durbin, R., Gotta, M., Kanapin, A., Le Bot, N., Moreno, S., Sohrmann, M.*, et al.* (2003). Systematic functional analysis of the *Caenorhabditis elegans* genome using RNAi. Nature *421*, 231-237.

Karashima, T., Sugimoto, A., and Yamamoto, M. (2000). *Caenorhabditis elegans* homologue of the human azoospermia factor DAZ is required for oogenesis but not for spermatogenesis. Development *127*, 1069-1079.

Kerr, J. F., Wyllie, A. H., and Currie, A. R. (1972). Apoptosis: a basic biological phenomenon with wide-ranging implications in tissue kinetics. Br J Cancer *26*, 239-257.

Kim, D. H., Feinbaum, R., Alloing, G., Emerson, F. E., Garsin, D. A., Inoue, H., Tanaka-Hino, M., Hisamoto, N., Matsumoto, K., Tan, M. W., and Ausubel, F. M. (2002). A conserved p38 MAP kinase pathway in *Caenorhabditis elegans* innate immunity. Science *297*, 623-626.

Kim, M. R., and Tilly, J. L. (2004). Current concepts in Bcl-2 family member regulation of female germ cell development and survival. Biochim Biophys Acta *1644*, 205-210.

Klemke, R. L., Leng, J., Molander, R., Brooks, P. C., Vuori, K., and Cheresh, D. A. (1998). CAS/Crk coupling serves as a "molecular switch" for induction of cell migration. J Cell Biol *140*, 961-972.

Lettre, G., Kritikou, E. A., Jaeggi, M., Calixto, A., Fraser, A. G., Kamath, R. S., Ahringer, J., and Hengartner, M. O. (2004). Genome-wide RNAi identifies p53-dependent and -independent regulators of germ cell apoptosis in *C. elegans*. Cell Death Differ *11*, 1198-1203.

Li, L. Y., Luo, X., and Wang, X. (2001). Endonuclease G is an apoptotic DNase when released from mitochondria. Nature *412*, 95-99.

Li, M. O., Sarkisian, M. R., Mehal, W. Z., Rakic, P., and Flavell, R. A. (2003). Phosphatidylserine receptor is required for clearance of apoptotic cells. Science *302*, 1560-1563.

Liu, Q. A., and Hengartner, M. O. (1998). Candidate adaptor protein CED-6 promotes the engulfment of apoptotic cells in *C. elegans*. Cell *93*, 961-972.

Liu, Q. A., and Hengartner, M. O. (1999). Human CED-6 encodes a functional homologue of the *Caenorhabditis elegans* engulfment protein CED-6. Curr Biol *9*, 1347-1350.

Luciani, M. F., and Chimini, G. (1996). The ATP binding cassette transporter ABC1, is required for the engulfment of corpses generated by apoptotic cell death. Embo J *15*, 226-235.

McCall, K. (2004). Eggs over easy: cell death in the *Drosophila* ovary. Dev Biol *274*, 3-14.

Metzstein, M. M., Hengartner, M. O., Tsung, N., Ellis, R. E., and Horvitz, H. R. (1996). Transcriptional regulator of programmed cell death encoded by *Caenorhabditis elegans* gene *ces-2*. Nature *382*, 545-547.

Metzstein, M. M., and Horvitz, H. R. (1999). The *C. elegans* cell death specification gene *ces-1* encodes a snail family zinc finger protein. Mol Cell *4*, 309-319.

Nagata, S. (2000). Apoptotic DNA fragmentation. Exp Cell Res *256*, 12-18.

Nakano, K., and Vousden, K. H. (2001). PUMA, a novel proapoptotic gene, is induced by p53. Mol Cell *7*, 683-694.

Navarro, R. E., Shim, E. Y., Kohara, Y., Singson, A., and Blackwell, T. K. (2001). *cgh-1*, a conserved predicted RNA helicase required for gametogenesis and protection from physiological germline apoptosis in *C. elegans*. Development *128*, 3221-3232.

Oda, E., Ohki, R., Murasawa, H., Nemoto, J., Shibue, T., Yamashita, T., Tokino, T., Taniguchi, T., and Tanaka, N. (2000). Noxa, a BH3-only member of the Bcl-2 family and candidate mediator of p53-induced apoptosis. Science *288*, 1053-1058.

Parrish, J., Li, L., Klotz, K., Ledwich, D., Wang, X., and Xue, D. (2001). Mitochondrial endonuclease G is important for apoptosis in *C. elegans*. Nature *412*, 90-94.

Parrish, J. Z., and Xue, D. (2003). Functional genomic analysis of apoptotic DNA degradation in *C. elegans*. Mol Cell *11*, 987-996.

Parrish, J. Z., Yang, C., Shen, B., and Xue, D. (2003). CRN-1, a *Caenorhabditis elegans* FEN-1 homologue, cooperates with CPS-6/EndoG to promote apoptotic DNA degradation. Embo J *22*, 3451-3460.

Reddien, P. W., Cameron, S., and Horvitz, H. R. (2001). Phagocytosis promotes programmed cell death in *C. elegans*. Nature *412*, 198-202.

Reddien, P. W., and Horvitz, H. R. (2000). CED-2/CrkII and CED-10/Rac control phagocytosis and cell migration in *Caenorhabditis elegans*. Nat Cell Biol *2*, 131-136.

Reddien, P. W., and Horvitz, H. R. (2004). The Engulfment Process of Programmed Cell Death in *Caenorhabditis elegans*. Annu Rev Cell Dev Biol.

Rospert, S., Dubaquie, Y., and Gautschi, M. (2002). Nascent-polypeptide-associated complex. Cell Mol Life Sci *59*, 1632-1639.

Savill, J., and Fadok, V. (2000). Corpse clearance defines the meaning of cell death. Nature *407*, 784-788.

Schumacher, B., Hofmann, K., Boulton, S., and Gartner, A. (2001). The *C. elegans* homolog of the p53 tumor suppressor is required for DNA damage-induced apoptosis. Curr Biol *11*, 1722-1727.

Shaham, S., and Horvitz, H. R. (1996). Developing *Caenorhabditis elegans* neurons may contain both cell-death protective and killer activities. Genes Dev *10*, 578-591.

Speliotes, E. K., Uren, A., Vaux, D., and Horvitz, H. R. (2000). The survivin-like *C. elegans* BIR-1 protein acts with the Aurora-like kinase AIR-2 to affect chromosomes and the spindle midzone. Mol Cell *6*, 211-223.

Su, H. P., Nakada-Tsukui, K., Tosello-Trampont, A. C., Li, Y., Bu, G., Henson, P. M., and Ravichandran, K. S. (2002). Interaction of CED-6/GULP, an adapter protein involved in engulfment of apoptotic cells with CED-1 and CD91/low density lipoprotein receptor-related protein (LRP). J Biol Chem *277*, 11772-11779.

Sulston, J. E., and Horvitz, H. R. (1977). Post-embryonic cell lineages of the nematode, *Caenorhabditis elegans*. Dev Biol *56*, 110-156.

Sulston, J. E., Schierenberg, E., White, J. G., and Thomson, J. N. (1983). The embryonic cell lineage of the nematode *Caenorhabditis elegans*. Dev Biol *100*, 64-119.

Tenor, J. L., McCormick, B. A., Ausubel, F. M., and Aballay, A. (2004). *Caenorhabditis elegans*-based screen identifies *Salmonella* virulence factors required for conserved host-pathogen interactions. Curr Biol *14*, 1018-1024.

Thellmann, M., Hatzold, J., and Conradt, B. (2003). The Snail-like CES-1 protein of *C. elegans* can block the expression of the BH3-only cell-death activator gene *egl-1* by antagonizing the function of bHLH proteins. Development *130*, 4057-4071.

Tilly, J. L. (2001). Commuting the death sentence: how oocytes strive to survive. Nat Rev Mol Cell Biol *2*, 838-848.

Wang, X., Wu, Y. C., Fadok, V. A., Lee, M. C., Gengyo-Ando, K., Cheng, L. C., Ledwich, D., Hsu, P. K., Chen, J. Y., Chou, B. K.*, et al.* (2003). Cell corpse engulfment mediated by *C. elegans* phosphatidylserine receptor through CED-5 and CED-12. Science *302*, 1563-1566.

Wang, X., Yang, C., Chai, J., Shi, Y., and Xue, D. (2002). Mechanisms of AIF-mediated apoptotic DNA degradation in *Caenorhabditis elegans*. Science *298*, 1587-1592.

Wu, Y. C., and Horvitz, H. R. (1998a). The *C. elegans* cell corpse engulfment gene *ced-7* encodes a protein similar to ABC transporters. Cell *93*, 951-960.

Wu, Y. C., and Horvitz, H. R. (1998b). *C. elegans* phagocytosis and cell-migration protein CED-5 is similar to human DOCK180. Nature *392*, 501-504.

Wu, Y. C., Stanfield, G. M., and Horvitz, H. R. (2000). NUC-1, a *Caenorhabditis elegans* DNase II homolog, functions in an intermediate step of DNA degradation during apoptosis. Genes Dev *14*, 536-548.

Wu, Y. C., Tsai, M. C., Cheng, L. C., Chou, C. J., and Weng, N. Y. (2001). *C. elegans* CED-12 acts in the conserved crkII/DOCK180/Rac pathway to control cell migration and cell corpse engulfment. Dev Cell *1*, 491-502.

Wyllie, A. H. (1980). Glucocorticoid-induced thymocyte apoptosis is associated with endogenous endonuclease activation. Nature *284*, 555-556.

Wyllie, A. H., Kerr, J. F., and Currie, A. R. (1980). Cell death: the significance of apoptosis. Int Rev Cytol *68*, 251-306.

Xue, D., and Horvitz, H. R. (1995). Inhibition of the *Caenorhabditis elegans* cell-death protease CED-3 by a CED-3 cleavage site in baculovirus p35 protein. Nature *377*, 248-251.

Xue, D., Shaham, S., and Horvitz, H. R. (1996). The *Caenorhabditis elegans* cell-death protein CED-3 is a cysteine protease with substrate specificities similar to those of the human CPP32 protease. Genes Dev *10*, 1073-1083.

Yan, N., Gu, L., Kokel, D., Chai, J., Li, W., Han, A., Chen, L., Xue, D., and Shi, Y. (2004). Structural, Biochemical, and Functional Analyses of CED-9 Recognition by the Proapoptotic Proteins EGL-1 and CED-4. Mol Cell *15*, 999-1006.

Yuan, J., and Horvitz, H. R. (1992). The *Caenorhabditis elegans* cell death gene *ced-4* encodes a novel protein and is expressed during the period of extensive programmed cell death. Development *116*, 309-320.

Yuan, J., Shaham, S., Ledoux, S., Ellis, H. M., and Horvitz, H. R. (1993). The *C. elegans* cell death gene *ced-3* encodes a protein similar to mammalian interleukin-1 beta-converting enzyme. Cell *75*, 641-652.

Zhou, Z., Caron, E., Hartwieg, E., Hall, A., and Horvitz, H. R. (2001a). The *C. elegans* PH domain protein CED-12 regulates cytoskeletal reorganization via a Rho/Rac GTPase signaling pathway. Dev Cell *1*, 477-489.

Zhou, Z., Hartwieg, E., and Horvitz, H. R. (2001b). CED-1 is a transmembrane receptor that mediates cell corpse engulfment in *C. elegans*. Cell *104*, 43-56.

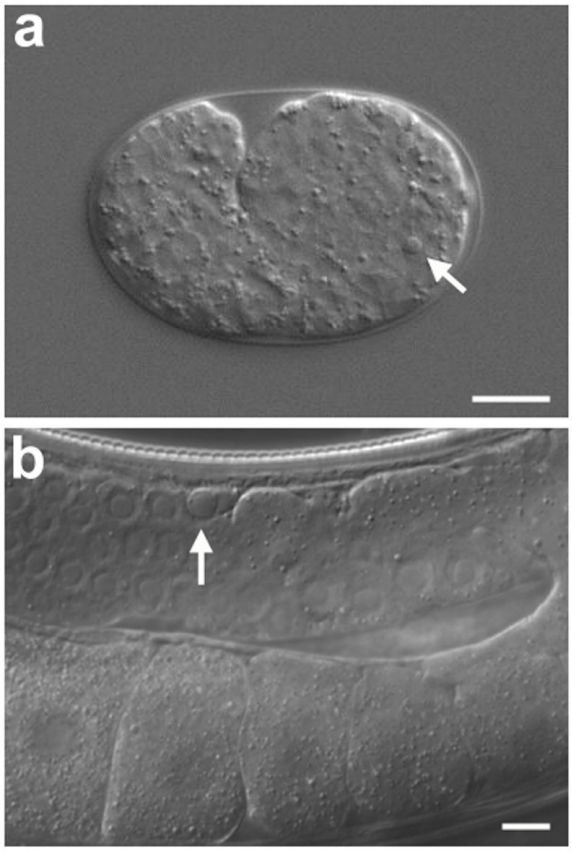

FIGURE 1.1 Morphology of apoptotic cells in *C. elegans*

(a) Somatic cell death in *C. elegans*. Picture of a wild-type embryo at an early 1.5-fold stage was taken by Nomarski optics. The white arrow indicates a highly refractile apoptotic cell. Scale bar, 10 μm. (Picture from Lukas Neukomm).

(b) Germ cell apoptosis in *C. elegans* hermaphrodite. Nomarski optics picture of a wild-type hermaphrodite gonad taken ~24 hours post larval stage L4. The white arrow indicates a highly refractile apoptotic germ cell. Anterior is to the left and dorsal to the top. Scale bar, 10 μm.

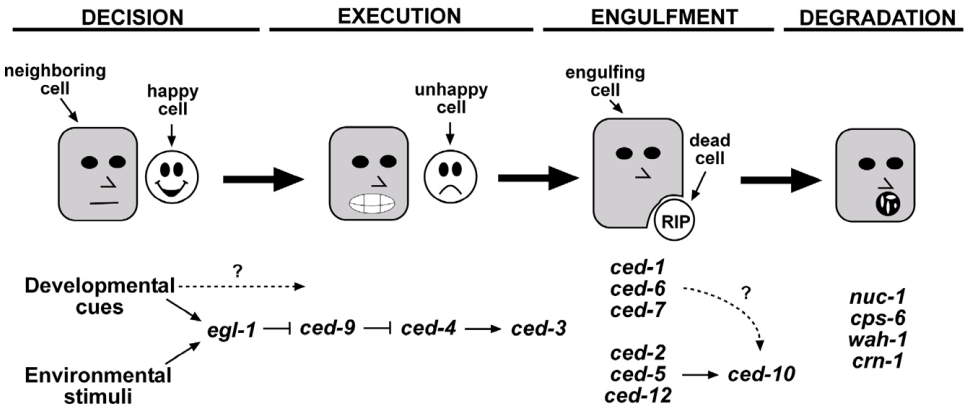

FIGURE 1.2 The *C. elegans* apoptotic pathway

The general 'four steps' programmed cell death pathway in *C. elegans*. Positive (→) and negative (—|) genetic interactions are shown. (Adapted from Hengartner, 1997).

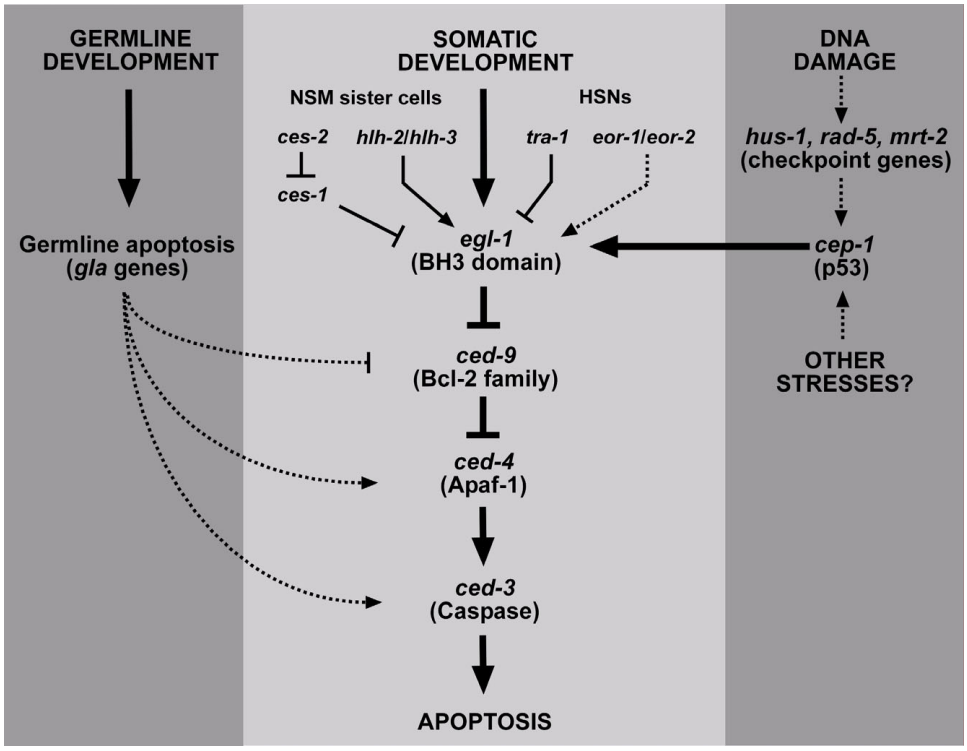

FIGURE 1.3 Regulation of apoptosis in *C. elegans*

Three different pathways lead to apoptosis in *C. elegans*. The pale grey box contains the canonical apoptotic pathway, whereas the dark grey boxes indicate germline-specific components. Dashed arrows represent either unknown or indirect interactions.

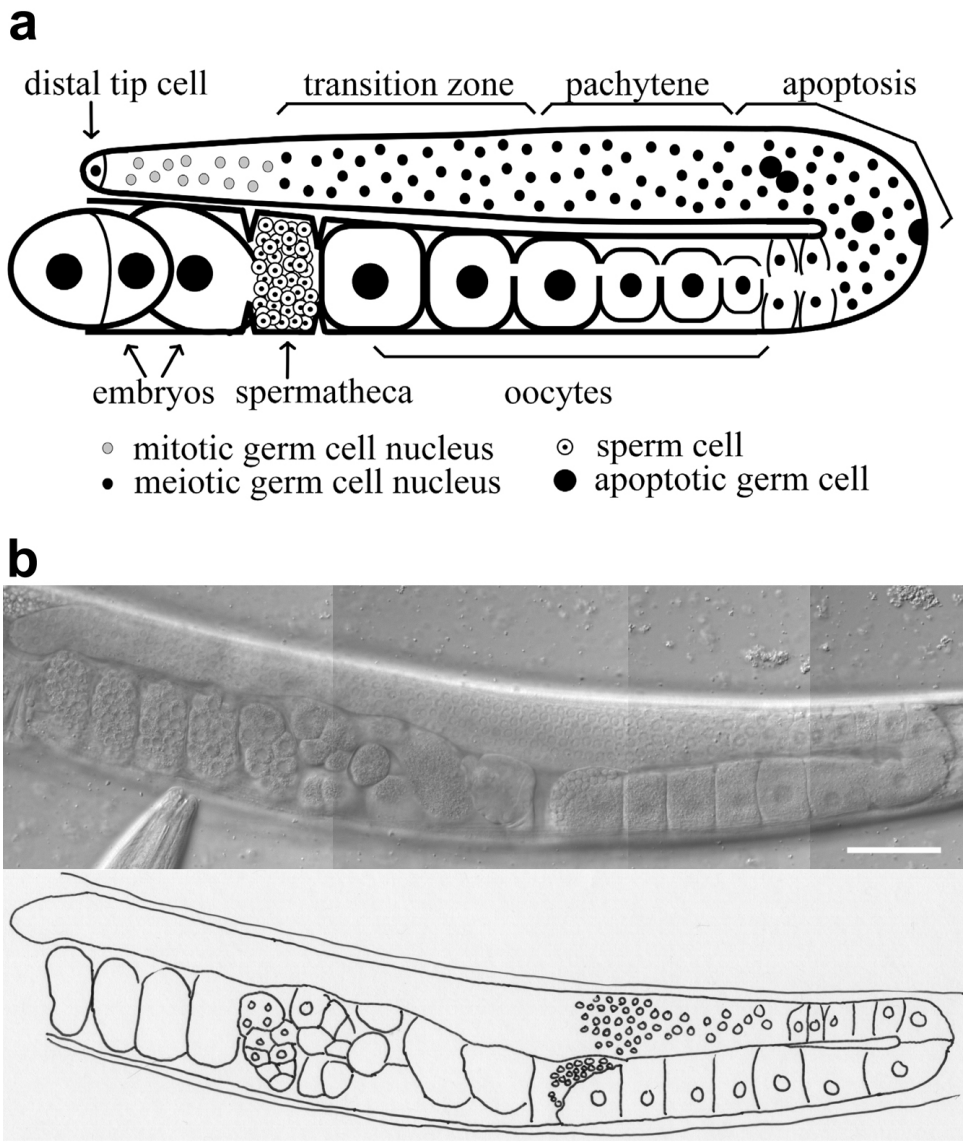

FIGURE 1.4 *C. elegans* adult hermaphrodite germ line

(a) Schematic diagram of an adult hermaphrodite *C. elegans* gonad. Apoptotic corpses are normally observed at and distal to the bend. (Adapted from Lettre et al., 2004).

(b) Picture, and corresponding drawing, of a hermaphrodite *C. elegans* gonad taken ~36 hours post the larval stage L4 by Normaski optics. Anterior is to the left and dorsal to the top. Scale bar, 50 μm.

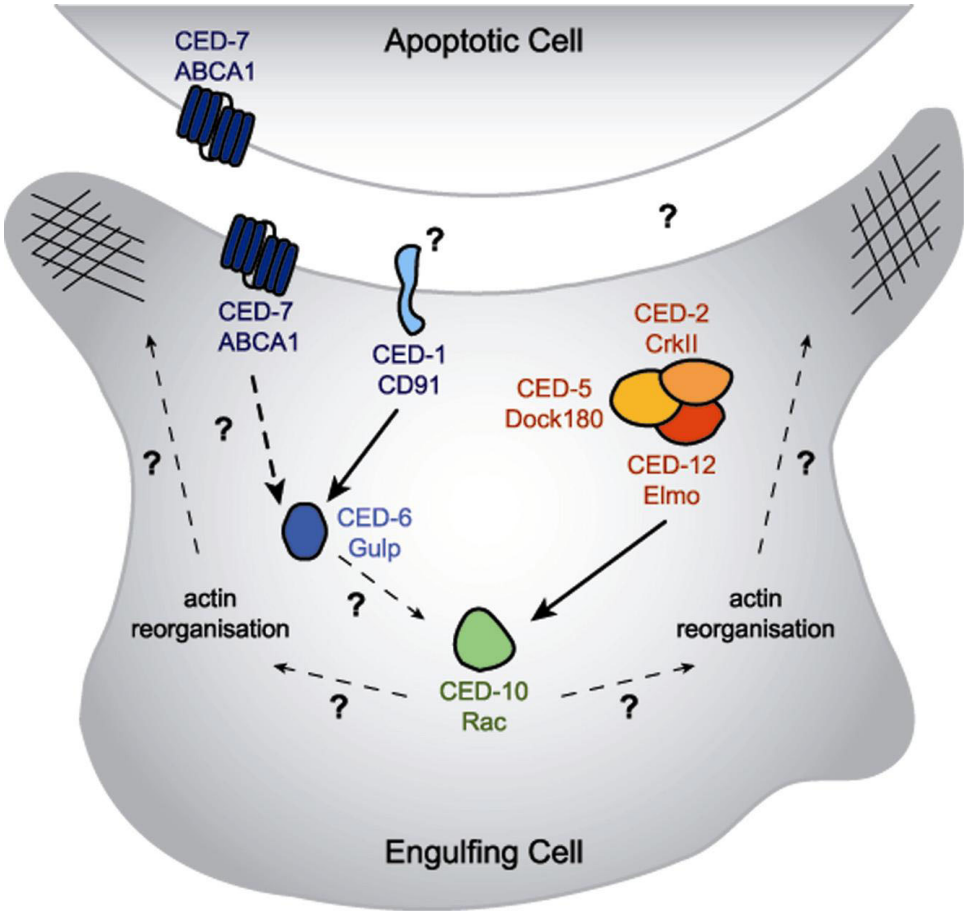

FIGURE 1.5 Phagocytosis of apoptotic cells in *C. elegans*

Molecular model for cell corpse removal in *C. elegans*. Two redundant genetic pathways have been described: one comprised of *ced-1*, *-6*, and *-7*, and the other of *ced-2*, *-5*, *-10*, and *-12*. Question marks indicate missing components. (This model is a courtesy of Steffi Züllig).

• CHAPTER 2 •

GENETIC MAPPING AND CLONING OF *GLA-1(OP208)*, *TEG-1(OP152)*, AND *GLA-4(OP199)*

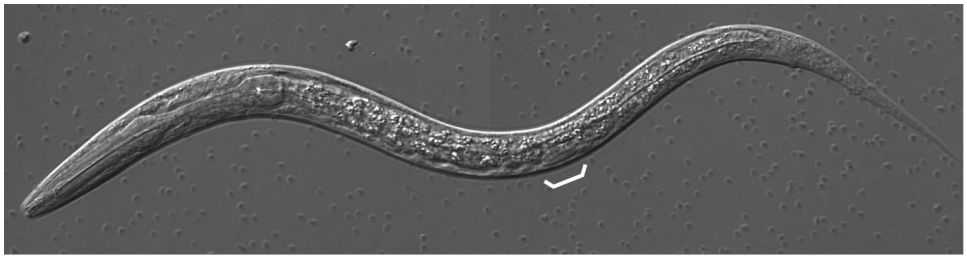

L1 larva - 4 cell stage gonad (Z1 and Z2 are visible)

• CHAPTER 2 •

GENETIC MAPPING AND CLONING OF *GLA-1(OP208)*, *TEG-1(OP152)*, AND *GLA-4(OP199)*

2.1 ABSTRACT

In a forward genetic screen for mutants with increased germline apoptosis *op208*, *op152*, and *op199* were previously isolated. Here, I show that *op208* is an allele of *cpb-3/gla-1*, a gene encoding a CPEB-like RNA binding protein, and that *op152* is a mutation in the gene *teg-1*, which is involved in germ cell proliferation and differentiation. Finally, *op199* was not cloned, but mapped to a genetic interval that contains 24 predicted genes.

2.2 INTRODUCTION

As mentioned in chapter 1, an important fraction of germ cells in the *C. elegans* hermaphrodite germ line undergo apoptosis; we refer to this process as 'physiological germ cell death' because it occurs without exogenous stresses (Gumienny et al., 1999). Interestingly, few genes are known to either promote or block the physiological germ cell death pathway, and we still do not know why ~50% of the developing germ cells die by apoptosis. On the assumption that identification of new regulators of this pathway might lead to further insights into the cause(s) of these germ cell deaths, a forward genetic screen was performed for mutants with increased levels of germline apoptosis (S. Milstein and M.O. Hengartner, unpublished). Briefly, wild-type worms were mutagenized with ethyl-methane-sulfinate (EMS), and the F_2 population was screened using acridine orange (AO) to visualize apoptotic cells. AO can be used as a vital dye to specifically stain engulfed apoptotic corpses in the *C. elegans* germ line (S.M. and M.O.H., unpublished). Approximately 45 000 haploid genomes were screened and 21 mutants were isolated. Milstein cloned *gla-1* and *gla-3*, two of the genes identified in this screen. *gla-1* encodes a member of the CPEB family of RNA binding proteins, and *gla-3* a TIS11-like zinc finger domain containing protein (S.M. and M.O.H., unpublished). In this chapter, I describe my efforts to map and clone three other mutants found in the 'Gla screen': *op208, op152,* and *op199*.

2.3 RESULTS

2.3.1 op208 represents a new allele of gla-1

op208 mutant worms have a strong *g*erm*l*ine *a*poptosis (Gla) phenotype (Figure 2.1 and 2.2c), but are otherwise phenotypically normal. Using two-factor mapping, Milstein had mapped *op208* on chromosome I, close to the physical marker *dpy-5*. I carried out three-factor mapping with the two following sets of markers: *unc-57* (-1.0 cM) *dpy-5* (0 cM), and *dpy-5 unc-29* (+3.3 cM). The cross between *op208* and *unc-57 dpy-5* revealed that *op208* is on the right, or close to the left, of *dpy-5* because 6/6 Unc non-Dpy recombinants were Gla and 0/6 Dpy non-Unc recombinants were Gla. The cross between *op208* and *dpy-5 unc-29* was even more informative: 9/17 Unc non-Dpy recombinants were Gla and 5/21 Dpy non-Unc recombinants were Gla. Furthermore, among the Gla animals picked in the F_2 generation to confirm the interval, one threw Dpy worms and another threw Unc worms. These data strongly suggest that *op208* lies between the markers *dpy-5* and *unc-29*, on the right arm of chromosome I (Figure 2.2a). To narrow down the genetic interval where *op208* is located, single nucleotide polymorphism (SNP) mapping was used. Recombinants between *dpy-5 op208 unc-29* animals and the polymorphic *C. elegans* strain CB4856 put *op208* between the molecular markers C04F1[2] (+0.35 cM) on the left and C34G6[3] (+0.50 cM) on the right (Figure 2.2a). On the physical map, this genetic interval corresponds to ~151 kb, which contains 40 predicted genes. One of the genes in this interval is *gla-1* itself, which has a strong Gla phenotype when mutated. Although Milstein had performed complementation tests between *op208* and the canonical *gla-1* allele *op234* and found complementation, I decided to repeat that experiment. The F_1 non-Dpy animals from a cross between *op208* males and *dpy-5 gla-1(op234)* hermaphrodites were Gla, suggesting that *op208* is in fact a new allele of *gla-1*. Indeed, sequencing the *gla-1* locus of *op208* animals revealed a single point mutation: a G-to-A transition in exon 4 (base pair 1572 of ORF) that changes methionine 524 into an isoleucine (Figure 2.2b). This mutation does not affect a conserved residue, but occurs within a very conserved region of the GLA-1 protein (Figure 3.2b). The *op234* mutation in *gla-1* is also a missense G-to-A transition (base pair 1577 of ORF) that changes a conserved cysteine at position 526 into a tyrosine (Figure 3.2b). Clearly, *op208* represents an hypomorphic allele of *gla-1* as the Gla phenotype of

op208 worms is weaker that the Gla phenotype of *op234* mutants (Figure 2.2c). It remains to be determined whether *op234* is a null allele, and therefore what the true phenotype caused by a complete loss of *gla-1* function will be.

2.3.2 op152 represents a new allele of teg-1

op152 is a temperature-sensitive allele identified in the forward genetic screen for mutants with increased germ cell death. At 20°C, *op152* mutants do not have a Gla phenotype, but at 25°C, the Gla phenotype of *op152* animals is strong (Figure 2.1 and 2.3c). *op152* also has pleiotropic effects: it causes cold-sensitive sterility at 15°C and a highly penetrant Mog (*M*asculinization *o*f *g*erm line) phenotype, i.e. an over-production of sperm cells and an accumulation of residual bodies in the proximal arm of the gonads. Intriguingly, blocking apoptosis in *op152* mutants through inactivation of the essential caspase *ced-3* results in the appearance of large necrotic-like structures in the germ line (Figure 2.1). The biological significance of this phenotype is still puzzling, and requires further analysis.

Two- and three-factor mapping was previously used to map *op152* on the right arm of chromosome III, close to the physical marker *dpy-18* (Figure 2.3a) (S.M. and M.O.H., unpublished). To refine the map position of *op152*, I used SNP mapping. By picking, at 15°C, Unc non-Sterile F_2 recombinants from crosses between the polymorphic strain CB4856 and *unc-49 dpy-18/op152* or *dpy-18/op152 unc-25* animals, I could place *op152* on the left of *dpy-18*, between the molecular markers Y47D3[13] (+7.4 cM) and *pkP3060* (+8.7 cM) (Figure 2.3a). The size of this interval is ~115 kb, and it is predicted to contain 20 genes. One of these genes, *teg-1*, was cloned in Tim Schedl's laboratory (University of Washington, St-Louis) as a regulator of germ cell proliferation and/or differentiation (D. Hansen and T. Schedl, unpublished). TEG-1 does not have any recognizable domains and its closest human match is the CD2 antigen cytoplasmic tail-binding protein 2. The gene is characterized by cold-sensitive sterility and a Mog phenotype when mutated; therefore an obvious candidate for *op152*. Complementation test was performed between *op152* and the canonical *teg-1* allele *oz230*, and non-complementation was found for the sterility and the Mog phenotypes. Sequencing of the six exons of *teg-1* in *op152* mutants revealed a single point mutation in exon 3 (base pair 618 of ORF), which changes

tryptophan 206 (UGG) into an opal stop codon (UGA). Furthermore, the *op152* mutation abrogates a *Hae*III restriction site, allowing detection after PCR amplification and restriction digest of genomic DNA extracted from *op152* mutants (Figure 2.3b).

The identification of *op152* as an allele of *teg-1* was surprising because, whereas *op152* is clearly Gla at 25°C (Figure 2.3c), the predicted null allele *oz230* is not (D.H. and T.S., personal communication). One explanation could be that *op152* is an usual *teg-1* allele (e.g. neomorph), although genetically it behaves as a recessive hypomorph. Another possibility is that an additional lesion, closely linked to *teg-1(op152)*, causes the Gla phenotype. To distinguish between these two possibilities, I performed a rescue experiment. By biolistic transformation, I created transgenic animals bearing few copies of the following transgene: $P_{pie\text{-}1}$*::gfp::teg-1*. The *pie-1* regulatory sequence was used to drive expression of the transgene in germ cells (Seydoux et al., 1996). The fusion protein GFP::TEG-1 showed nuclear localization and could only be observed in the distal arm of the gonads. When this transgene was crossed into *teg-1(op152)* worms, it rescued the sterility and the Mog phenotype, suggesting that the fusion protein is functional and that the activity of TEG-1 is required in germ cells. Moreover, time course analysis revealed that the transgene completely rescues the Gla phenotype of *op152* animals at 25°C (Figure 2.3c). These observations suggest that *op152* is an unusual recessive *teg-1* allele, although further genetic characterization is required to confirm this hypothesis.

2.3.3 gla-4(op199) maps at ~+17.5 cM on chromosome I

gla-4(op199) is the only mutant found in the forward genetics 'Gla screen' that has unusual corpse morphology. Indeed, *gla-4(op199)* worms do not have more germline apoptosis, but rather have three-to-four times bigger apoptotic corpses relative to wild-type (Figure 2.1). Furthermore, the corpses in *gla-4(op199)*, do not show the characterisitic button-like appearance, but are granular and have a visible nucleus (Figure 2.1). *op199* was mapped on the right of *unc-29* (+3.3 cM), on chromosome I by Milstein. I used SNP mapping to find a small interval for this mutation. However, this task was tedious due to the lack of good physical markers close to the region of interest. Consequently, most recombinants isolated from the different crosses were non-informative. I built the double mutants *unc-101* (+13.3 cM) *op199* and *op199 unc-54*

(+27.4 cM), which I crossed into CB4856 to pick Gla non-Unc recombinants in the F_2 generation (Figure 2.4). Genotyping these recombinants for polymorphisms allowed me to place *op199* between the molecular marker Y26D4[2] (+17.4 cM) and ZK1225[1] (+18.1 cM) (Table 2.1). This interval corresponds to 122 kb, and contains 24 predicted genes. Thorough bioinformatic analysis of these 24 genes did not reveal an obvious candidate for *gla-4*. To clone *gla-4(op199)*, available clones from the Ahringer RNAi feeding library were used to knock down 18 of these genes in a wild-type background (Table 2.2) (Fraser et al., 2000; Kamath et al., 2003). Unfortunately, these experiments were unsuccessful as the *op199* phenotype could not be phenocopied by RNAi. These results indicate that either *op199* is one of the six genes not tested by RNAi, or that RNAi feeding does not work efficiently to knock down *gla-4* expression.

2.4 DISCUSSION

2.4.1 mRNA translation, GLA-1, and germ cell death

gla-1, annotated in Wormbase as *cpb-3*, encodes a CPEB protein. CPEBs (cytoplasmic polyadenylation element-binding protein) are highly conserved RNA binding proteins that modulate translational repression and mRNA localization (Figure 2.2b) (Mendez and Richter, 2001). In *Drosophila*, the CPEB protein Orb is crucial for anteroposterior and dorsoventral patterning during oogenesis, as well as for the formation of the egg chamber and entry into meiosis (Lantz et al., 1992). Similarly, the *Xenopus* CPEB orthologue plays an important role during oogenesis (Stebbins-Boaz et al., 1996). In the mouse, disruption of the CPEB gene is viable, but causes sterility. Detailed molecular analysis revealed that the sterility is due to an arrest during the early pachytene to diplotene transition in prophase of meiosis I (Tay et al., 2003; Tay and Richter, 2001). Furthermore, male meiotic germ cells undergo apoptosis in $CPEB^{-/-}$ mice (Tay and Richter, 2001). This is a very similar phenotype than in *gla-1(lf) C. elegans* hermaphrodite mutants, where increased germline apoptosis is seen only once germ cells escape pachytene arrest.

C. elegans has four CPEB proteins: FOG-1, CPB-1, -2, and -3. Surprisingly, two of these proteins, FOG-1 and CPB-1, are required for spermatogenesis but dispensable for oogenesis (Luitjens et al., 2000). FOG-1 is necessary for the cell fate decision to develop

into sperm rather than oocyte, and CPB-1 plays an essential role for progression through meiosis during spermatogenesis. Luitjens et al. did not identify any functions for *cpb-2* and *cpb-3/gla-1* (Luitjens et al., 2000). Therefore, our work is the first to assign a function to a worm CPEB gene in oogenesis, namely the anti-apoptotic activity of *cpb-3/gla-1* (Figure 3.2c). We still ignore how CPB-3/GLA-1 regulates germ cell apoptosis, but we suspect that it might be through binding of specific mRNA targets. One might be able to identify putative targets by using the strategy developed to identify *in vivo* targets for the RNA-binding protein GLD-1 in *C. elegans* (Lee and Schedl, 2001). Briefly, transgenic animals with an epitope-tagged GLA-1 would be lysed and the protein-RNA complexes would be pulled-down. The mRNAs present in these complexes would be identified through hybridization to microarrays. Another important question to be addressed is what the null phenotype for *cpb-3/gla-1* really is? Indeed, *op208* and *op234* are unlikely to be null alleles as both are missense mutations (Figure 2.2b). Furthermore, we have not tested whether additional phenotypes are visible when the *gla-1* alleles are put *in trans* over deficiencies. Because CPEBs play an essential role during oogenesis in several organisms, it would not be surprising if the *trans*-heterozygote combination *gla-1(op234)/Df* produces a more severe phenotype (complete sterility?) than homozygous *gla-1(op234)*.

In *Xenopus*, many dormant mRNAs in oocytes have short poly(A) tails; it is only when these tails are elongated that translation can occur. CPEB binds the 3' untranslated region (UTR) of these mRNAs and, through interactions with the proteins Maskin and the 5'UTR-bound eIF4E, causes circularization and repression of the transcripts. However, when CPEB is phosphorylated, it facilitates translation: it recruits the cleavage and polyadenylation specificity factor (CPSF) and poly(A) polymerase. Interestingly, it has recently been shown in *C. elegans* that GLD-2, a regulator of mitosis/meiosis decision in the germ line, and GLD-3, a Bicaudal-C homologue, form a complex with poly(A) polymerase activity (Eckmann et al., 2002; Wang et al., 2002). It has also been proposed that this enzymatic activity is required for translation of mRNAs important for germ cell proliferation and/or differentiation (Wang et al., 2002). It will be interesting to test whether the CPEB *cpb-3/gla-1* gene genetically interacts with the *gld-2/gld-3* pathway.

As a first step to test this hypothesis, I scored *gld-2(q497)* animals for germline apoptosis, but could not detect any abnormal phenotypes.

2.4.2 teg-1 links germ cell proliferation and differentiation to apoptosis

In the distal arm of the *C. elegans* hermaphrodite germ line, germ cells must decide between proliferation and differentiation, that is, entry into meiosis. The GLP-1/Notch signaling pathway promotes cell division and/or inhibits differentiation through inactivation of two key redundant genes: *gld-1* and *gld-2*. In *glp-1(gf)* or *gld-2(lf) gld-1(lf)* mutants, germ cells remain proliferative and form a tumorous germ line (Seydoux and Schedl, 2001). To identify new genes involved in the switch between mitosis and meiosis, Hansen and Schedl performed a genetic screen for *t*umorous *e*nhancers of a weak *glp-1(gf)* mutation (*teg* genes) (D.H. and T.S., unpublished). They identified and cloned *teg-1*, a gene that encodes a protein similar to a human protein that interacts with the T-lymphocyte receptor, CD2. Therefore, it was surprising to find out that *op152*, one of the mutants identified in the 'Gla screen', is a new allele of *teg-1*. One can imagine a model where TEG-1 is a repair protein required throughout meiosis: it might be involved in entry into meiosis at the distal end of the gonad, and also during pachytene progression at the bend of the gonad. Maybe our *teg-1(op152)* allele only affects the pachytene role of TEG-1, whereas *teg-1(oz230)*, which is a predicted null, influences the earlier event, i.e. meiotic entry. This model could explain the phenotypic discrepancies between *op152* and *oz230*. Also, it could provide an explanation for the phenotype of the *teg-1(op152); ced-3(n717)* double mutants. In these animals, germ cell death is completely blocked, but necrotic-like vacuoles appear in the gonad (Figure 2.1). Assuming a role in repair for TEG-1, its absence in the death-sensitive zone of the germ line would lead to apoptotic death of impaired germ cells. If apoptosis cannot be used to eliminate these defective germ cells, as in *teg-1; ced-3* worms, the cells would lyse and die by necrosis.

Recently, it has been shown that GLD-1 binds the mRNA of the worm p53 homologue *cep-1* (B. Schumacher and A. Gartner, unpublished). In a screen for mutants hyper-sensitive to DNA damage, the authors of the study found an unusual *gld-1* allele, which encodes a protein unable to specifically repress the *cep-1* mRNA. Presumably, in this mutant, more CEP-1 is present and upon genotoxic stress, more germline apoptosis

occur. Because *teg-1* genetically interacts with the *gld-1* pathway (D.H. and T.S., unpublished), it would be interesting to check if the level of *cep-1* mRNA and CEP-1 protein are normal in *teg-1(op152)* animals. Importantly, irradiation experiments should be carried out to investigate whether the *teg-1(op152)* mutants are hyper-sensitive to DNA damage. Clearly, more work needs to be done to understand how germ cell proliferation and differentiation are linked to apoptosis.

2.4.3 gla-4(op199) remains a stranger

Using SNP mapping, I could map *op199* in a 0.7 cM interval on the right arm of chromosome I (Figure 2.4). RNAi knock down of 18 of the 24 predicted genes in that interval did not allow me to phenocopy the *gla-4(op199)* phenotype, suggesting that *gla-4* is one of the six genes not tested, or that *gla-4(RNAi)* does not work (Table 2.2). To clone *gla-4(op199)*, I propose the following strategy: (1) create RNAi feeding vectors for the six genes in the interval that have not been tested yet, (2) perform RNAi-feeding in the RNAi-hyper-sensitive strain *rrf-3(pk1426)* (Simmer et al., 2002), (3) use RNAi soaking or injection, and (4) create low-copy integrants of the most promising genes to rescue the *op199* phenotype. The very peculiar morphology of the apoptotic corpses in *gla-4(op199)* worms makes this mutant very interesting, and justify further efforts to clone this gene.

2.5 MATERIALS AND METHODS

2.5.1 Nematode strains and culture

Standard procedures for nematode culture and genetic manipulation were followed with growth at 20°C, unless otherwise noted (Brenner, 1974; Gumienny et al., 1999; Sulston and Hodgkin, 1988). The wild-type N2 Bristol strain was used. *C. elegans* gene mutations relevant to this study are as followed: LGI: *unc-57(e406), dpy-5(e61), gla-1(op234), gla-1(op208), unc-101(m1), gla-4(op199), unc-54(e1092);* LGIII: *unc-49(e382), unc-119(ed3), teg-1(op152), teg-1(oz230), dpy-18(e364), unc-25(e156);* LGIV: *ced-3(n717)*. Phenotypes are described either by Riddle (Riddle et al., 1997), or in this thesis. The polymorphic strain CB4856 was used for single nucleotide polymorphism (SNP) mapping as described by Plasterk and co-workers (Wicks et al., 2001).

2.5.2 Light and fluorescent microscopy

Microscopic analysis of cells was done using standard live-animal techniques: worms were mounted on 4% agarose pad and anesthetized with 30 mM NaN_3 in M9 buffer. Observations were done using a Leica DM RXA2 microscope fitted with Nomarski optics. Images were captured with a ORCA-ER digital CCD camera (Hamamatsu) and processed with OpenLab software. Fluorescence stereomicroscopy was done with a Leica MZ FLIII or a Zeiss Stemi SV11 M^2BIO stereomicroscope.

2.5.3 Biolistic transformation

GFP::TEG-1 lines were constructed with pID3.01B_teg-1 (the original vector, pID3.01B, is a gift from Dr. Geraldine Seydoux, John Hopkins University). The plasmid contains a translational fusion of *gfp* (N-terminus) with the full-length genomic sequences of *teg-1* (ATG to stop codon). Cloning was performed using Gateway Cloning™ technology (Invitrogen) according to the protocol from the Seydoux laboratory. The plasmid also contains the rescuing *unc-119* genomic sequence from pDPMM016. The constructs was bombarded into *unc-119(ed3)* worms as previously described (Praitis et al., 2001). To obtain germline expression, 0.5 µg of DNA per bombardment was used. Integration of the construct was determined by loss of visible Unc-119 offspring.

2.5.5 Cloning

Cloning was performed according to standard molecular biology techniques described by Sambrook and Russel (Sambrook and Russell, 2001). Some ligation reactions were done using the Rapid DNA Ligation Kit (Roche). TOPO TA Cloning® and Gateway Cloning™ were performed according to the protocols provided by the manufacturer (Invitrogen).

2.5.6 Polymerase chain reaction (PCR)

PCR was performed using Biotaq DNA polymerase (Bioline), *Pfu Turbo* DNA polymerase (Stratagene), or the Expand High Fidelity PCR system (Roche) according to the manufacturers' protocols.

2.6 REFERENCES

Brenner, S. (1974). The genetics of *Caenorhabditis elegans*. Genetics *77*, 71-94.

Eckmann, C. R., Kraemer, B., Wickens, M., and Kimble, J. (2002). GLD-3, a bicaudal-C homolog that inhibits FBF to control germline sex determination in *C. elegans*. Dev Cell *3*, 697-710.

Fraser, A. G., Kamath, R. S., Zipperlen, P., Martinez-Campos, M., Sohrmann, M., and Ahringer, J. (2000). Functional genomic analysis of *C. elegans* chromosome I by systematic RNA interference. Nature *408*, 325-330.

Gumienny, T. L., Lambie, E., Hartwieg, E., Horvitz, H. R., and Hengartner, M. O. (1999). Genetic control of programmed cell death in the *Caenorhabditis elegans* hermaphrodite germline. Development *126*, 1011-1022.

Kamath, R. S., Fraser, A. G., Dong, Y., Poulin, G., Durbin, R., Gotta, M., Kanapin, A., Le Bot, N., Moreno, S., Sohrmann, M.*, et al.* (2003). Systematic functional analysis of the *Caenorhabditis elegans* genome using RNAi. Nature *421*, 231-237.

Lantz, V., Ambrosio, L., and Schedl, P. (1992). The Drosophila orb gene is predicted to encode sex-specific germline RNA-binding proteins and has localized transcripts in ovaries and early embryos. Development *115*, 75-88.

Lee, M. H., and Schedl, T. (2001). Identification of in vivo mRNA targets of GLD-1, a maxi-KH motif containing protein required for *C. elegans* germ cell development. Genes Dev *15*, 2408-2420.

Luitjens, C., Gallegos, M., Kraemer, B., Kimble, J., and Wickens, M. (2000). CPEB proteins control two key steps in spermatogenesis in *C. elegans*. Genes Dev *14*, 2596-2609.

Mendez, R., and Richter, J. D. (2001). Translational control by CPEB: a means to the end. Nat Rev Mol Cell Biol *2*, 521-529.

Praitis, V., Casey, E., Collar, D., and Austin, J. (2001). Creation of low-copy integrated transgenic lines in *Caenorhabditis elegans*. Genetics *157*, 1217-1226.

Riddle, D. L., Blumenthal, T., Meyer, B. J., and Priess, J. R. (1997). *C. elegans II*. Cold Spring Harbor Laboratory Press, Cold Spring Harbor, NY.

Sambrook, J., and Russell, D. W. (2001). Molecular Cloning - A Laboratory Manual. Cold Spring Harbor, NY: Cold Spring Harbor Laboratory Press.

Seydoux, G., Mello, C. C., Pettitt, J., Wood, W. B., Priess, J. R., and Fire, A. (1996). Repression of gene expression in the embryonic germ lineage of *C. elegans*. Nature *382*, 713-716.

Seydoux, G., and Schedl, T. (2001). The germline in *C. elegans*: origins, proliferation, and silencing. Int Rev Cytol *203*, 139-185.

Simmer, F., Tijsterman, M., Parrish, S., Koushika, S. P., Nonet, M. L., Fire, A., Ahringer, J., and Plasterk, R. H. (2002). Loss of the putative RNA-directed RNA polymerase RRF-3 makes *C. elegans* hypersensitive to RNAi. Curr Biol *12*, 1317-1319.

Stebbins-Boaz, B., Hake, L. E., and Richter, J. D. (1996). CPEB controls the cytoplasmic polyadenylation of cyclin, Cdk2 and c-mos mRNAs and is necessary for oocyte maturation in Xenopus. Embo J *15*, 2582-2592.

Sulston, J. E., and Hodgkin, J. (1988). Methods. In *The nematode Caenorhabditis elegans*. Cold Spring Harbor Laboratory, Cold Spring Harbor, NY, 587-606.

Tay, J., Hodgman, R., Sarkissian, M., and Richter, J. D. (2003). Regulated CPEB phosphorylation during meiotic progression suggests a mechanism for temporal control of maternal mRNA translation. Genes Dev *17*, 1457-1462.

Tay, J., and Richter, J. D. (2001). Germ cell differentiation and synaptonemal complex formation are disrupted in CPEB knockout mice. Dev Cell *1*, 201-213.

Wang, L., Eckmann, C. R., Kadyk, L. C., Wickens, M., and Kimble, J. (2002). A regulatory cytoplasmic poly(A) polymerase in *Caenorhabditis elegans*. Nature *419*, 312-316.

Wicks, S. R., Yeh, R. T., Gish, W. R., Waterston, R. H., and Plasterk, R. H. (2001). Rapid gene mapping in *Caenorhabditis elegans* using a high density polymorphism map. Nat Genet *28*, 160-164.

TABLE 2.1 SNP mapping for *gla-4(op199)*

	pkP1073 +17.4 cM	Y26D4[2] +17.4 cM	F22G12[1] +17.8 cM	ZK1225[1] +18.1 cM	ZK1053[2] +18.2 cM
CB4856 X *unc-101(m1) gla-4(op199)*					
	4/4	2/4	0/4	0/4	0/4
CB4856 X *gla-4(op199) unc-54(e1092)*					
	0/11	0/11	0/11	3/11	11/11

The Gla-4 non-Unc-101 recombinants and the Gla-4 non-Unc-54 recombinants determine the left and right boundaries of the genetic interval, respectively. Only the few informative recombinants for this interval are included. Numbers represent the fraction of worms that retains the CB4856(Hawaii)-specific allele.

TABLE 2.2 Candidate genes for *gla-4(op199)*

Gene	RNAi	Description[1]
Y26D4A.8	Y	Connect nuclear MT to spindle body assembly
Y26D4A.9	Y	Serpin domain
		DNA DSB repair rad50 ATPase
Y26D4A.10	N	
Y26D4A.11	N	Integrase and Chromo domain
C17H1.1	Y	
C17H1.2	Y	
C17H1.3	N	ER to Golgi transport
C17H1.4	Y	ER to Golgi transport
C17H1.5	Y	INCENP
		ER to Golgi transport
C17H1.6	Y	ER to Golgi transport
C17H1.7	Y	Caldesmon
		Enzyme that transfers mannosylphosphate to cell wall
C17H1.8	N	Translocation between nucleoplasm and NPC
F22G12.1	Y	ER to Golgi complex
		Myosin heavy chain
F22G12.2	N	Integrase domain, DNA recombination – binding
		POL polyprotein (RT)
		DNA-damage inducible, production or recovery of mutations
F22G12.3	Y	Cyclin-like F-box
F22G12.4	Y	Ank repeat, FYVE zinc finger
		Ankhzn protein – Mouse ES cells – endosomes
F22G12.5	Y	Pleckstrin homology domain (intracellular signaling or cytoskeleton)
F22G12.6	N	Ankhzn protein
F17B5.1	Y	Enzyme that transfers mannosylphosphate to cell wall
		Thioredoxin
F17B5.2	Y	Acetyltransferase domain, C-type lectin
F17B5.3	Y	C-type lectin, Beta and gamma crystalline
F17B5.4	Y	Galactoside 2-L-fucosyltransferase 1
F17B5.5	Y	C-type lectin
ZK1225.1	Y	DUF235

[1]As annotated in Wormbase. For the RNAi column, 'Y' indicates that RNAi knockdown of the gene was performed at 15°C, 20°C, and 25°C in a wild-type N2 background (P_o generation). 'N' indicates that the corresponding clone was not present in the Ahringer feeding library, or that sequencing revealed that it contained the wrong insert.

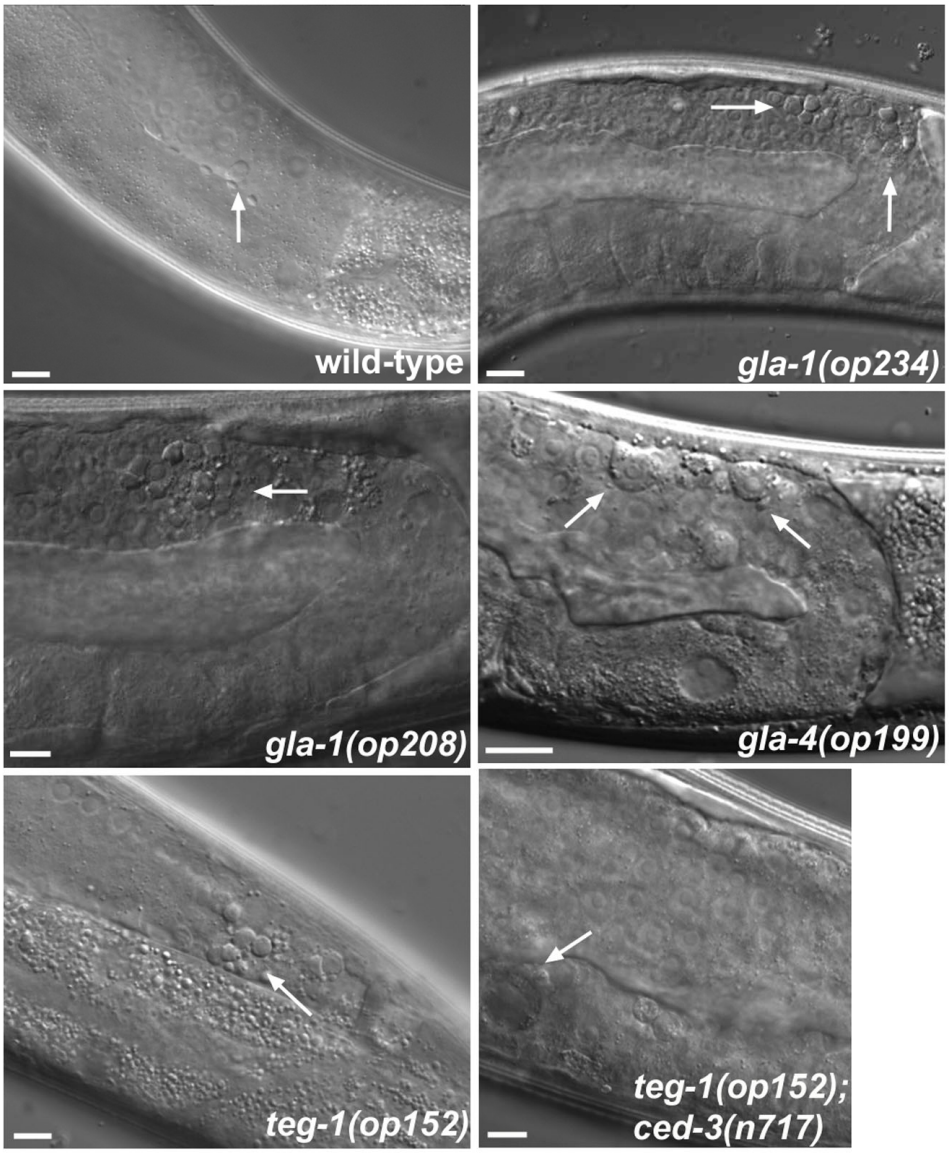

FIGURE 2.1 Phenotypes of Gla mutants

Mutants which are characterized by increased levels of germ cell death. DIC pictures of worms grown at 20°C (25°C for *teg-1*) were taken 24 hours post larval stage L4. Apoptotic germ cells can be seen as highly refractile disks (arrows). For the picture of *teg-1; ced-3* animal, the arrow indicates a necrotic vacuole. For all the pictures, anterior is to the left and dorsal to the top. Scale bar, 10 μm.

FIGURE 2.2 Cloning and characterization of *gla-1(op208)* (next page)

(a) Schematic diagram of the cloning strategy used to identify the *op208* locus. The main physical and molecular markers used are indicated. *gla-1/cpb-3* encodes a gene with six exons on chromosome I. It is transcribed from right to left along the chromosome.

(b) Partial alignment of the protein sequence of *C. elegans* GLA-1, *D. melanogaster* Orb, zebrafish ZOR-1, and mouse CPEB. The aligned region of the protein corresponds to part of the zinc finger. The *gla-1(op208)* and *gla-1(op234)* missense mutations, and the corresponding amino acid changes, are indicated.

(c) Time-course analysis of germ cell death in wild-type, *gla-1(op234)*, and *gla-1(op208)* mutants. Worms were synchronized and scored for germ cell apoptosis by DIC every 12 hours post L4 stage. Data shown represent mean ±s.d. of three experiments (n=20 gonads for each experiment).

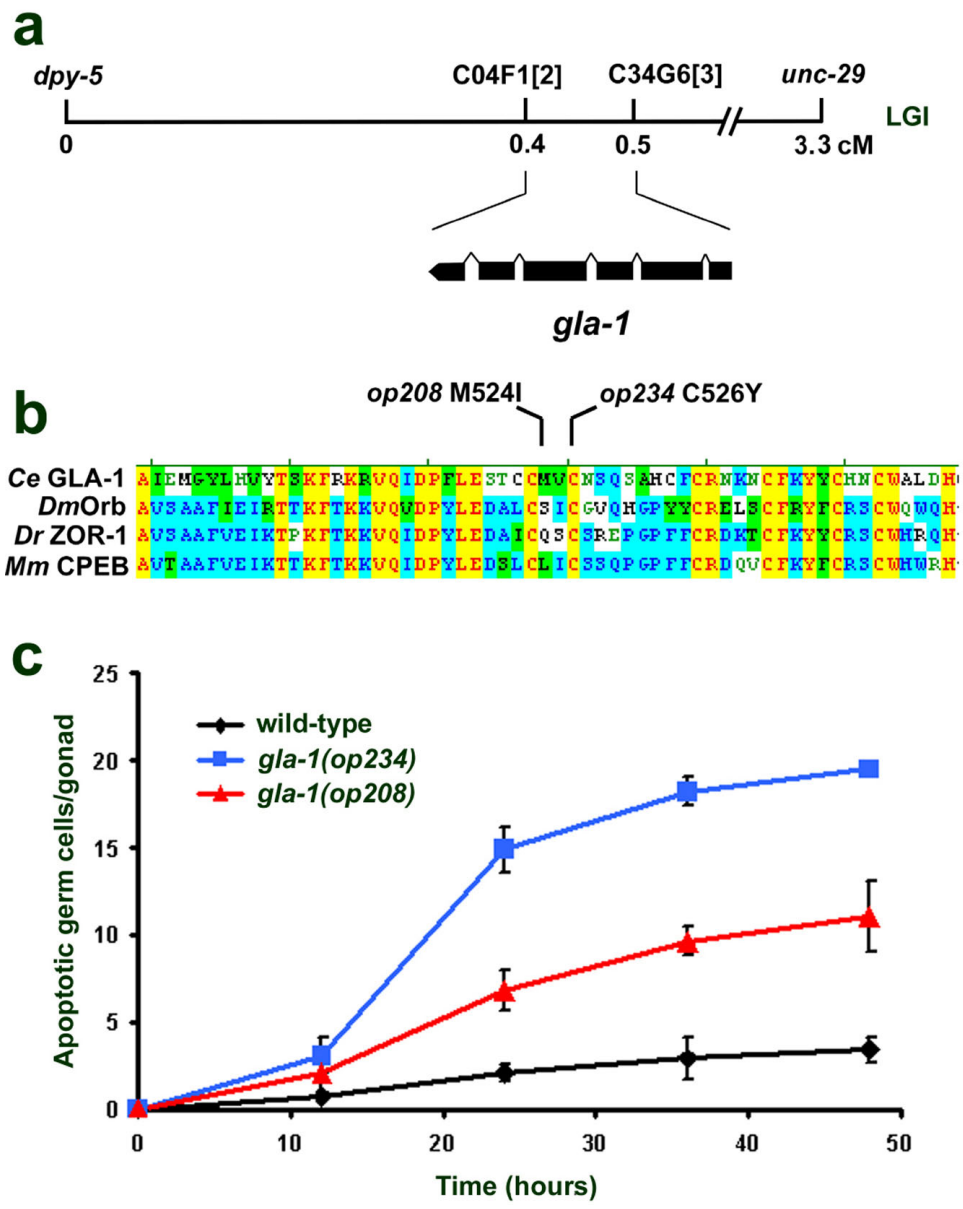
a
dpy-5
C04F1[2]
C34G6[3]
unc-29
LGI
0
0.4
0.5
3.3 cM
gla-1
b
op208 M524I
op234 C526Y
Ce GLA-1
DmOrb
Dr ZOR-1
Mm CPEB
c
wild-type
gla-1(op234)
gla-1(op208)
Apoptotic germ cells/gonad
Time (hours)
0
5
10
15
20
25
0
10
20
30
40
50

FIGURE 2.3 Cloning and characterization of *teg-1(op152)* (next page)

(a) Schematic diagram of the cloning strategy used to identify the *op152* locus. The main physical and molecular markers used are indicated. *teg-1* encodes a gene with six exons on chromosome III. It is transcribed from right to left along the chromosome.

(b) *op152* abrogates a *Hae*III restriction site in exon 3 of the *teg-1* locus. PCR amplification of exon 3 with specific primers (5'-ATTGAGCGTAGCATGAATTTTCTGG-3' and 5'-AAATTTCCGGTAAACCGACAATTGC-3') gives a 393 bp product. After restriction digest with *Hae*III and agarose gel electrophoresis, two bands are obtained from wild-type animals [246, 147 bp], three bands from heterozygote animals [393, 246, 147 bp], and one band from homozygote worms [393 bp]. Wild-type: N2 Bristol; Heterozygote: *teg-1(op152)/hT2[qIs48]*; Homozygote: *teg-1(op152)*. M: molecular weight marker.

(c) Time-course analysis of germ cell death in wild-type, *teg-1(op152)*, and *teg-1(op152); opIs115[*$P_{pie\text{-}1}$*::gfp::teg-1]* animals grown at 25^{o}C. Worms were synchronized and scored for germ cell apoptosis by DIC every 12 hours post L4 stage. For *teg-1(op152)* homozygotes, GFP negative progeny from *teg-1(op152)/hT2[qIs48]* heterozygote mothers were picked and scored. Data shown represent mean ±s.d. of two experiments (n=20 gonads for each experiment).

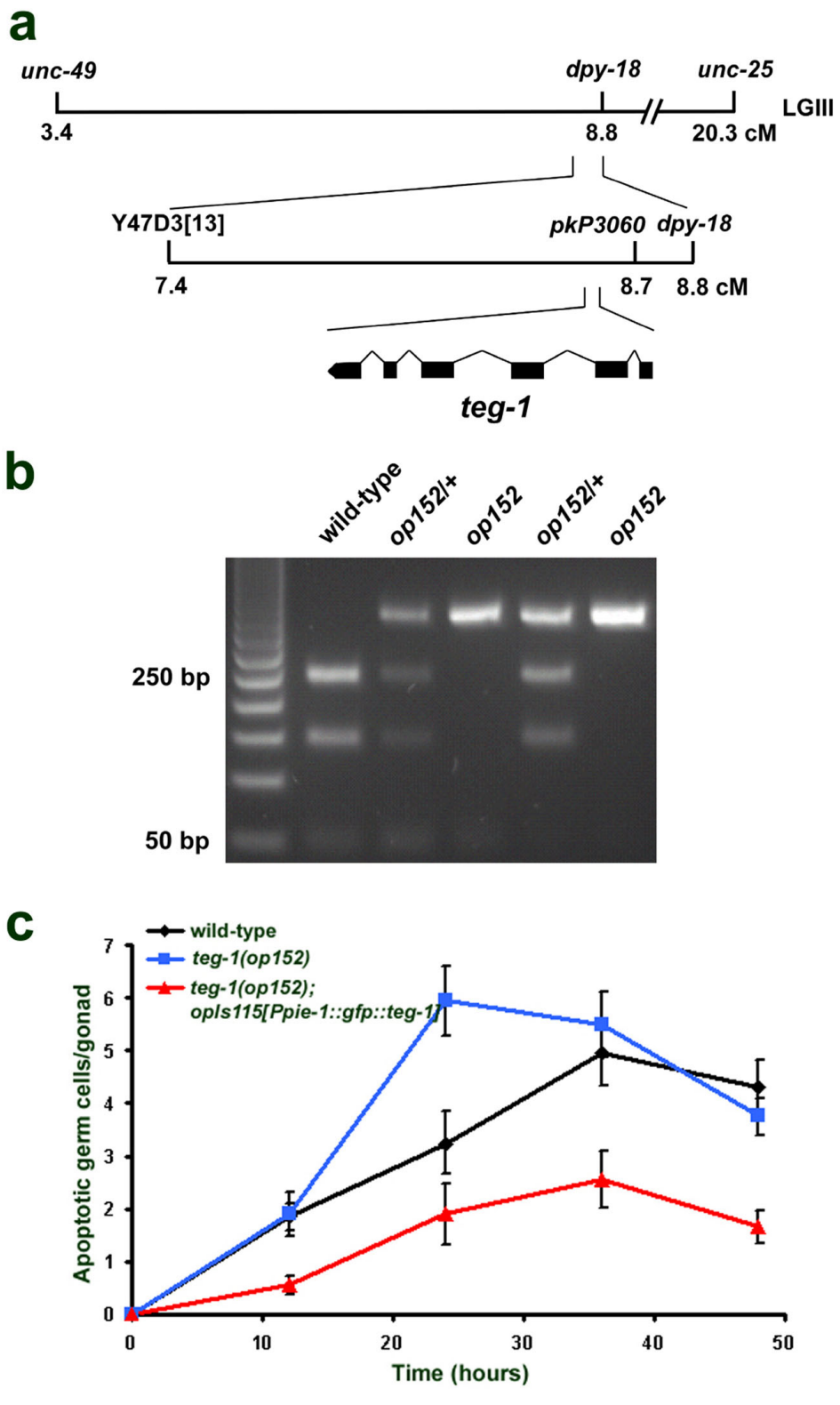
a
unc-49
dpy-18
unc-25
LGIII
3.4
8.8
20.3 cM
Y47D3[13]
pkP3060
dpy-18
7.4
8.7
8.8 cM
teg-1
b
wild-type
op152/+
op152
op152/+
op152
250 bp
50 bp
c
wild-type
teg-1(op152)
teg-1(op152);
opIs115[Ppie-1::gfp::teg-1]
Apoptotic germ cells/gonad
0
1
2
3
4
5
6
7
0
10
20
30
40
50
Time (hours)

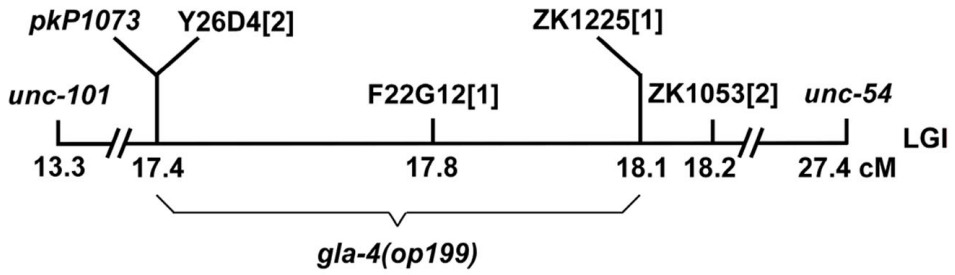

FIGURE 2.4 Molecular cloning of *gla-4(op199)*

Schematic diagram of the cloning strategy used to map *gla-4(op199)*. The main physical and molecular markers used are shown. The 0.7 cM (122 kb) interval where *gla-4(op199)* maps is indicated.

• CHAPTER 3 •

GENOME-WIDE RNAI IDENTIFIES P53-DEPENDENT AND -INDEPENDENT REGULATORS OF GERM CELL APOPTOSIS IN *C. ELEGANS*

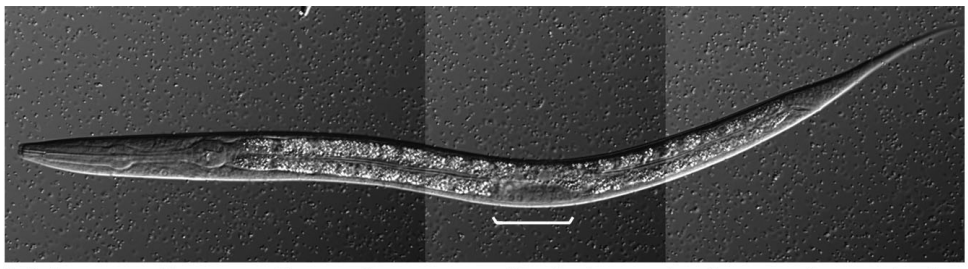

L2 larva - Separation of germ cells into anterior and posterior populations by the somatic gonad blast cells

• CHAPTER 3 •

GENOME-WIDE RNAI IDENTIFIES P53-DEPENDENT AND -INDEPENDENT REGULATORS OF GERM CELL APOPTOSIS IN *C. ELEGANS*

Reprinted by permission from Cell Death and Differentiation
Volume 11, Pages 1198-1203, November 2004

3.1 PREFACE

In this chapter, I described a functional genomics approach used by our laboratory to discover most of the worm genes that protect germ cell from undergoing apoptosis. We performed a genome-wide RNAi screen using the RNAi feeding library from the Ahringer laboratory and looked for gene knockdowns that cause a Gla phenotype, that is, increased *g*erm*l*ine *a*poptosis.

Dr. E. Kritikou and myself did most of the primary screen, with help from M. Jaeggi and A. Calixto for chromosome I. Dr. Kritikou and I did the secondary screen. I performed all the epistasis analysis presented in Table 1 of the article. Dr. Kritikou characterized the *bmk-1(ok391)* mutant, whereas I focused my work on the *pmk-3(ok169)* mutant. Extensive genetic characterization of the *pmk-3(lf)* phenotype will be given in chapter 4. I wrote the article, which was then edited by Dr. Kritikou and Professor M.O. Hengartner.

At the end of this chapter, I included Supplementary Table 3.1 and Supplementary Figure 3.1. Although not essential for the comprehension of the article, these data might be useful for future lab members.

Cell Death and Differentiation (2004) 11, 1198–1203

www.nature.com/cdd

Genome-wide RNAi identifies p53-dependent and -independent regulators of germ cell apoptosis in *C. elegans*

G Lettre[1,4], EA Kritikou[1,4], M Jaeggi[1], A Calixto[2], AG Fraser[3,5], RS Kamath[3], J Ahringer[3] and MO Hengartner*[,1]

[1] Institute for Molecular Biology, University of Zurich, Winterthurerstrasse 190, 8057 Zurich, Switzerland
[2] Department of Biological Sciences, Columbia University, 1012 Fairchild Center, 1212 Amsterdam Avenue, New York, NY 10027, USA
[3] Wellcome CRC Institute and Department of Genetics, University of Cambridge, Tennis Court Road, Cambridge CB2 IQR, UK
[4] G Lettre and EA Kritikou contributed to this work equally
[5] Current address: The Wellcome Trust Sanger Institute, Wellcome Trust Genome Campus, Hinxton, Cambridge CB10 1SA, UK
* Corresponding author: MO Hengartner, Institute for Molecular Biology, University of Zurich, Winterthurerstrasse 190, 8057 Zurich, Switzerland. Tel: +41-1-635-3140; Fax: +41-1-635-6861; E-mail: michael.hengartner@molbio.unizh.ch

Received 11.3.04; revised 18.5.04; accepted 03.6.04; published online 23.7.04
Edited by G Melino

Abstract

We used genome-wide RNA interference (RNAi) to identify genes that affect apoptosis in the *C. elegans* germ line. RNAi-mediated knockdown of 21 genes caused a moderate to strong increase in germ cell death. Genetic epistasis studies with these RNAi candidates showed that a large subset (16/21) requires p53 to activate germ cell apoptosis. Apoptosis following knockdown of the genes in the p53-dependent class also depended on a functional DNA damage response pathway, suggesting that these genes might function in DNA repair or to maintain genome integrity. As apoptotic pathways are conserved, orthologues of the worm germline apoptosis genes presented here could be involved in the maintenance of genomic stability, p53 activation, and fertility in mammals.
Cell Death and Differentiation (2004) **11,** 1198–1203.
doi:10.1038/sj.cdd.4401488
Published online 23 July 2004

Keywords: apoptosis; germline development; p53; RNAi; *C. elegans*

Abbreviations: AO, acridine orange; DIC, differential interference contrast; DTC, distal tip cell; *gf*, gain-of-function; *gla*, *g*erm*l*ine *a*poptosis; *lf*, loss-of-function; RNAi, RNA-mediated interference

Introduction

Apoptosis is a physiological mechanism by which unneeded, harmful, or damaged cells commit suicide. It plays an important role in development and homeostasis, and its misregulation has been associated with various pathologies.[1–3] Although we understand the molecular events occurring during apoptosis relatively well, less is known about the regulatory signals that trigger this cell fate.

Here we describe a systematic approach to identify new genes that regulate germ cell apoptosis in *Caenorhabditis elegans*. RNA interference (RNAi) was used to knockdown expression of 16 757 worm genes to find antiapoptotic factors that prevent excess germ cell death. Knockdown of 21 genes reproducibly resulted in a moderate to strong increase in germ cell apoptosis in wild-type animals. By epistasis analysis, we show that a large subset of our RNAi candidates require p53 and a functional DNA damage response pathway to activate germ cell apoptosis. Furthermore, we characterize mutations in two genes identified in our screen, *pmk-3* and *bmk-1*, and show that these mutants indeed have more germ cell deaths than wild-type worms. The identification of new *C. elegans* *g*erm*l*ine *a*poptosis (*gla*) genes, many of which have mammalian homologues, should shed light on the different pathways that regulate apoptosis during metazoan development.

Results

C. elegans hermaphrodites possess two U-shaped gonads connected at a common uterus (Figure 1a). Each gonad has a distal-to-proximal polarity, the most distal part being capped by the somatic distal tip cell (DTC). The DTC expresses a growth factor, LAG-2, which promotes the mitotic proliferation of the adjacent germ cells. In the distal arms, germ cell nuclei are not completely enclosed by membrane, and thus form a large syncytium. Nevertheless, because each nucleus acts independently of its neighbour, we will refer to these syncytial nuclei as germ cells. Once germ cells escape the influence of the DTC, they enter meiosis (transition zone in Figure 1a) and progress into the pachytene stage of meiosis I; exit from pachytene requires the activation of the RAS/MAPK pathway.[4,5] Germ cells can then further differentiate into oocytes, or die by apoptosis. Germ cell apoptosis depends on the caspase CED-3 and the Apaf-1 homologue CED-4, and is blocked by the Bcl-2-like protein CED-9.[6] Animals with a conditional loss-of-function (*lf*) mutation in *ced-9* have five times more apoptotic corpses in their germ line than wild-type worms.[6] This result can readily be phenocopied by inactivating *ced-9* with RNAi (Figure 1b).[7]

To identify other antiapoptotic genes, we inactivated 86% of the ~19 500 predicted *C. elegans* protein-coding genes using a RNAi feeding library.[8] To visualize apoptotic germ cells by fluorescent microscopy, the vital dye acridine orange (AO) was used. Ingestion of AO-stained *Escherichia coli* by *C. elegans* specifically labels engulfed apoptotic corpses in the germ line (Figure 1c).[6] Using this assay combined with the RNAi library, we identified 21 gene inactivations that cause a Gla phenotype, that is, more germ cell apoptosis than

observed in wild-type worms (Table 1). Sequence analysis of these candidates revealed that knockdown of a large variety of genes, belonging to several functional classes, induce germ cell apoptosis (Table 1; sequences can be retrieved at Wormbase; www.wormbase.org). Many of the genes identified in our screen encode proteins with known antiapoptotic functions in other systems, thereby validating our approach. For example, as has previously been shown,[9,10] we found that knocking down RAD50 or the RecA-like protein RAD51, two proteins involved in homologous recombination and DNA double-strand break repair, results in a Gla phenotype (Table 1). Similarly, mice carrying a mutation in either Rad50 or Rad51 show increased apoptosis.[11,12] Moreover, it has recently been reported that inactivation of the p53 inhibitor iASPP, and its worm counterpart *ape-1*, induces apoptosis in a p53-dependent manner.[13] We independently identified *ape-1* in our RNAi screen, and confirmed that its inactivation requires p53 to cause a Gla phenotype (Table 1 and see below).

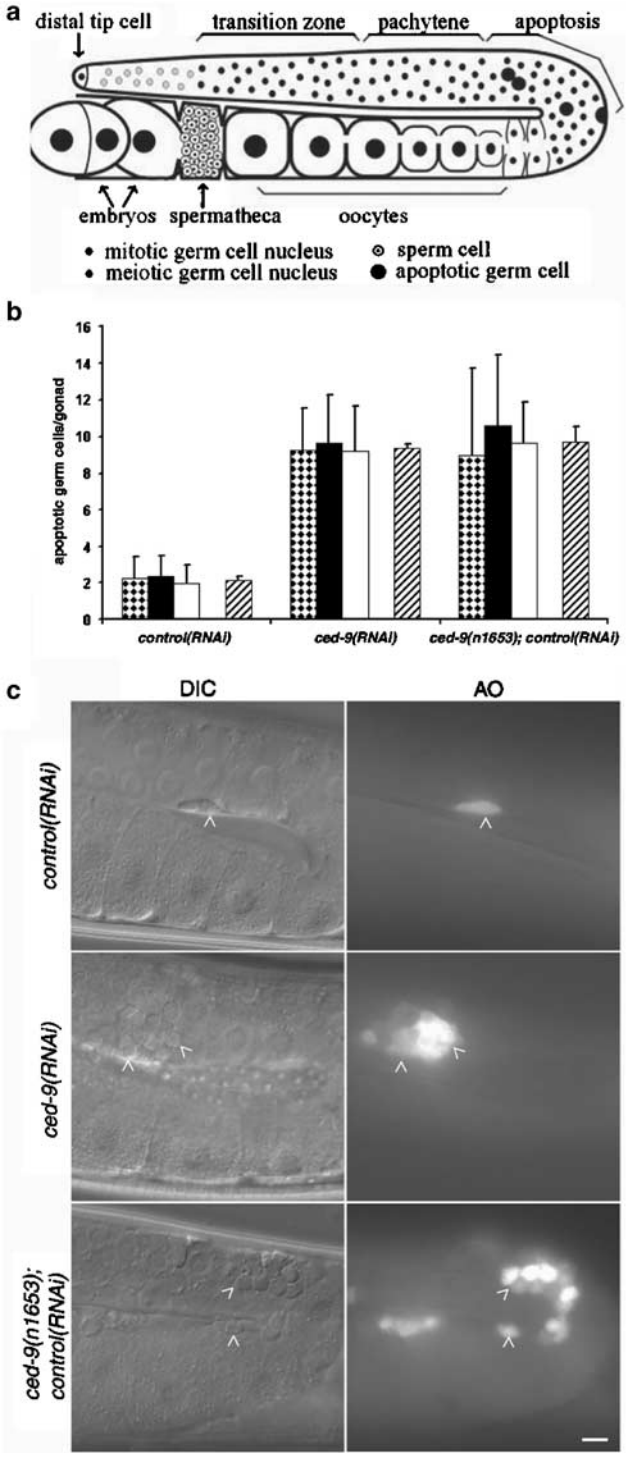

Why do so many different gene inactivations cause germ cell death? In an effort to address this issue, we performed epistasis analysis with our RNAi candidates. First, we showed that in all cases a strong *lf* mutation in the caspase *ced-3* completely suppresses the Gla phenotype, thus confirming the apoptotic nature of the cell deaths detected by AO and differential interference contrast (DIC) (Table 1). Apoptosis in the hermaphrodite *C. elegans* germ line can be triggered by genotoxic treatment, such as γ-irradiation.[10] It has been shown that these DNA damage-induced germ cell deaths are dependent on the worm p53 homologue *cep-1*[14,15] and the checkpoint gene *hus-1*.[16] To test if the gene candidates found in our screen activate the DNA damage response pathway, their expression was also inactivated by RNAi in *cep-1* and *hus-1* mutants. The basal level of germ cell death in these mutant backgrounds is lower than in wild-type worms (in Table 1, compare *control(RNAi)* for each mutant). The reason for this difference is unknown; one possibility is that in the absence of HUS-1 or CEP-1, endogenous DNA damage (e.g. aberrant meiotic intermediates) remains undetected and therefore cannot cause apoptosis. We found that *cep-1(lf)* and *hus-1(lf)* completely suppress the Gla phenotype of all but five genes, suggesting that p53 is a key sensor of germ cell stresses in *C. elegans* and that many of our RNAi candidates indirectly affect germ cell apoptosis through the activation of quality control checkpoint pathways (Table 1).[16,17] For the five gene knockdowns that are not suppressed by *cep-1* or *hus-1*, a reduction in the number of apoptotic germ cells was observed in comparison to wild-type worms (Table 1, p53-independent class). As already mentioned, these mutant strains have initially less germ cell deaths than the wild-type strain; this could explain the differences observed. Epistasis analysis with *ced-9(gf)*, a mutation that completely blocks *cep-1*-dependent germ cell death, but does not affect physiological germline apoptosis,[6,10] confirmed the above results (Table 1).

Figure 1 RNAi and acridine orange can be combined for a high-throughput, genome-wide screen for apoptotic germ cell death. (**a**) Schematic diagram of an adult hermaphrodite *C. elegans* gonad. Apoptotic cells are normally observed at and distal to the bend. (**b**) Knockdown of *ced-9* by RNAi can phenocopy a conditional loss-of-function mutation in *ced-9*. For each genotype, three independent experiments are shown; the checked, black, and white bars represent mean $\pm$ S.D. for each individual experiment ($n = 20$ gonads), whereas the dashed bars represent mean $\pm$ S.D. of the three experiments. See Materials and methods for a description of the statistics used in this study. (**c**) Left column shows representative pictures of a gonad after RNAi feeding observed by differential interference contrast (DIC) microscopy. Apoptotic germ cells can be seen as highly refractile disks (arrowheads). Right column shows that acridine orange (AO) stains specifically apoptotic corpses in the germ line. For all the pictures, anterior is to the left and dorsal to the top. Scale bar, 8 μm

Table 1 Gene candidates that increase germline apoptosis following RNAi

Gene(*locus*)	Description[a]	Germ cell deaths per gonad[b]				
		wild-type (*t*-test)	*ced-3(lf)*	*cep-1(lf)* (*t*-test)	*hus-1(lf)* (*t*-test)	*ced-9(gf)* (*t*-test)
Control	Vector+*gfp*	2.2±0.2	0	1.5±0.2	1.0±0.1	1.5±0.2
p53-independent						
T07C4.8(*ced-9*)	Bcl-2 homologue	9.4±0.2 (*P*=1.2E-41)	0	5.1±0.7 (*P*=3.7E-11)	6.0±1.8 (*P*=2.4E-19)	5.9±0.6 (*P*=1.2E-13)
T02E1.3a	Zinc-finger domain, TIS11 family	9.1±1.1 (*P*=4.5E-26)	0	5.7±0.6 (*P*=3.4E-12)	4.6±0.2 (*P*=5.2E-22)	5.2±0.7 (*P*=1.7E-12)
B0414.5(*cpb-3*)	RNA-binding protein, CPEB family	8.7±0.5 (*P*=4.4E-28)	0	6.1±0.4 (*P*=3.6E-14)	6.2±2.5 (*P*=2.4E-21)	5.2±1.5 (*P*=1.0E-9)
R05D3.4	RING domain	8.0±1.4 (*P*=2.0E-18)	0	5.1±1.9 (*P*=6.1E-10)	4.8±0.6 (*P*=7.2E-26)	7.4±1.7 (*P*=1.5E-15)
F42G8.4(*pmk-3*)	p38 MAPK	4.1±1.7 (*P*=3.5E-6)	0	2.3±0.2 (*P*=0.003)	2.3±0.3 (*P*=1.2E-8)	3.0±0.3 (*P*=1.4E-5)
p53-dependent						
Y43C5A.6(*rad-51*)	DNA repair protein RAD51 homologue	7.9±1.2 (*P*=1.8E-30)	0	1.4±0.2 (*P*=0.24)	1.1±0.1 (*P*=0.28)	1.4±0.3 (*P*=0.43)
F23B12.8(*bmk-1*)	BimC kinesin-like homologue	4.4±1.1 (*P*=1.7E-11)	0	1.3±0.1 (*P*=0.24)	1.4±0.6 (*P*=0.04)	1.8±0.8 (*P*=0.20)
C16C8.14	Ubiquitin domain-containing protein	4.0±0.9 (*P*=3.8E-8)	0	1.5±0.3 (*P*=0.46)	1.4±0.4 (*P*=0.03)	2.1±0.1 (*P*=0.015)
Y38H6C.17	Amino acid/polyamine transporter	3.9±0.6 (*P*=2.0E-9)	0	1.6±0.3 (*P*=0.28)	1.4±0.1 (*P*=0.03)	2.4±0.3 (*P*=0.005)
K02F3.5	bZIP transcription factor	3.9±0.8 (*P*=6.9E-9)	0	1.3±0.4 (*P*=0.29)	1.6±0.5 (*P*=0.002)	2.0±0.3 (*P*=0.07)
T04H1.4(*rad-50*)	DNA repair protein RAD50 homologue	3.8±0.1 (*P*=1.1E-9)	0	1.4±0.2 (*P*=0.43)	1.0±0.1 (*P*=0.40)	1.5±0.4 (*P*=0.44)
F38H12.3	Nuclear hormone receptor	3.8±0.4 (*P*=5.2E-8)	0	1.7±0.5 (*P*=0.18)	1.1±0.3 (*P*=0.34)	1.4±1.0 (*P*=0.41)
Y23H5A.2	Novel	3.8±0.9 (*P*=8.0E-7)	0	1.4±0.2 (*P*=0.42)	1.2±0.5 (*P*=0.28)	2.4±0.0 (*P*=0.013)
F46F3.4(*ape-1*)	p53-binding protein (iASPP) like	3.7±0.6 (*P*=2.3E-7)	0	1.5±0.0 (*P*=0.47)	1.3±0.4 (*P*=0.09)	1.9±0.3 (*P*=0.11)
H06H21.9	PDZ/DHR/GLGF domain	3.5±1.2 (*P*=4.5E-6)	0	1.5±0.3 (*P*=0.46)	1.1±0.6 (*P*=0.30)	1.9±0.1 (*P*=0.15)
R11G11.7(*pqn-60*)	Glutamine/asparagines-rich domain, DUF148	3.5±0.4 (*P*=6.6E-7)	0	1.6±0.7 (*P*=0.32)	1.3±0.1 (*P*=0.08)	1.6±0.6 (*P*=0.35)
R03D7.6(*gst-5*)	Glutathione *S*-transferase	3.5±0.7 (*P*=4.8E-6)	0	1.1±0.1 (*P*=0.05)	1.2±0.1 (*P*=0.23)	1.4±0.3 (*P*=0.35)
F28A10.1	DUF13	3.5±0.9 (*P*=4.1E-5)	0	1.4±0.1 (*P*=0.42)	1.3±0.5 (*P*=0.05)	1.4±0.2 (*P*=0.39)
K02F2.6(*ser-3*)	Rhodopsin-like GPCR	3.4±1.2 (*P*=3.6E-5)	0	1.4±0.0 (*P*=0.46)	1.3±0.0 (*P*=0.05)	1.7±0.0 (*P*=0.24)
F29F11.2	UDP-glucoronosyltransferase	3.4±0.6 (*P*=6.7E-5)	0	1.9±0.6 (*P*=0.08)	1.4±0.2 (*P*=0.08)	1.8±0.2 (*P*=0.10)
K11D12.6	Trypsin inhibitor domain	3.4±0.3 (*P*=6.0E-5)	0	1.7±0.4 (*P*=0.21)	1.4±0.7 (*P*=0.02)	2.0±0.6 (*P*=0.05)

[a]As annotated in Wormbase. [b]Synchronized L1 worms were fed dsRNA-expressing bacteria until 24 h post-L4 stage, and then scored using DIC microscopy for a germline apoptosis phenotype. Data shown are mean number of apoptotic corpses per gonad±S.D. of three independent experiments for wild-type, two experiments for *cep-1(lf)*, *hus-1(lf)*, and *ced-9(gf)*, and one experiment for *ced-3(lf)* ($n=20$ gonads for each experiment). Wild-type: N2; *ced-3(lf)*: *ced-3(n717); cep-1(lf)*: *cep-1(gk138); hus-1(lf)*: *hus-1(op244); ced-9(gf)*: *ced-9(n1950)*. *t*-test values were obtained by comparing the number of germ cell corpses in each experimental group with the respective *control(RNAi)* group

As RNAi does not always faithfully reproduce the known *lf* phenotypes, we sought to confirm our RNAi results with genetic mutants. As a first step towards this aim, we obtained and characterized deletion alleles for two of our RNAi candidates, *pmk-3* and *bmk-1*. Neither mutant has any obvious growth defects (data not shown),[18] but both *pmk-3(lf)* and *bmk-1(lf)* mutants displayed an increased number of germ cell corpses when compared with wild-type worms (Figure 2a). PMK-3 is one of the three p38 MAPK isoforms in *C. elegans*, which are all present on the same operon.[18] The worm p38 PMK-1 has been implicated in stress responses and innate immunity, whereas the role of PMK-2 and PMK-3 is still unclear.[18–20] Contrary to the *pmk-3(lf)* Gla phenotype, knockdown of either *pmk-1* or *pmk-2* does not increase germ cell death (Figure 2b), suggesting a specific involvement of the PMK-3 isoform of p38 in the protection against germ cell apoptosis. *bmk-1* encodes a *C. elegans* homologue of the BimC kinesin-like motor protein involved in spindle formation.[21] Double-mutant analysis revealed that *ced-3* is epistatic to both *pmk-3* and *bmk-1* (Figure 2b). In contrast, *cep-1(lf)*,

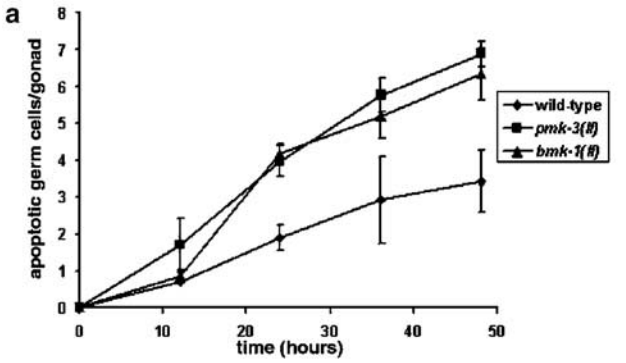

b

Genotype	Germ cell deaths per gonad[1]
wild-type	1.9±0.6
pmk-3(lf)	4.0±0.2
bmk-1(lf)	4.5±0.5
ced-3(lf)	0
pmk-3(lf) ced-3(lf)	0
ced-3(lf); bmk-1(lf)	0
cep-1(lf)	1.2±0.4
cep-1(lf); pmk-3(lf)	3.7±0.6
cep-1(lf); bmk-1(lf)	1.3±0.6
hus-1(lf)	1.0±0.1
hus-1(lf); pmk-3(lf)	3.4±0.2
hus-1(lf); bmk-1(lf)	1.4±0.2
ced-9(gf)	1.4±0.3
ced-9(gf); pmk-3(lf)	3.3±0.1
ced-9(gf); bmk-1(lf)	1.1±0.2
pmk-1(RNAi)	1.7±0.2
pmk-2(RNAi)	1.7±0.2

[1]Data shown are mean number of apoptotic corpses per gonad ±s.d. of 3 independent experiments (n=20 gonads for each experiment). Wild-type: N2. *pmk-3(lf)*: *pmk-3(ok169)*. *bmk-1(lf)*: *bmk-1(ok391)*. *ced-3(lf)*: *ced-3(n717)*. *cep-1(lf)*: *cep-1(gk138)*. *hus-1(lf)*: *hus-1(op244)*. *ced-9(gf)*: *ced-9(n1950)*.

Figure 2 *pmk-3(ok169)* and *bmk-1(ok391)* mutants exhibit a Gla phenotype. (**a**) Time-course of germ cell death in *pmk-3(ok169)* and *bmk-1(ok391)* mutants. Worms were synchronized and scored for germ cell apoptosis by DIC every 12 h post-L4 stage. Data shown represent mean ± S.D. of three experiments ($n = 20$ gonads for each experiment). (**b**) *ced-3(lf)* prevents germ cell death in *pmk-3* and *bmk-1* mutants, whereas *cep-1(lf)*, *hus-1(lf)*, and *ced-9(gf)* block only *bmk-1(lf)*-induced germ cell death. Worms were scored 24 h post-L4 stage

hus-1(lf), and *ced-9(gf)* abrogated *bmk-1(lf)*-induced germ cell death, but not the Gla phenotype of *pmk-3(lf)* worms (Figure 2b). These results corroborate our RNAi data (Table 1), and imply that loss of *bmk-1* activates p53-dependent germ cell death, whereas *pmk-3* acts in a p53-independent germ cell apoptotic pathway.

Discussion

In this paper, we describe the results of a genome-wide RNAi screen for genes that affect apoptosis in the *C. elegans* adult hermaphrodite germ line. We identified 21 genes that reproducibly induce germ cell death when knocked down by RNAi, confirmed that the additional germ cell deaths were apoptotic in nature, and used various cell death mutants to determine which death-inducing pathways were activated in each case.

Interestingly, knockdown of most of the genes identified in our screen appears to cause germ cell death indirectly, through activation of p53-dependent checkpoint or quality control mechanisms. The *C. elegans* p53 protein CEP-1 has been shown to participate in a conserved signalling pathway in response to DNA damage,[16] suggesting that at least some of these *gla* genes will be involved in the maintenance of genome stability. Consistent with this hypothesis, the p53-dependent class contains genes such as *rad-50* and *rad-51*, which are required for DNA repair and meiotic recombination, as well as genes predicted to protect from reactive oxygen species, such as *gst-5*.

We also identified in our screen *ape-1*, the worm orthologue of the p53-binding protein iASPP. Mammalian iASPP is the most phylogenetically conserved inhibitor of p53 identified so far.[13] It has been proposed that the primary function of iASPP is to inhibit the proapoptotic activity of p53 in the absence of genotoxic stress. As previously reported,[13] we found that *ape-1(RNAi)* induces germ cell apoptosis in a p53-dependent manner, consistent with the hypothesis that *C. elegans* iASPP APE-1 might also act as a p53 inhibitor by binding and regulating CEP-1's pro-apoptotic function. However, we found that *ape-1(RNAi)* resulted in *cep-1*-dependent apoptosis only in the presence of a functional upstream DNA damage response pathway (Table 1). This indicates that releasing CEP-1 from APE-1 inhibition is not sufficient by itself to trigger p53-dependent germ cell death. It is possible that effective activation of the apoptotic response might require not only release from APE-1, but also modification of CEP-1 by checkpoint regulators of the DNA damage response pathway. Further genetic and biochemical analysis is clearly required in order to understand the role of *C. elegans* iASPP in regulating p53-mediated apoptosis.

In mammals, p53 has been shown to mediate apoptosis in response not only to DNA damage, but also other stresses, such as oncogene activation and hypoxia.[22] In contrast, we have been unable so far to identify a DNA damage-independent death pathway for CEP-1 in *C. elegans*: all the *cep-1*-dependent RNAi candidates that we report here also showed a significantly reduced Gla phenotype in animals mutant for the gene *hus-1* (Table 1), which acts early in the DNA damage response pathway. We suspect that the ability of p53 to respond to oncogene activation might be a more recent evolution than its ability to respond to DNA damage, as tumour development is not much of a threat for simple, short-lived invertebrates such as *C. elegans*. Alternatively, our screen might simply have been unable to generate stresses that activate other p53-dependent pathways.

Our screen led to the identification of a small number of genes that, upon knockdown, induce germ cell apoptosis in a p53-independent manner. One of these, *ced-9*, encodes the *C. elegans* homologue of mammalian Bcl-2.[23] CED-9 acts downstream of p53 in the regulation of germ cell apoptosis,[16] readily explaining the observed epistasis. The mechanism of action of the other four genes – two predicted RNA-binding proteins, a p38 MAPK, and the *C. elegans* homologue of the *S. cerevisiae* Ring-finger protein Bre1p– is more obscure. We have previously shown that about half of all potential oocytes undergo apoptosis in the adult *C. elegans* germ line, and have suggested that many of these deaths serve a homeostatic function: to eliminate nuclei that served transiently as nurse cells and thereby reduce the nuclear/cytoplasmic ratio of the

mature syncytial gonad.[6] It is tempting to suggest that these four genes function in the regulation of this physiological germ cell death process. Alternatively, knockdown of these four genes might simply activate another, p53-independent quality control pathway that results in germ cell apoptosis.

Did our screen identify all the genes that can induce germ cell death upon inactivation? Most certainly not. First, the RNAi collection we used contained only about 85% of all predicted *C. elegans* genes. Thus, about a seventh of the *C. elegans* genome was not tested in our screen. Second, because of the intrinsic variability and limited efficiency of RNAi,[24] we likely missed a significant number of positive genes in our primary and secondary screens due to false negative results. Third, the particular feeding protocol used in our screen (feeding of P_o L1 larvae, screening of P_o adults) would have precluded us from identifying any genes that are required not only for germ cell survival but also for larval growth, as well as genes that need to be fed for more than one generation for the RNAi phenotype to become evident.

Indeed, we recovered in our screen only a fraction of the genes previously described to affect germ cell apoptosis. For example, we identified only two of the more than 12 DNA damage response genes previously shown to induce germ cell apoptosis upon RNAi-mediated knockdown.[9,10,25,26] However, many of these genes needed to be fed for several generations at high dsRNA concentrations for the apoptosis phenotype to become evident. We also failed to identify in our screen *daz-1* and the ste13/ME31B/RCK/p54 homologue *cgh-1*; both genes have been shown to induce germ cell apoptosis through as yet unknown mechanisms upon inactivation.[27,28] We did however identify in our screen CPB-3, one of four *C. elegans* CPEB family members. In clam and Xenopus oocytes, CPEB has been shown to interact functionally and physically with p47/p54, the orthologue of *C. elegans* CGH-1.[29] Whether CPB-3 and CGH-1 also interact in *C. elegans*, and whether they cooperate to control germ cell apoptosis, possibly by regulating the translation of mRNA targets, remains to be determined.

Previous genome-wide RNAi screens in *C. elegans* have been used to determine new gene functions[8,24] as well as to identify genes involved in body fat regulation[30] and genome stability.[31,32] Our results demonstrate that systematic RNAi screens can also successfully be used to identify genes that affect apoptosis. Indeed, based on our RNAi data, we identified two new genetic mutants that have excess germ cell death, confirming our reverse genomic approach. Further analysis of the apoptotic genes identified in our screen will provide useful genetic entry points into the study of mechanisms that control germ cell survival, genomic stability and of the genetic networks that regulate p53 activation.

Materials and Methods

Strains

C. elegans was cultivated using standard methods.[33] All strains were grown at 20°C. The strains used in this study were the following: wild-type N2 Bristol, *hus-1(op244)*, *cep-1(gk138)*, *ced-9(n1653)*, *ced-9(n1950gf)*, *pmk-3(ok169)*, *ced-3(n717)*, *bmk-1(ok391)*. *ok169* and *ok391* were backcrossed to the wild-type strain three times before phenotypical analysis. The deletion alleles were detected by PCR using the following primer sequences: for *ok169* 5′-CCCATTTTTCACTGCGTCTCAATCG-3′ and 5′-TCTGCTTCTCCAGGGATTAACGGTG-3′, and for *ok391* 5′-ATTTGCTGCGAACCTTGACT-3′ and 5′-GCCGCGAATCATTGTATTTC-3′.

RNAi germ cell apoptosis screen

We carried out RNAi as described.[34] In total, 30–50 synchronized L1 worms were placed on NGM agarose plates seeded with *E. coli* producing double-stranded RNA (dsRNA). Worms were grown for 3 days, then stained for 1 h in the dark by adding 500 μl of M9 buffer containing AO (Molecular Probes; 0.02 mg/ml) to the plate. Worms were then transferred to fresh agar plates, and allowed to destain for 1 h in the dark. AO staining was assessed by fluorescent microscopy. RNAi candidates that induced a Gla phenotype were tested again in duplicate. The presence of increased germ cell corpses was confirmed by Nomarski optics 24 h post-L4 stage. For all clones that produced a Gla phenotype, plasmids were isolated and the DNA sequence encoding the dsRNA was sequenced to confirm the identity of the inactivated gene.

Statistical analysis

In Figure 1b, the checked, black, and white bars represent mean $\pm$S.D. for each experiment ($n=20$ gonads), to illustrate variation within each experiment. The dashed bar represent mean $\pm$S.D. for the three experiments, to illustrate variation amongst experiments. This latter statistical representation is also used in Table 1 and Figure 2. Genes were considered to cause increased cell death only if they reproducibly caused significant increases in germ cell apoptosis (cutoff for inclusion in Table 1 was $P<0.0001$ *versus* wild-type). In Table 1, the cutoff value to establish epistatic groups was chosen as $P<0.001$ (RNAi *versus* respective mutant control). Although the *P*-value for *cep-1(gk138); pmk-3(RNAi)* ($P=0.003$) is above the cutoff value, we decided to group *pmk-3* into the p53-independent class based on the clear phenotype of the double mutant (Figure 2b).

Acknowledgements

We thank the *C. elegans* Gene Knockout Consortium and the *Caenorhabditis* Genetics Center, which is supported by NIH's National Center for Research Resources, for providing *cep-1(gk138)*, *pmk-3(ok169)*, and *bmk-1(ok391)* mutant strains. We thank A Hajnal and ER Hofmann for critical reading of the manuscript, and members of the Hengartner lab for comments. This work was supported by a grant from the Swiss National Science Foundation, the Josef Steiner Foundation, the Ernst Hadorn Foundation, and NIH grant GM52240. G Lettre is supported by a fellowship from the Fonds Québécois de la Recherche sur la Nature et les Technologies.

References

1. Hanahan D and Weinberg RA (2000) The hallmarks of cancer. Cell 100: 57–70
2. Meier P, Finch A and Evan G (2000) Apoptosis in development. Nature 407: 796–801
3. Yuan J and Yankner BA (2000) Apoptosis in the nervous system. Nature 407: 802–809
4. Hubbard EJ and Greenstein D (2000) The *Caenorhabditis elegans* gonad: a test tube for cell and developmental biology. Dev. Dyn. 218: 2–22

5. Seydoux G and Schedl T (2001) The germline in *C. elegans*: origins, proliferation, and silencing. Int. Rev. Cytol. 203: 139–185
6. Gumienny TL, Lambie E, Hartwieg E, Horvitz HR and Hengartner MO (1999) Genetic control of programmed cell death in the *Caenorhabditis elegans* hermaphrodite germline. Development 126: 1011–1022
7. Fraser AG, James C, Evan GI and Hengartner MO (1999) *Caenorhabditis elegans* inhibitor of apoptosis protein (IAP) homologue BIR-1 plays a conserved role in cytokinesis. Curr. Biol. 9: 292–301
8. Kamath RS, Fraser AG, Dong Y, Poulin G, Durbin R, Gotta M, Kanapin A, Le Bot N, Moreno S, Sohrmann M, Welchman DP, Zipperlen P and Ahringer J (2003) Systematic functional analysis of the *Caenorhabditis elegans* genome using RNAi. Nature 421: 231–237
9. Boulton SJ, Gartner A, Reboul J, Vaglio P, Dyson N, Hill DE and Vidal M (2002) Combined functional genomic maps of the *C. elegans* DNA damage response. Science 295: 127–131
10. Gartner A, Milstein S, Ahmed S, Hodgkin J and Hengartner MO (2000) A conserved checkpoint pathway mediates DNA damage-induced apoptosis and cell cycle arrest in *C. elegans*. Mol. Cell 5: 435–443
11. Lim DS and Hasty P (1996) A mutation in mouse rad51 results in an early embryonic lethal that is suppressed by a mutation in p53. Mol. Cell. Biol. 16: 7133–7143
12. Bender CF, Sikes ML, Sullivan R, Huye LE, Le Beau MM, Roth DB, Mirzoeva OK, Oltz EM and Petrini JH (2002) Cancer predisposition and hematopoietic failure in Rad50(S/S) mice. Genes Dev. 16: 2237–2251
13. Bergamaschi D, Samuels Y, O'Neil NJ, Trigiante G, Crook T, Hsieh JK, O'Connor DJ, Zhong S, Campargue I, Tomlinson ML, Kuwabara PE and Lu X (2003) iASPP oncoprotein is a key inhibitor of p53 conserved from worm to human. Nat. Genet. 33: 162–167
14. Derry WB, Putzke AP and Rothman JH (2001) *Caenorhabditis elegans* p53: role in apoptosis, meiosis, and stress resistance. Science 294: 591–595
15. Schumacher B, Hofmann K, Boulton S and Gartner A (2001) The *C. elegans* homolog of the p53 tumor suppressor is required for DNA damage-induced apoptosis. Curr. Biol. 11: 1722–1727
16. Hofmann ER, Milstein S, Boulton SJ, Ye M, Hofmann JJ, Stergiou L, Gartner A, Vidal M and Hengartner MO (2002) *Caenorhabditis elegans* HUS-1 is a DNA damage checkpoint protein required for genome stability and EGL-1-mediated apoptosis. Curr. Biol. 12: 1908–1918
17. Hofmann ER, Milstein S and Hengartner MO (2000) DNA-damage-induced checkpoint pathways in the nematode *Caenorhabditis elegans*. Cold Spring Harb. Symp. Quant. Biol. 65: 467–473
18. Berman K, McKay J, Avery L and Cobb M (2001) Isolation and characterization of *pmk-(1–3)*: three p38 homologs in *Caenorhabditis elegans*. Mol. Cell. Biol. Res. Commun. 4: 337–344
19. Aballay A, Drenkard E, Hilbun LR and Ausubel FM (2003) *Caenorhabditis elegans* innate immune response triggered by *Salmonella enterica* requires intact LPS and is mediated by a MAPK signaling pathway. Curr. Biol. 13: 47–52
20. Kim DH, Feinbaum R, Alloing G, Emerson FE, Garsin DA, Inoue H, Tanaka-Hino M, Hisamoto N, Matsumoto K, Tan MW and Ausubel FM (2002) A conserved p38 MAP kinase pathway in *Caenorhabditis elegans* innate immunity. Science 297: 623–626
21. Kashina AS, Rogers GC and Scholey JM (1997) The bimC family of kinesins: essential bipolar mitotic motors driving centrosome separation. Biochim. Biophys. Acta. 1357: 257–271
22. Pluquet O and Hainaut P (2001) Genotoxic and non-genotoxic pathways of p53 induction. Cancer Lett. 174: 1–15
23. Hengartner MO and Horvitz HR (1994) *C. elegans* cell survival gene *ced-9* encodes a functional homolog of the mammalian proto-oncogene bcl-2. Cell 76: 665–676
24. Simmer F, Moorman C, Van Der Linden AM, Kuijk E, Van Den Berghe PV, Kamath R, Fraser AG, Ahringer J and Plasterk RH (2003) Genome-wide RNAi of *C. elegans* using the hypersensitive *rrf-3* strain reveals novel gene functions. PLoS Biol. 1: E12
25. Chin GM and Villeneuve AM (2001) *C. elegans mre-11* is required for meiotic recombination and DNA repair but is dispensable for the meiotic G(2) DNA damage checkpoint. Genes. Dev. 15: 522–534
26. Boulton SJ, Martin JS, Polanowska J, Hill DE, Gartner A and Vidal M (2004) BRCA1/BARD1 orthologs required for DNA repair in *Caenorhabditis elegans*. Curr. Biol. 14: 33–39
27. Karashima T, Sugimoto A and Yamamoto M (2000) *Caenorhabditis elegans* homologue of the human azoospermia factor DAZ is required for oogenesis but not for spermatogenesis. Development 127: 1069–1079
28. Navarro RE, Shim EY, Kohara Y, Singson A and Blackwell TK (2001) *cgh-1*, a conserved predicted RNA helicase required for gametogenesis and protection from physiological germline apoptosis in *C. elegans*. Development 128: 3221–3232
29. Minshall N, Thom G and Standart N (2001) A conserved role of a DEAD box helicase in mRNA masking. RNA 7: 1728–1742
30. Ashrafi K, Chang FY, Watts JL, Fraser AG, Kamath RS, Ahringer J and Ruvkun G (2003) Genome-wide RNAi analysis of *Caenorhabditis elegans* fat regulatory genes. Nature 421: 268–272
31. Pothof J, van Haaften G, Thijssen K, Kamath RS, Fraser AG, Ahringer J, Plasterk RH and Tijsterman M (2003) Identification of genes that protect the *C. elegans* genome against mutations by genome-wide RNAi. Genes Dev. 17: 443–448
32. Vastenhouw NL, Fischer SE, Robert VJ, Thijssen KL, Fraser AG, Kamath RS, Ahringer J and Plasterk RH (2003) A genome-wide screen identifies 27 genes involved in transposon silencing in *C. elegans*. Curr. Biol. 13: 1311–1316
33. Brenner S (1974) The genetics of *Caenorhabditis elegans*. Genetics 77: 71–94
34. Fraser AG, Kamath RS, Zipperlen P, Martinez-Campos M, Sohrmann M and Ahringer J (2000) Functional genomic analysis of *C. elegans* chromosome I by systematic RNA interference. Nature 408: 325–330

SUPPLEMENTARY TABLE 3.1 List of RNAi clones that cause a Gla phenotype in the primary screen

Predicted gene (*locus*)	Description	Chromosome	Physical map (Mbp)
Protein degradation			
C16C8.14	Ubiquitin domain-containing protein	II	3.45
T12B5.3	F-box domain	III	0.95
T10F2.3	Ulp1 protease family	III	5.17
R05D3.4	RING domain	III	8.36
C06A6.4	Peptidase M20/M25/M40; ArgE/dapE/ACY1/CPG2/yscS	IV	7.83
K03D3.8	Retroviral aspartyl protease	IV	16.31
K11D12.6	Trypsin inhibitor domain	V	5.03
F35B12.6	Serine protease inhibitor	V	11.62
T04G9.2	Neutral zinc metallopeptidase; astacin	X	0.78
B0294.3	F-box domain	X	1.89
T25B6.2	Neutral zinc metallopeptidase; similar to human endothelin-converting enzyme 1	X	9.03
C27C12.7	Dipeptidyl aminopeptidase-like	X	14.83
Redox regulation			
F55A3.5	Glutathione peroxidase	I	10.79
R03D7.6 (*gst-5*)	Glutathione S-transferase	II	10.95
F37B1.1 (*gst-24*)	Glutathione S-transferase	II	13.61
C06A6.5	Thioredoxin domain	IV	7.83
Transcription			
F40G9.4	BTB/POZ domain	III	0.19
K02F3.4	Basic-leucine zipper transcription factor	III	0.83
F56B3.9	Zinc-finger, C_2H_2-type	IV	0.77
F53B2.5	Armadillo/beta-catenin-like repeat	IV	12.53
Y45F10B.1 (*tsp-5*)	Tetraspanin	IV	13.59
Y32F6A.1	SET domain	V	10.44
F48D6.3 (*hlh-13)*	Helix-loop-helix DNA binding domain	X	4.25
K09F5.5	SET domain	X	7.74
F54B11.6	MYND zinc finger domain	X	13.60
C11G6.1 (*taf-3*)	Member of the TAF family	X	16.33
Signal transduction			
C37A2.4 (*cye-1*)	Cyclin E	I	6.79
K02F2.6 (*ser-3*)	Rhodopsin-like GPCR	I	6.83
F15A4.9	Arrestin	II	12.48
Y55B1AR.1	FTH domain	III	0.60
Y55B1AR.3	FTH domain	III	0.60
B0244.8	Low density lipoprotein (LDL) receptor	III	5.73
C05D10.2	Protein kinase	III	6.07
W03G1.6	Protein kinase	IV	0.52
Y38F2AL.5	Calcium-binding EF-hand	IV	2.33
T26C12.4 (*gcy-23*)	Adenylate/guanylate cyclase catalytic domain	IV	3.29
H06H21.9	PDZ/DHR/GLGF domain	IV	4.83
C33H5.6	G-protein beta WD-40 repeat	IV	7.78
F42G8.4 (*pmk-3*)	p38 MAPK	IV	8.14
C10C5.6a	G-protein beta WD-40 repeat	IV	9.39
K11E8.1a (*unc-43*)	Calcium/calmodulin-dependent protein kinase	IV	10.34
Y24F12A.2	Gtr1/RagA G-protein	IV	11.60
F38H12.3	Nuclear hormone receptor	V	4.09
C03A7.6	Rhodopsin-like GPCR	V	5.16
R13D7.6	Rhodopsin-like GPCR	V	7.40
H27A22.1	Guanylate cyclase	V	10.61
B0240.3 (*daf-11*)	Guanylate cyclase	V	11.73
E02A10.3	Calmodulin-like protein	V	12.59
R11D1.6 (*str-181*)	7 TM chemoreceptor	V	12.72
T01G5.1	Tyrosine-protein kinase (KIN15/KIN16 subfamily)	V	15.12
T10H4.5 (*srw-16*)	7 TM chemoreceptor, sri family	V	15.28
ZK1037.5	Ligand-binding domain of nuclear hormone receptor	V	15.33

T14E8.3	Rhodopsin-like GPCR	X	6.57
K11G12.2 (*acr-2*)	Nicotinic acetylcholine receptor subunit	X	6.70
F22F1.2	Serine/threonine protein kinase	X	8.15
ZC504.5 (*gur-3*)	Gustatory receptor	X	10.41
F19H6.1	Protein kinase; similar to human NEK7	X	12.39
Metabolism			
T15D6.2 (*gly-16*)	Acetylglucosaminyltransferase	I	12.39
F31C3.3	Glycoside hydrolase, family 10	I	15.06
Y57A10C.6	Thiolase	II	12.43
R13A5.10	Cytidine/deoxycytidylate deaminase	III	7.58
F13H6.4	Carboxylesterase	V	6.37
F15H10.6	Mitochondrial substrate carrier	V	10.41
F29F11.2	UDP-glucoronosyltransferase	V	10.66
T22G5.2 (*lbp-7*)	Lipid binding protein	V	13.88
T06C12.10	Glycosyl transferase	V	15.89
C31A11.7	Acyltranferase 3 family	V	16.31
Y38H6C.17	Amino acid/polyamine transporter	V	20.54
F47B10.2	Phenylalanine/histidine ammonia lyase	X	10.90
DNA damage response			
Y43C5A.6 (*rad-51*)	DNA repair protein RAD51 homologue	IV	10.28
F46F3.4 (*ape-1*)	p53-binding protein like	V	11.68
T04H1.4 (*rad-50*)	DNA repair protein RAD50 homologue	V	12.25
Ion homeostasis			
C46A5.2	Na^+ channel; amiloride-sensitive	IV	7.76
C09H5.2	Cation transport ATPase	V	8.08
W06D12.5	Potassium channel	V	17.72
C05E11.4 (*amt-1*)	Ammonium transporter	X	4.57
B0395.1 (*nhx-1*)	Sodium/proton antiporter	X	16.01
Structure			
F54D8.1	Nematode cuticule collagen	III	5.11
F53F1.1	Cuticlin	V	13.41
ZK1193.1 (*col-19*)	Cuticular collagen	X	0.42
R04E5.10 (*ifd-1*)	Cytoplasmic intermediate filament protein	X	8.82
Other			
B0414.5 *(cpb-3*)	RNA binding protein, CPEB family	I	5.80
T02E1.3a	Zinc finger domain, TIS11 family	I	8.22
F25H5.4 (*eft-2*)	Elongation factor Tu	I	9.17
F46F5.4	DUF273	II	0.81
C14A4.11	Similar to human Programmed Cell Death 10 protein	II	10.61
F35C5.12	Knottin	II	12.91
F28A10.1	DUF13	II	0.83
K02F3.5	C-type lectin	III	0.82
T07C4.8 (*ced-9)*	Bcl-2 homologue	III	10.34
C23H5.1	S-adenosylmethionine-dependent methyltransferase activity	IV	2.13
R11E3.3	RNA-directed DNA polymerase	IV	4.77
F17E9.12 (*his-31*)	Histone	IV	8.33
F38E11.1 (*hsp-12.3*)	Alpha-B-crystallin	IV	9.45
R11G11.7 (*pqn-60*)	Glutamine/asparagines-rich domain, DUF148	V	0.50
C02A12.6	DUF40	V	3.49
C10F3.1	Aggrecan core protein repeat	V	6.00
T10H9.4 (*snb-1*)	Synapyobrevin- vesicle transport – neurotransmitter release	V	6.66
F40G12.2	DUF263	V	14.26
F40G12.9	CC domain	V	14.29
F23B12.8 (*bmk-1*)	BimC kinesin-like homologue	V	14.46
T26H8.1	Transposase	V	15.30
F36G9.11	C-type lectin	V	15.98
Y68A4B.2	C-type lectin	V	17.25
R04A9.2	PAZ domain	X	0.37
F21E9.3	Transthyretin-like	X	1.34
H02F09.3	Similar to human Mucin 5	X	1.57
F38B6.2	Worm-specific repeat type 1	X	6.70
T23E7.4 (*nlp-6*)	Neuropeptide-like protein gene	X	17.66

Novel		
Y23H5A.2	I	2.62
F58D5.8	I	12.04
K09F6.5	II	2.27
Y38E10A.13	II	12.62
Y38E10A.16	II	12.63
Y38E10A.24	II	12.68
F35C5.1	II	12.88
F42G4.5	II	13.07
Y55B1AR.2	III	0.60
K01A11.1	III	3.43
C44B12.1	IV	1.13
F36A4.1	IV	4.27
W03B1.1	IV	4.33
F19C7.5	IV	4.60
C17H12.10	IV	6.80
F38A5.11	IV	6.59
C25A8.2	IV	7.01
C46A5.6	IV	7.76
C49H3.12	IV	7.93
F42G8.9	IV	8.12
T28A11.4	V	3.27
T20D4.18	V	3.42
C24G6.3	V	5.52
F32B6.11	V	10.91
C01G10.4	V	15.09
F21H7.2	V	16.23
T27C5.8	V	17.42
ZK262.4	V	18.43
M02E1.1	X	0.33
F52D1.2	X	0.45
T13G4.5	X	1.20
R09H3.1	X	1.66
T25B6.3	X	9.03
F17H10.4	X	13.13
C31E10.5	X	14.00
F31B9.3	X	15.92

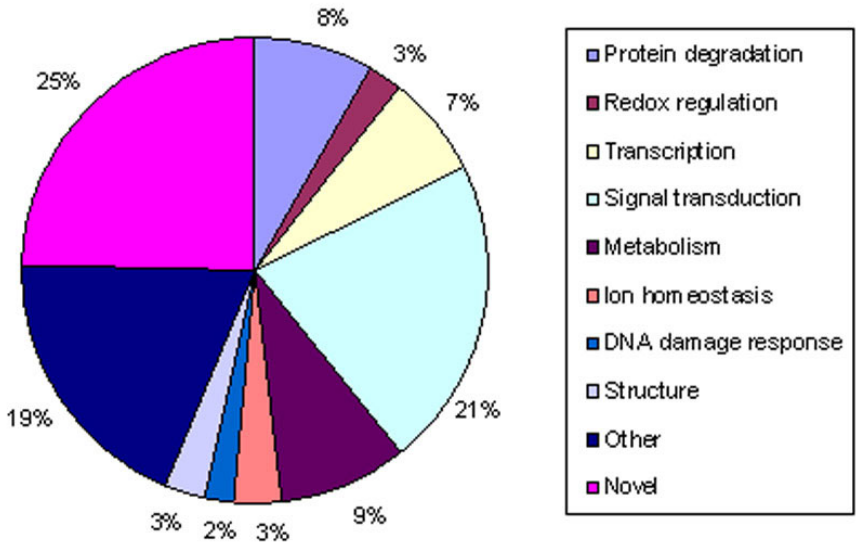

SUPPLEMENTARY FIGURE 3.1 *In silico* classification of RNAi candidates

gla genes identified in the genome-wide RNAi screen were placed into functional classes using data from Proteome, Pfam, and InterPro. The 'other' and 'novel' classes contain genes that could not be grouped, or with no recognizable domains, respectively.

• CHAPTER 4 •

A P38 MAPK PATHWAY REGULATES APOPTOSIS IN THE *C. ELEGANS* GERM LINE

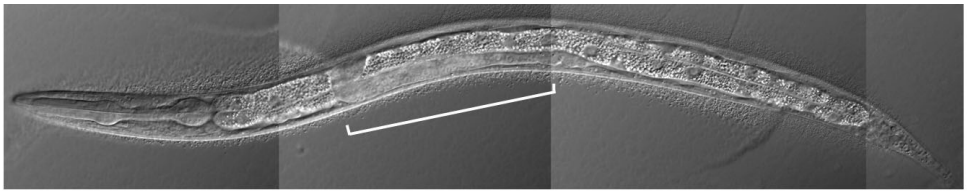

L3 larva - Migration of the DTC to form the bend of the gonad

• CHAPTER 4 •

A P38 MAPK PATHWAY REGULATES APOPTOSIS IN THE *C. ELEGANS* GERM LINE

4.1 ABSTRACT

In this chapter, the characterization of mutations in *pmk-3*, a gene that encodes a p38 MAPK, is described. *pmk-3* loss-of-function mutations causes p53-independent germ cell apoptosis. I show that *pmk-3* is expressed in the *C. elegans* hermaphrodite germ line, and that its activity is required in this tissue. Also, I demonstrate that the MAPKKK MTK-1, the MAPKK MKK-4, and the p38 MAPK PMK-3 act in the same genetic pathway to promote germ cell survival. Finally, preliminary results are presented which suggest that the transcription factor MEF-2 mediates PMK-3's anti-apoptotic activity.

4.2 INTRODUCTION

Mitogen-activated protein kinases (MAPKs) compose a family of protein kinases whose function and regulation have been conserved during evolution from yeast to humans. Metazoans have three well-characterized subfamilies of MAPKs: the extracellular signal-regulated kinases (ERKs), which control cell division, and the c-Jun amino-terminal kinases (JNKs) and p38 MAPKs, which become activated in response to environmental stresses (Johnson and Lapadat, 2002; Widmann et al., 1999). Each MAPK is part of a canonical phosphorelay where the MAPK is phosphorylated by a MAPK kinase (MAPKK), which is itself phosphorylated by a MAPKK kinase (MAPKKK). The level of regulation of these different phosphorylation cascades is very complex: it is tissue-specific, stimulus-specific, and many different MAPKKs and MAPKKKs can activate the same MAPK. For instance, in the presence of inflammatory cytokines, the MAPKKs MKK3 and MKK6 activate p38, whereas MKK4 and MKK7 activate JNK (Brancho et al., 2003). Furthemore, because of cross-talks between the different MAPK pathways, and also the multitude of known targets, the study of MAPK signaling cascades in mammalian cells is very challenging. For this reason, researchers have turned towards simpler systems to unravel the regulation of MAPK pathways. The yeast *S. cerevisiae* was particularly useful to study the oncogenic Ras-ERK pathway, and the fly

D. melanogaster to study the developmental functions of JNK (e.g. in dorsal closure). The worm *C. elegans* has members of each subfamily of MAPKs: the ERK pathway plays major roles during vulva development and germ cell meiotic progression, whereas the JNK and p38 pathways are involved in stress responses and innate immunity. In this chapter, I describe a novel p38 MAPK pathway that regulates germ cell survival.

p38 MAPKs are serine/threonine kinases important for cellular responses to inflammatory cytokines and environmental stresses (e.g. osmotic shock). In mammals, they also regulate the differentiation and survival of various cell types (e.g. cardiomyocytes). p38 MAPKs can be pro- or anti-apoptotic, depending on the cell type and the stimulus. For instance, activation of the transcription factor MEF2 by p38 MAPK upon excitotoxic insults (e.g. *N*-methyl-*D*-aspartate (NMDA)) is anti-apoptotic during neuron development, but pro-apoptotic in mature neurons (Okamoto et al., 2002). Mammals have four p38 MAPKs, only one of which (*p38*α) has been studied through gene targeting in the mouse: *p38*$\alpha^{-/-}$ mice are embryonic lethal owing to placental defects (Adams et al., 2000; Tamura et al., 2000).

C. elegans has three genes encoding p38 MAPKs: *pmk-1*, *-2*, and *-3*. These genes are arranged into a single operon on chromosome IV (Figure 4.1a) (Berman et al., 2001). Recently, an elegant genetic screen for mutants with impaired innate immunity showed that the PMK-1 isoform plays an important role in the worm's response to pathogen infections (Kim et al., 2002). The authors mutagenized wild-type worms, and then looked for mutants hyper-sensitive to *Pseudomonas* infections. They found that mutations in *nsy-1* (a MAPKKK), *sek-1* (a MAPKK), or RNAi knockdown of *pmk-1* (a p38 MAPK) enhance susceptibility to pathogens. Using an antibody that recognizes active PMK-1, they could also show that NSY-1 and SEK-1 act upstream of PMK-1, in a linear pathway. Another recent article took this result further, by assigning a pro-apoptotic activity to PMK-1 (Aballay et al., 2003). It was already known that *Salmonella* infections trigger an innate immune response in worms, resulting in increase germ cell death (Aballay and Ausubel, 2001). The Ausubel laboratory demonstrated that these *Salmonella*-induced germ cell deaths are completely dependent on the NSY-1→SEK-1→PMK-1 pathway (Aballay et al., 2003). Unfortunately, the authors could not provide a molecular model to

explain how PMK-1 signaling activates the core apoptotic machinery, although their epistasis analysis suggested that it acts upstream of *ced-9*.

In chapter 3, I reported that we had identified, in our genome-wide RNAi screen, *pmk-3* as a candidate regulator of germ cell apoptosis. We found that RNAi of or mutations in *pmk-3* increased germ cell apoptosis in a p53-independent manner (Lettre et al., 2004). This suggests that, in contrary to PMK-1, PMK-3 has an anti-apoptotic role in the *C. elegans* hermaphrodite germ line. In this chapter, I characterize the *pmk-3* gene, and identify the upstream components of this novel p38 MAPK pathway as well as one possible downstream effector. Finally, I discuss the possibility that ectopic activation of the PMK-1 pathway might be responsible, to some extent, for p53-independent germ cell apoptosis.

4.3 RESULTS

4.3.1 Mutations in pmk-3 cause p53-independent germ cell apoptosis

pmk-3 is the most 5' gene in the '*pmk*' operon on linkage group IV (Figure 4.1a). The gene has seven exons and codes for a protein of 474 amino acids. I obtained from the *C. elegans* gene knockout consortium the deletion allele *ok169*: this mutation removes a large part of the 5' end of the gene, including exon 1 and intron 1 completely (Figure 4.1b). Because *ok169* eliminates the translational start site, I expect this mutation to be a strong loss-of-function, and likely a null. From the Mitani laboratory in Japan, I obtained *pmk-3(tm745)*. In this mutant, a 733 base pairs deletion removes exons 2 and 3, and most of intron 3, thus eliminating part of the PMK-3 kinase domain (Figure 4.1b).

In a first step, I showed that *pmk-3(ok169)* mutants have a Gla phenotype (Figure 4.2) (Lettre et al., 2004). The same phenotype for the second *pmk-3* allele, *tm745*, was also observed (Figure 4.2b). The Gla phenotype of *pmk-3(tm745)* animals is weaker compared to *ok169* animals, maybe reflecting the nature of the mutations (see above). Since the phenotype of *ok169* appears stronger than *tm745*, and is therefore more likely to reflect the true *pmk-3* loss-of-function phenotype, the remaining experiments presented in this chapter were performed with *ok169*.

We had also shown that *pmk-3(ok169)* or *pmk-3(RNAi)* increase germline apoptosis in a p53-independent manner, because the number of apoptotic corpses is not reduced in

cep-1(gk138); pmk-3(ok169) double mutants (Lettre et al., 2004). The results from this epistasis study can be found in Table 4.1; I also included the results from the *pmk-3(ok169); egl-1(n1084 n3082)* strain, which were omitted in the original publication. The pro-apoptotic BH3-domain gene *egl-1* is the main transcriptional target of CEP-1 upon DNA damage. As expected, the loss-of-function mutation in *egl-1* does not suppress *pmk-3(lf)*-induced germ cell death, confirming that the CEP-1→EGL-1 pathway is not required for the Gla phenotype observed in *pmk-3(lf)* animals (Table 4.1).

4.3.2 Characterization of pmk-3(ok169)

The *ok169* deletion allele was obtained using a TMP/UV mutagenesis protocol. In the past, it has been reported that this mutagen can cause genes to move from their endogenous positions to other genomic locations, such that there is a deletion in the locus but still a wild-type copy of the gene in the genome (Derry et al., 2001). To address this possibility, I analyzed the *pmk-3* locus by Southern blotting. The genomic region surrounding *pmk-3* is depicted in Figure 4.3a: I used a probe that anneals downstream of *ok169*, and the restriction enzymes *Bam*HI or *Apa*LI. Beside the *Bam*HI star activity products, I exactly obtained the predicted restriction fragments (Figure 4.3b). Based on these results, and the fact that it is impossible to amplify a PCR fragment with primers that anneal within the *ok169* deletion, I conclude that *ok169* is a 'clean' deletion and that there is no wild-type copy of *pmk-3* in *ok169* animals.

There is no obvious phenotype associated with *pmk-3(ok169)* other than the Gla phenotype. The worms grow normally, the brood size is normal (269±35 vs. 265±28 for wild-type and *pmk-3(ok169)*, respectively (mean ±s.d., n=10)), and there is no sign of embryonic lethality. However, there is a synthetic phenotype with *unc-119* mutant animals. While I was trying to build the double mutant *unc-119(ed3); pmk-3(ok169)* for bombardment, I realized that the strain grew very slowly and that most animals arrested at the L1 or L2 larval stage. This might suggest that *pmk-3* is involved in some aspects of neuronal cell fate determination. This result is interesting because it is already known that the NSY-1→SEK-1→PMK-1 pathway is important for the cell fate of the AWC neurons in *C.elegans* (Takeda and Ichijo, 2002).

4.3.3 pmk-3 is expressed in the germ line

Berman et al. used a GFP reporter to show that the '*pmk*' operon is expressed in intestinal cells (Berman et al., 2001). They did not report any expression in the germ line or the somatic gonad. However, this result was expected because they used extra-chromosomal arrays for their expression analysis; since these arrays contain several copies of the transgene, they tend to be silenced in the germ line.

To determine whether *pmk-3* is expressed in germ cells, I performed RNA *in situ* hybridization with the full-length *pmk-3* cDNA as probe. I dissected gonads from wild-type and *pmk-3(ok169)* animals, and incubated them with sense or antisense probes labeled with digoxigenin. The results presented in Figure 4.4 show very clearly that *pmk-3* is expressed in the death-sensitive zone of the germ line (at and distal to the bend), consistent with the idea that *pmk-3* is important for germ cell survival. *pmk-3* also seems to be expressed in the proximal arm of the gonad, although this observation needs to be confirmed because few intact gonads were observed (i.e. with both distal and proximal arms). As control, hybridization of *pmk-3(ok169)* gonads with the antisense probe, or wild-type gonads with the sense probe, did not give any specific signal (Figure 4.4). This control experiment suggests that there is no *pmk-3* mRNA in *ok169* mutants, maybe because the mutation affects the stability of the transcript, or prevents *trans*-splicing from the poly-cistronic message. Northern blot experiments are required to definitely solve this issue.

4.3.4 Over-expression of pmk-3 in germ cells rescues the pmk-3(ok169) Gla phenotype

Disruptions of *pmk-3* by two different alleles, *ok169* and *tm745*, as well as its RNAi knockdown, cause a Gla phenotype. However, one could argue that these 'inactivations' also affect the neighboring genes in the '*pmk*' operon (i.e. *pmk-1* and *pmk-2*), and that the Gla phenotype observed is due to general inactivation of the three p38 MAPK isoforms. For this reason, it was important to show that the Gla phenotype in *pmk-3(lf)* animals can be rescued by over-expressing wild-type *pmk-3*.

Rescue experiments in the *C. elegans* germ line are never trivial because multiple copies of transgenes are silenced by RNAi-based mechanisms. For this reason, I used biolistic transformation to obtain transgenic lines carrying but a few tandem copies of

transgene, integrated randomly on one of the chromosome. The transgene was built such that the coding part from the *pmk-3* locus was fused to the C-terminus of green fluorescent protein (GFP), and expressed under the control of the *pie-1* regulatory sequences ($P_{pie\text{-}1}$*::gfp::pmk-3*). The *pie-1* gene is a transcriptional repressor normally expressed in germ cells and early embryos; its enhancer/promoter elements have been used in the past to drive transgene expression into germ cells (Seydoux et al., 1996).

I obtained two different lines with integrated transgenes: *opIs137* and *opIs138*. I crossed these transgenes into *pmk-3(ok169)* worms, and performed time course analysis to investigate if they could rescue the Gla phenotype. Both transgenes bring the number of germ cell deaths back to wild-type level, suggesting that, indeed, the Gla phenotype observed is only due to *pmk-3(lf)* (Figure 4.5a). This result is a very strong proof that *pmk-3* has a major role in germ cell survival.

Interestingly, I found that the fusion protein GFP::PMK-3 exclusively localized to germ cell nuclei (Figure 4.5b). This result agrees with the dogma that active MAPKs translocate to the nucleus (Lee et al., 2000), and suggests that the downstream targets of PMK-3 are nuclear. Two reasons can explain why cytoplamic GFP::PMK-3 could not be observed: (1) maybe PMK-3 is constitutively active, or (2) maybe this over-expression setup leads to GFP::PMK-3 auto-activation.

4.3.5 MKK-4 and MTK-1 are in the same pathway than PMK-3

I was interested to identify which MAPKK and MAPKKK act upstream of the p38 MAPK PMK-3 to regulate germ cell death. There was no obvious candidate from the dataset obtained from the RNAi screen for Gla genes (see Chapter 3). Therefore, I decided to systematically inactivate, by RNAi or with genetic mutations, every worm gene encoding a putative MAPKK or MAPKKK. At this stage of this project, I was fortunate to obtain several deletion mutants for MAPKK and MAPKKK genes from the laboratory of Professor Kunihiro Matsumoto in Nagoya, Japan. I tested for a Gla phenotype inactivation of the MAPKK genes *mek-1*, *mek-2*, *mkk-4*, *jkk-1*, and *gck-1*, as well as the MAPKKK genes *dlk-1*, *mtk-1*, *mlk-1*, *zak-1*, and *gck-2*. Only the *mkk-4(km23)* and *mtk-1(km33)* mutant strains had increased germ cell death compared to wild-type animals (Figures 4.6b and 4.7b). *km23* removes exons 4-to-10 of *mkk-4*, and *km33*

removes exons 6-to-8 of *mtk-1* (Figures 4.6a and 4.7a). Importantly, neither the double mutants *pmk-3(ok169); mkk-4(km23)* and *mtk-1(km33); pmk-3(ok169)*, nor the triple mutant *mtk-1(km33); pmk-3(ok169); mkk-4(km23)* showed any increase in the Gla phenotype compared to the single mutants, suggesting that all these genes lie in the same genetic pathway: *mtk-1→mkk-4→pmk-3* (Figures 4.6b, 4.7b, and 4.7c).

Why were *mkk-4* and *mtk-1* not identified in the RNAi screen? The RNAi clone for *mtk-1* did not grow during the original screen such that *mtk-1(RNAi)* could not be checked for a Gla phenotype. The clone for *mkk-4* grew, but no Gla phenotype was observed, maybe because the *mkk-4(RNAi)* Gla phenotype is too weak. Indeed, Figure 4.6b shows that the Gla phenotype in *mkk-4(km23)* animals is not as strong as in *pmk-3(ok169)* worms. This would suggest that there is possibly redundancy in the cascade and that another unidentified MAPKK can phosphorylate PMK-3. This scenario is quite possible because, in mammals, at least two MAPKKs (MKK-3 and -6) can activate p38 MAPK.

4.3.6 What signals activate the MTK-1→MKK-4→PMK-3 cascade?

mtk-1 is a well-conserved gene, with homologues from yeast to humans. In *S. cerevisiae*, the MTK-1-like Ssk2p activates the high-osmolarity response pathway, which leads to the phosphorylation of the p38 MAPK Hog1p (Yuzyuk et al., 2002). To check whether osmotic stress is a pro-apoptotic stimulus in the *C. elegans* germ line, which is normally counter-balanced by the survival activity of PMK-3, I treated worms with high salt concentrations or sorbitol. Unfortunately, these experiments were not conclusive: weak osmotic stresses did not produce any germline phenotypes, whereas stronger stresses resulted in lethality or growth defects. Therefore, it remains unclear whether osmotic stresses can induce germline apoptosis. To properly realize this experiment, one would need to specifically stress germ cells, without affecting the somatic tissue. Thus, injection of highly osmotic solutions directly into the gonads could be attempted.

In mammals, MTK-1 is activated by the stress-inducible molecule GADD45 in response to TGF-β signaling (Takekawa et al., 2002). However, *C. elegans* does not have a GADD45 homologue. Nevertheless, because TGF-β is a well-described survival signal, I studied the importance of TGF-β signaling on germ cell survival. The worm has four

TGF-β-like proteins: DAF-7, DBL-1, UNC-129, and TIG-2. Genetic mutations or RNAi knockdowns of each of these genes, as well as all possible double inactivations, did not produce a Gla phenotype. This suggests that TGF-β signaling does not play a survival role in the *C. elegans* germ line.

In conclusion, I have been unable to determine what signals lead to the activation of the MTK-1→MKK-4→PMK-3 cascade. Genetic screens or biochemical approaches, such as the purification of the MTK-1 complex, could give us more insights into the regulation of this pathway.

4.3.7 MEF-2 might be a downstream effector of PMK-3

Several proteins, including many different transcription factors, are known substrates of p38 MAPKs in mammals. Myocyte enhancer factor-2 (MEF2) is a MADS (MCM1, Agamous, Deficiens, and Serum response factor) box-type transcription factor implicated in myogenesis and neurogenesis (McKinsey et al., 2002). p38α MAPK can directly phosphorylate MEF2 in cell culture experiments and this phosphorylation event is important for the role of MEF2 in neuronal differentiation and survival/apoptosis (Mao et al., 1999; Yang et al., 1999; Zhao et al., 1999). Transfection of neuronal precursor cells with dominant-negative (DN) forms of MEF2 or p38 MAPK induces apoptosis, and co-transfection of a constitutively active form of MEF2 with the p38 MAPK(DN) blocks the apoptotic response (Okamoto et al., 2000; Okamoto et al., 2002). These biochemical experiments put p38 MAPK upstream of MEF2, and clearly demonstrate that p38 MAPK can promote cell survival in mammals. Importantly, it is unknown how the p38 MAPK → MEF2 pathway ensures cell survival.

C. elegans has one MEF2 homologue, *mef-2*, which is not essential for myogenesis and development (Dichoso et al., 2000). Because of the anti-apoptotic activity of MEF2 in mammalian cells and its interaction with p38 MAPK, I was interested to check whether worm *mef-2* is an effector of *pmk-3* in the *C. elegans* germ line. Two deletion alleles of *mef-2* are available: *gv1* is a predicted null because it removes the DNA-binding domain of MEF-2, whereas *gv2* leaves the DNA-binding domain intact but affects the transactivation domain (Figure 4.8a) (Dichoso et al., 2000). The two mutant strains *mef-2(gv1)* and *mef-2(gv2)* were scored for germline apoptosis; assuming that *C. elegans*

MEF-2 plays a similar role in the germ line than its mammalian homologue in developing neurons, loss of *mef-2* function should cause increased germ cell death. Indeed, time-course analysis showed that both deletion mutants have a modest, but significant, increase in the levels of germline apoptosis (Figures 4.8b and 4.8c). Surprinsingly, the Gla phenotype of *mef-2(gv2)* is stronger than the Gla phenotype of the putative null *mef-2(gv1)*. There are two possible explanations for this result: (1) *mef-2(gv1)* animals have an egg-laying defect (Egl) phenotype such that the accumulation of embryos within the animal renders apoptotic corpse count difficult, and (2) *mef-2(gv2)* is an antimorph (dominant-negative) allele because the encoded protein still have a DNA-binding domain but only a truncated transactivation domain. It should be possible to test the latter possibility by scoring germline apoptosis in *mef-2(gv2)*/+ heterozygotes. The double mutants *mef-2(gv1); pmk-3(ok169)* and *mef-2(gv2); pmk-3(ok169)* have a Gla phenotype equivalent to the Gla phenotype of *pmk-3(ok169)* single mutant (Figures 4.8b and 4.8c). The results of this epistasis analysis suggest that MEF-2 might be one of the proteins that mediate the survival activity of PMK-3 in *C. elegans* germ cells.

At this point, caution must be raised concerning the interpretation of the results presented above. I have shown that for one assay (apoptotic germ cell count), there are genetic interactions between *mtk-1*, *mkk-4*, *pmk-3*, and *mef-2*. However, one would like to test this model by so-called gain-of-function experiments, to show the specificity of the phenotypes. To address this important point, I built a transgene where the DNA-binding domain of MEF-2 is fused to the strong transactivation domain of the viral protein VP16 (MEF-2 activated form). If the model is correct, MEF-2::VP16 should rescue the Gla phenotype of all the genes in this p38 MAPK pathway. I have also created a transgene encoding a dominant negative form of MEF-2. If MEF-2 is downstream of PMK-3, this MEF-2(DN) should cause a Gla phenotype even when PMK-3 is over-expressed (Figure 4.5). Unfortunately, although these two constructs are ready, I have been unable to obtain transgenic animals with germline expression so far.

4.3.8 Does PMK-1 activation induce physiological germ cell death?

In the introduction of this chapter, I mentioned that *Salmonella* infections can induce germ cell death in *C. elegans*, and that this induction depends on the p38 MAPK isoform

PMK-1 (Aballay and Ausubel, 2001; Aballay et al., 2003). Therefore, two genes, expressed from the same operon (Figure 4.1a), have antagonistic functions: PMK-1 is pro-apoptotic in the germ line upon bacterial infection, whereas PMK-3 is anti-apoptotic in the same tissue. It is possible that these p38 MAPKs interfere with each other: in this model, the Gla phenotype of *pmk-3(lf)* could be caused by ectopic activation of PMK-1. To test this model, I performed immunoblots with an antibody that recognizes the phosphorylated form of PMK-1 (active PMK-1), and another antibody that recognizes PMK-1 (Figure 4.9a). As controls, I used protein extracts from *pmk-1(km25)* (no PMK-1 protein), *sek-1(ag1)* and *nsy-1(ag3)* (no phosphorylated PMK-1 because SEK-1 and NSY-1 are the MAPKK and MAPKKK upstream of PMK-1), and *vhp-1(sa366)* animals (more phosphorylated PMK-1, because VHP-1 is the phosphatase that inactivates PMK-1). Interestingly, *pmk-3(ok169)*, but also *gla-1(op234)*, *gla-3(op212)*, and *gla-3(op216)* mutants have elevated level of active PMK-1 when compared to wild-type worms (Figure 4.9a). Inactivation of these three genes (*pmk-3*, *gla-1*, *gla-3*) causes p53-independent germ cell death (Chapter 3), and we have suggested that they regulate the physiological germ cell death pathway. Hyper-activation of PMK-1 in these mutant backgrounds is not a by-product of increased germline apoptosis *per se*, because *ced-9(n1653)* or irradiated worms, which have a Gla phenotype, do not have high level of active PMK-1. Also, although *vhp-1(sa366)* mutants have more active PMK-1 (Figure 4.9a), I could not observe a Gla phenotype in these worms because they have a severe growth delay phenotype.

If ectopic activation of PMK-1 is responsible for physiological germ cell death, disrupting *pmk-1* should suppress the Gla phenotype of *pmk-3(lf)*, *gla-1(lf)*, and *gla-3(lf)*. I built the *gla-1(op234); pmk-1(km25)* and *gla-3(op216); pmk-1(km25)* double mutants and scored them for germline apoptosis (obviously, the *pmk-3(ok169) pmk-1(km25)* strain could not be built as these genes are ~five kb apart on LG IV). Data presented in Figure 4.9b shows that a mutation in *pmk-1* suppresses by ~30% the Gla phenotype of *gla-1(op234)* and *gla-3(op216)*. Therefore, *pmk-1* might be one of the genes that activate physiological germline apoptosis in *C. elegans* (see discussion).

4.4 DISCUSSION

4.4.1 A novel p38 MAPK pathway regulates germ cell survival in C. elegans

p38 MAPKs are involved in stress responses and cell differentiation in metazoans. In *C. elegans*, the p38 MAPK PMK-3 promotes germ cell survival because inactivation of *pmk-3* via mutations or RNAi results in increased germ cell apoptosis (Figure 4.2). Epistasis analysis has revealed that loss of *pmk-3* function causes germ cell apoptosis independently of the worm p53 homologue *cep-1* (Table 4.1), thus establishing *pmk-3* as a possible regulator of the physiological germ cell death pathway in worms. I have also shown, by RNA hybridization, that *pmk-3* is expressed in the death-sensitive zone of the germ line (Figure 4.4), and by tissue-specific rescue, that PMK-3 activity is required in the nuclei of germ cells (Figure 4.5).

MAPK are part of phosphorelays, involving upstream MAPKKK and MAPKK. Searching for the upstream components of the PMK-3 pathway, I found that mutations in the MAPKKK gene *mtk-1* and in the MAPKK gene *mkk-4* produce a Gla phenotype. Importantly, the triple mutant *mtk-1; pmk-3; mkk-4* did not have a stronger Gla phenotype than *pmk-3(ok169)*, suggesting that these genes all belong to the same genetic pathway (Figures 4.6 and 4.7). Because of the molecular nature of the proteins encoded by *mtk-1*, *mkk-4*, and *pmk-3*, it is tempting to propose a model where the MAPKKK MTK-1 activates the MAPKK MKK-4, which itself activates the p38 MAPK PMK-3. However, biochemical experiments, such as immunoblotting with an anti-phospho-PMK-3 antibody, will be required to confirm this hypothesis.

4.4.2 What is upstream and downstream of the pmk-3 pathway?

Unfortunately, I have been unable to identify the stimulus or developmental cue that activates the PMK-3 pathway. This is certainly a question of great interest because we still ignore what triggers physiological germ cell death; it is possible that the upstream components of the PMK-3 pathway would give us a hint concerning the nature of the inducer(s). The most upstream gene in the signaling cascade described in this chapter is *mtk-1*. Therefore, identification of the proteins that interact with MTK-1 should be a priority to understand what regulates the anti-apoptotic activity of PMK-3 in the germ line. Our collaborators in Japan, Dr. Naoki Hisamoto and Prof. Kunihiro Matsumoto

(Nagoya University) are currently developing a functional screening system in yeast to identify proteins that can interact with MTK-1, and will inform us of their future results. In addition, one could try to co-purify the proteins that interact with a tag version of MTK-1 *in vivo* in *C. elegans*.

I have presented preliminary data suggesting that the transcription factor MEF-2 might act downstream of PMK-3 to promote germ cell survival. Mutations in *mef-2* cause a Gla phenotype, and double mutants *mef-2(lf); pmk-3(lf)* do not have an additive Gla phenotype (Figure 4.8). To test the PMK-3→MEF-2 interaction, I built transgenes encoding an activated form (MEF-2::VP16) and a dominant negative form (MEF-2DN) of MEF-2, but I have not yet been able to obtain transgenic lines that express the constructs in the germ line. These transgenic strains would also be useful to address another very important issue concerning the identification of the MEF-2 targets that promote germ cell survival. Indeed, *in silico* approaches to identify MEF-2 target genes have so far been unsucessful. For the proposed experiment, RNA from $P_{pie\text{-}1}$*::gfp::mef-2::VP16* and $P_{pie\text{-}1}$*::gfp::mef-2DN* animals would be isolated, amplified and labeled, and hybridized on a microarray. This strategy should yield the genes that are regulated by MEF-2 in germ cells, including those with anti-apoptotic activity.

In *C. elegans*, MEF-2 has been shown to physically interact with the class II histone deacetylase (HDAC) HDA-4 by yeast-two-hybrid and *in vitro* pull-down assays (Choi et al., 2002). Histone deacetylation by HDACs is associated with heterochromatin and other transcriptionally silent genomic regions. As such, HDACs are thought to act as transcriptional repressors. Work in mammalian cells has revealed that MEF2 can interact with several class II HDACs, and that MEF2 phosphorylation by calcium/calmodulin-dependent protein kinase (CaMK) is required to disrupt MEF2-HDAC interactions (Lu et al., 2000). If PMK-3 activates MEF-2 in the *C. elegans* germ line by disrupting the interaction between MEF-2 and HDA-4, the model predicts that removing *hda-4* activity should suppress the Gla phenotype of *pmk-3(lf)* mutants. I obtained the *hda-4(ok518)* allele and built a double mutant strain with *pmk-3(ok169)*: preliminary data show that *pmk-3(ok169); hda-4(ok518)* animals have a wild-type level of germline apoptosis (Apoptotic germ cells/gonad 24 hours post stage L4 (mean ±s.d.): wild-type 1.9±0.6; *pmk-3(ok169)* 4.0±0.2; *pmk-3(ok169); hda-4(ok518)* 2.0±0.2). If correct, this result

suggests that PMK-3 function is to release MEF-2 from HDA-4 repressing activity; in the absence of HDA-4, MEF-2 can recruit the transcriptional machinery required for the expression of germ cell-specific anti-apoptotic genes. Although very speculative, this model is nevertheless very seducing. Of course, additional experiments are required before it is proven correct.

4.4.3 PMK-1 activation and physiological germ cell death

It was rather surprising to discover that a high level of active PMK-1 is present in some mutants (*gla-1*, *gla-3*, *pmk-3*) with increased levels of germline apoptosis (Figure 4.9a). This finding suggests that PMK-1 might be one of the key inducer of physiological germ cell death. Indeed, the double mutants *gla-1(lf); pmk-1(lf)* and *gla-3(lf); pmk-1(lf)* have significantly less apoptotic germ cells compared to the single mutant *gla-1(lf)* and *gla-3(lf)*, demonstrating that PMK-1 activation is partially responsible for the Gla phenotype of these animals (Figure 4.9b). However, there has to be other genes than *pmk-1* that contribute to physiological germ cell death because *pmk-1(lf)* does not completely suppress the Gla phenotype of *gla-1* and *gla-3*.

We have shown that mutations in genes of the DNA damage pathway, such as *cep-1*, weakly suppress the Gla phenotype of genes, like *gla-1*, that presumably act in the physiological germ cell death pathway (Chapter 3, Table 1). To explain this weak suppression, we have proposed that mutants with a strong Gla phenotype have more endogenous DNA damage, and that this damage leads to few *cep-1*-dependent apoptotic deaths. At this stage, it is unclear whether *pmk-1* is in a p53-independent pathway (p38 MAPK can directly phosphorylate p53 in mammalian cells) and therefore whether the suppression presented in Figure 4.9b is due (partially) to the absence of apoptotic deaths induced by endogenous DNA damage.

4.5 MATERIALS AND METHODS

4.5.1 Nematode strains and culture

Standard procedures for nematode culture and genetic manipulation were followed with growth at 20°C, unless otherwise noted (Brenner, 1974; Gumienny et al., 1999; Sulston and Hodgkin, 1988). The wild-type N2 Bristol strain was used. *C. elegans* gene mutations relevant to this study are as followed: LGI: *hus-1(op244), mtk-1(km33), gla-1(op234), gla-3(op212), gla-3(op212), cep-1(gk138), mef-2(gv1), mef-2(gv2);* LGII: *nsy-1(ag3), vhp-1(sa366);* LGIII: *ced-9(n1653ts), ced-9(n1950gf), unc-119(ed3);* LGIV: *pmk-1(km25), pmk-3(ok169), pmk-3(tm745), ced-3(n717);* LGV: *egl-1(n1084n3082);* LGX: *sek-1(ag1), mkk-4(km23).* Phenotypes are described either by Riddle (Riddle et al., 1997), or in this thesis.

The following PCR primers were used to genotype the deletion mutants:

Primers to genotype deletion mutants

Mutation	Forward primer (5'→3')	Reverse primer (5'→3')	WT product size (bp)	Mutant product size (bp)
mtk-1(km33)	CATGAACCTATGTTTAGCCTTTAAC	CGAAAACAATACATGATGGTTATGG	1777	573
mef-2(gv1)	CCTTAATTAATTAATGCTGCTGCTC	TAATGCAAAATTACGGTAAACGGTC	2396	1020
mef-2(gv2)	CCTTAATTAATTAATGCTGCTGCTC	TAATGCAAAATTACGGTAAACGGTC	2396	1636
pmk-1(km25)	TTTGTGTCCCTAATTCCTTGATCTC	TGAGTCCACGAAGAATTTGATAGAC	868	493
pmk-3(ok169)	CCCATTTTTCACTGCGTCTCAATCG	TCTGCTTCTCCAGGGATTAACGGTG	3681	2397
pmk-3(tm745)	CCCATTTTTCACTGCGTCTCAATCG	TCTGCTTCTCCAGGGATTAACGGTG	3681	2947
mkk-4(km23)	ATCCGAGAAAGGACCAAATATCGTG	AATCGGAGGGAAGAGAGAGAGAAAG	1712	309

4.5.2 Light and fluorescent microscopy

Microscopic analysis of cells was done using standard live-animal techniques: worms were mounted on 4% agarose pad and anesthetized with 30 mM NaN_3 in M9 buffer. Observations were done using a Leica DM RXA2 microscope fitted with Nomarski optics. Images were captured with a ORCA-ER digital CCD camera (Hamamatsu) and processed with OpenLab software. Fluorescence stereomicroscopy was done with a Leica MZ FLIII or a Zeiss Stemi SV11 M^2BIO stereomicroscope.

4.5.3 Biolistic transformation

GFP::PMK-3 lines were constructed with pID3.01B_pmk-3 (the original vector, pID3.01B, is a gift from Dr. Geraldine Seydoux, John Hopkins University). The plasmid contains a translational fusion of *gfp* (N-terminus) with the full-length genomic

sequences of *pmk-3* (ATG to stop codon). Cloning was performed using Gateway Cloning™ technology (Invitrogen) according to the protocol from the Seydoux laboratory. The plasmid also contains the rescuing *unc-119* genomic sequence from pDPMM016. The construct was bombarded into *unc-119(ed3)* worms as previously described (Praitis et al., 2001). To obtain germline expression, 0.5 µg of DNA per bombardment was used. Integration of each construct was determined by loss of visible Unc-119 offspring.

4.5.4 Cloning

Cloning was performed according to standard molecular biology techniques described by Sambrook and Russel (Sambrook and Russell, 2001). Some ligation reactions were done using the Rapid DNA Ligation Kit (Roche). TOPO TA Cloning® and Gateway Cloning™ were performed according to the protocols provided by the manufacturer (Invitrogen).

4.5.5 Polymerase chain reaction (PCR)

PCR was performed using Biotaq DNA polymerase (Bioline), *Pfu Turbo* DNA polymerase (Stratagene), or the Expand High Fidelity PCR system (Roche) according to the manufacturers' protocols.

4.5.6 Southern blotting

Genomic DNA from wild-type and *pmk-3(ok169)* worms was extracted using the Purogene® DNA Isolation Kit (Gentra Systems). DNA transfer from agarose gel onto Hybond N+ membrane was done as described by Sambrook and Russel (Sambrook and Russell, 2001). The probe corresponds to the genomic fragment 25 137 - 26 089 of cosmid F42G8 (encompassing exons 2-5 of *pmk-3*) and was labeled using the PCR DIG Probe Synthesis Kit (Roche). Hybridization and detection were performed using the DIG DNA Labeling and Detection Kit (Roche).

4.5.7 RNA in situ hybridization

Gonads from 24 hours post L4 wild-type and *pmk-3(ok169)* worms were dissected in PBS/0.2 mM levamisole, and fixed for 2 hours at room temperature in 3% paraformaldehyde/0.25% glutaraldehyde/0.1M K_2HPO_4 (pH 7.2). The RNA sense and antisense probes were synthesized using the full-length *pmk-3* cDNA (cloned into pBluescript SK(-) (Stratagene)) as template and the DIG RNA Labelling Kit (Roche). The *pmk-3* cDNA is a gift from Dr. Melanie Cobb, University of Texas Southwestern. RNA hybridization was performed as described by Lee and Schedl (Lee and Schedl, 2004) and online at http://www.genetics.wustl.edu/tslab/gonad_in_situ.html, with the following modifications: 1) probes were diluted 1:5 in hybridization buffer, 2) the hybridization was done for 24 hours at 48^{o}C, and 3) gonads were incubated with the anti-DIG antibody for 14 hours at 4^{o}C.

4.5.8 Protein extraction

Adult worms were washed off the plates with water, and washed once more with water. Worm pellets were then frozen in liquid nitrogen and kept at –80^{o}C. To extract proteins, an equal volume of acid-washed glass beads (Sigma) was added to the frozen worm pellet, and the tubes were put in a bead beater (FastPrep™ FP120) for 35 seconds at speed 6.5. 100 µl – 300 µl of RIPA buffer [50 mM Tris (pH 8.0), 150 mM NaCl, 1% NP-40, 1% deoxycholate, 1% SDS, Complete Mini protease inhibitor 1 tablet/10 ml (Roche)] or immunoprecipitation buffer [25 mM HEPES-NaOH (pH 7.4), 150 mM Nacl, 0.2 mM DTT, 10% glycerol, 1% Triton X-100, Complete Mini protease inhibitor 1 tablet/10 ml (Roche)] was added to the tubes, vortexed, and incubated on ice for ten minutes. Extracts were centrifuged for 15 minutes at 13,200 RPM at 4^{o}C. Supernatants were collected and kept at -80^{o}C. Protein quantification was done using the Bio-Rad protein assay as recommended, with bovine serum albumin (BSA) as standard.

4.5.9 Protein gel electrophoresis

The Laemmli SDS-PAGE (sodium dodecyl sulfate polyacrylamide gel electrophoresis) technique for protein electrophoresis was used, as described by Westermeier (Westermeier, 2001), usually with a 10% acrylamide gel. Alternatively, pre-cast NuPAGE® 4-12% gradient gels from Invitrogen were used, as recommended. The

SeeBlue® Plus2 pre-stained standard (Invitrogen) was used as molecular size marker, and the SimplyBlue™ Safestain (Invitrogen) for protein visualization.

4.5.10 Western blotting

Primary antibodies used in this study were: anti-ACTIVE® p38 pAb, Rabbit (Promega) 1:2000; anti-PMK-1 pAb, Rabbit (gift from Dr. Kunihiro Matsumoto, Nagoya University) 1:1000; anti-GFP mAb, Mouse (Roche) 1:1000; anti-α-tubulin mAb, Rat (Immunologicals Direct), 1:1000. Secondary antibodies (peroxidase-conjugated) used in this study were: goat anti-rabbit (Pierce) 1:30 000; goat anti-mouse (Pierce) 1:10 000; goat anti-rat (Jackson Immuno Research) 1:10 000. Proteins were transferred onto PVDF membrane (30 volts, 75 minutes) using the wet transfer apparatus from Invitrogen. Blots were blocked for 1 hour with TBS-T (Tween 20 0.1%) plus 5% fat-free milk at room temperature, or, for the anti-phospho p38 antibody, overnight with TBS-T plus 1% immunoglobulin-free BSA at 4^{o}C. Primary antibodies were added (overnight at 4^{o}C for all except for the anti-phospho p38 antibody, which was incubated two hours at room temperature). Blots were washed three times ten minutes with TBS-T, and secondary antibodies were added for one hour at room temperature. Blots were washed three times ten minutes with TBS-T. Detection was done using homemade fluorescent peroxidase substrate (mixing equal volume of solution A [2.5 mM luminol, 0.4 mM *p*-coumeric acid, 0.1 M Tris-HCl (pH 8.5)] and solution B [0.1 M Tris-HCl (pH 8.5), 0.02% H_2O_2]).

4.6 REFERENCES

Aballay, A., and Ausubel, F. M. (2001). Programmed cell death mediated by *ced-3* and *ced-4* protects *Caenorhabditis elegans* from *Salmonella typhimurium*-mediated killing. Proc Natl Acad Sci U S A *98*, 2735-2739.

Aballay, A., Drenkard, E., Hilbun, L. R., and Ausubel, F. M. (2003). *Caenorhabditis elegans* Innate Immune Response Triggered by *Salmonella enterica* Requires Intact LPS and Is Mediated by a MAPK Signaling Pathway. Curr Biol *13*, 47-52.

Adams, R. H., Porras, A., Alonso, G., Jones, M., Vintersten, K., Panelli, S., Valladares, A., Perez, L., Klein, R., and Nebreda, A. R. (2000). Essential role of p38alpha MAP kinase in placental but not embryonic cardiovascular development. Mol Cell *6*, 109-116.

Berman, K., McKay, J., Avery, L., and Cobb, M. (2001). Isolation and characterization of *pmk-(1-3)*: three p38 homologs in *Caenorhabditis elegans*. Mol Cell Biol Res Commun *4*, 337-344.

Brancho, D., Tanaka, N., Jaeschke, A., Ventura, J. J., Kelkar, N., Tanaka, Y., Kyuuma, M., Takeshita, T., Flavell, R. A., and Davis, R. J. (2003). Mechanism of p38 MAP kinase activation in vivo. Genes Dev *17*, 1969-1978.

Brenner, S. (1974). The genetics of *Caenorhabditis elegans*. Genetics *77*, 71-94.

Choi, K. Y., Ji, Y. J., Jee, C., Kim do, H., and Ahnn, J. (2002). Characterization of CeHDA-7, a class II histone deacetylase interacting with MEF-2 in *Caenorhabditis elegans*. Biochem Biophys Res Commun *293*, 1295-1300.

Derry, W. B., Putzke, A. P., and Rothman, J. H. (2001). *Caenorhabditis elegans* p53: role in apoptosis, meiosis, and stress resistance. Science *294*, 591-595.

Dichoso, D., Brodigan, T., Chwoe, K. Y., Lee, J. S., Llacer, R., Park, M., Corsi, A. K., Kostas, S. A., Fire, A., Ahnn, J., and Krause, M. (2000). The MADS-Box factor CeMEF2 is not essential for *Caenorhabditis elegans* myogenesis and development. Dev Biol *223*, 431-440.

Gumienny, T. L., Lambie, E., Hartwieg, E., Horvitz, H. R., and Hengartner, M. O. (1999). Genetic control of programmed cell death in the *Caenorhabditis elegans* hermaphrodite germline. Development *126*, 1011-1022.

Johnson, G. L., and Lapadat, R. (2002). Mitogen-activated protein kinase pathways mediated by ERK, JNK, and p38 protein kinases. Science *298*, 1911-1912.

Kim, D. H., Feinbaum, R., Alloing, G., Emerson, F. E., Garsin, D. A., Inoue, H., Tanaka-Hino, M., Hisamoto, N., Matsumoto, K., Tan, M. W., and Ausubel, F. M. (2002). A conserved p38 MAP kinase pathway in *Caenorhabditis elegans* innate immunity. Science *297*, 623-626.

Lee, M. H., and Schedl, T. (2004). Translation repression by GLD-1 protects its mRNA targets from nonsense-mediated mRNA decay in *C. elegans*. Genes Dev *18*, 1047-1059.

Lee, S. H., Park, J., Che, Y., Han, P. L., and Lee, J. K. (2000). Constitutive activity and differential localization of p38alpha and p38beta MAPKs in adult mouse brain. J Neurosci Res *60*, 623-631.

Lettre, G., Kritikou, E. A., Jaeggi, M., Calixto, A., Fraser, A. G., Kamath, R. S., Ahringer, J., and Hengartner, M. O. (2004). Genome-wide RNAi identifies p53-dependent and -independent regulators of germ cell apoptosis in *C. elegans*. Cell Death Differ *11*, 1198-1203.

Lu, J., McKinsey, T. A., Nicol, R. L., and Olson, E. N. (2000). Signal-dependent activation of the MEF2 transcription factor by dissociation from histone deacetylases. Proc Natl Acad Sci U S A *97*, 4070-4075.

Mao, Z., Bonni, A., Xia, F., Nadal-Vicens, M., and Greenberg, M. E. (1999). Neuronal activity-dependent cell survival mediated by transcription factor MEF2. Science *286*, 785-790.

McKinsey, T. A., Zhang, C. L., and Olson, E. N. (2002). MEF2: a calcium-dependent regulator of cell division, differentiation and death. Trends Biochem Sci *27*, 40-47.

Okamoto, S., Krainc, D., Sherman, K., and Lipton, S. A. (2000). Antiapoptotic role of the p38 mitogen-activated protein kinase-myocyte enhancer factor 2 transcription factor pathway during neuronal differentiation. Proc Natl Acad Sci U S A *97*, 7561-7566.

Okamoto, S., Li, Z., Ju, C., Scholzke, M. N., Mathews, E., Cui, J., Salvesen, G. S., Bossy-Wetzel, E., and Lipton, S. A. (2002). Dominant-interfering forms of MEF2 generated by caspase cleavage contribute to NMDA-induced neuronal apoptosis. Proc Natl Acad Sci U S A *99*, 3974-3979.

Praitis, V., Casey, E., Collar, D., and Austin, J. (2001). Creation of low-copy integrated transgenic lines in *Caenorhabditis elegans*. Genetics *157*, 1217-1226.

Riddle, D. L., Blumenthal, T., Meyer, B. J., and Priess, J. R. (1997). *C. elegans II*. Cold Spring Harbor Laboratory Press, Cold Spring Harbor, NY.

Sambrook, J., and Russell, D. W. (2001). Molecular Cloning - A Laboratory Manual. Cold Spring Harbor, NY: Cold Spring Harbor Laboratory Press.

Seydoux, G., Mello, C. C., Pettitt, J., Wood, W. B., Priess, J. R., and Fire, A. (1996). Repression of gene expression in the embryonic germ lineage of *C. elegans*. Nature *382*, 713-716.

Sulston, J. E., and Hodgkin, J. (1988). Methods. In *The nematode Caenorhabditis elegans*. Cold Spring Harbor Laboratory, Cold Spring Harbor, NY, 587-606.

Takeda, K., and Ichijo, H. (2002). Neuronal p38 MAPK signalling: an emerging regulator of cell fate and function in the nervous system. Genes Cells *7*, 1099-1111.

Takekawa, M., Tatebayashi, K., Itoh, F., Adachi, M., Imai, K., and Saito, H. (2002). Smad-dependent GADD45beta expression mediates delayed activation of p38 MAP kinase by TGF-beta. Embo J *21*, 6473-6482.

Tamura, K., Sudo, T., Senftleben, U., Dadak, A. M., Johnson, R., and Karin, M. (2000). Requirement for p38alpha in erythropoietin expression: a role for stress kinases in erythropoiesis. Cell *102*, 221-231.

Westermeier, R. (2001). Electrophoresis in practice.Wiley-VCH.

Widmann, C., Gibson, S., Jarpe, M. B., and Johnson, G. L. (1999). Mitogen-activated protein kinase: conservation of a three-kinase module from yeast to human. Physiol Rev *79*, 143-180.

Yang, S. H., Galanis, A., and Sharrocks, A. D. (1999). Targeting of p38 mitogen-activated protein kinases to MEF2 transcription factors. Mol Cell Biol *19*, 4028-4038.

Yuzyuk, T., Foehr, M., and Amberg, D. C. (2002). The MEK kinase Ssk2p promotes actin cytoskeleton recovery after osmotic stress. Mol Biol Cell *13*, 2869-2880.

Zhao, M., New, L., Kravchenko, V. V., Kato, Y., Gram, H., di Padova, F., Olson, E. N., Ulevitch, R. J., and Han, J. (1999). Regulation of the MEF2 family of transcription factors by p38. Mol Cell Biol *19*, 21-30.

TABLE 4.1 Epistasis analysis with *pmk-3(ok169)*

Genotype	Germ cell deaths per gonad[1]
wild-type	1.9±0.6
pmk-3(lf)	4.0±0.2
ced-3(lf)	0
pmk-3(lf) ced-3(lf)	0
hus-1(lf)	1.0±0.1
hus-1(lf); pmk-3(lf)	3.4±0.2
cep-1(lf)	1.2±0.4
cep-1(lf); pmk-3(lf)	3.7±0.6
egl-1(lf)	**1.3±0.6**
pmk-3(lf); egl-1(lf)	**3.7±0.1**
ced-9(gf)	1.4±0.3
ced-9(gf); pmk-3(lf)	3.3±0.1

[1]The mean number of apoptotic corpses per gonad ± s.d. was obtained from 3 independent experiments. The total number of gonads scored for each experiment was 20. Wild-type: N2. *pmk-3(lf)*: *pmk-3(ok169)*. *ced-3(lf)*: *ced-3(n717)*. *hus-1(lf)*: *hus-1(op244)*. *cep-1(lf)*: *cep-1(gk138)*. *egl-1(lf)*: *egl-1(n1084 n3082)*. *ced-9(gf)*: *ced-9(n1950)*.

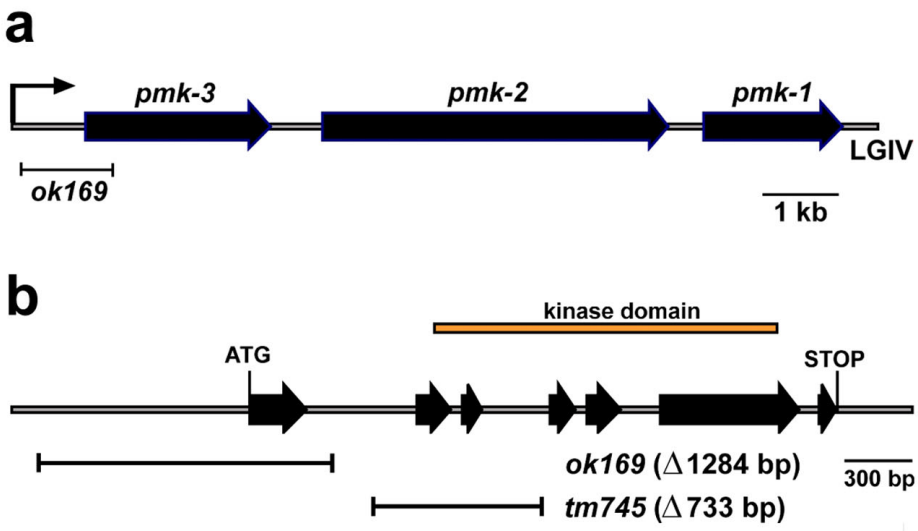

FIGURE 4.1 The *C. elegans pmk-3* locus

(a) Genomic organization of the *C. elegans* operon on chromosome IV that contains *pmk-1*, *pmk-2*, and *pmk-3*. The poly-cistronic message is transcribed from left-to-right, with *pmk-3* at the 5' end. The *pmk-3(ok169)* deletion is shown.

(b) Genomic structure of the *pmk-3* locus. The *pmk-3* gene has seven exons and encodes a protein of 474 amino acids. The two *pmk-3* deletions, *ok169* and *tm745*, are shown. *ok169* removes most of the 5'UTR and exon 1. *tm745* removes exon 2 and 3.

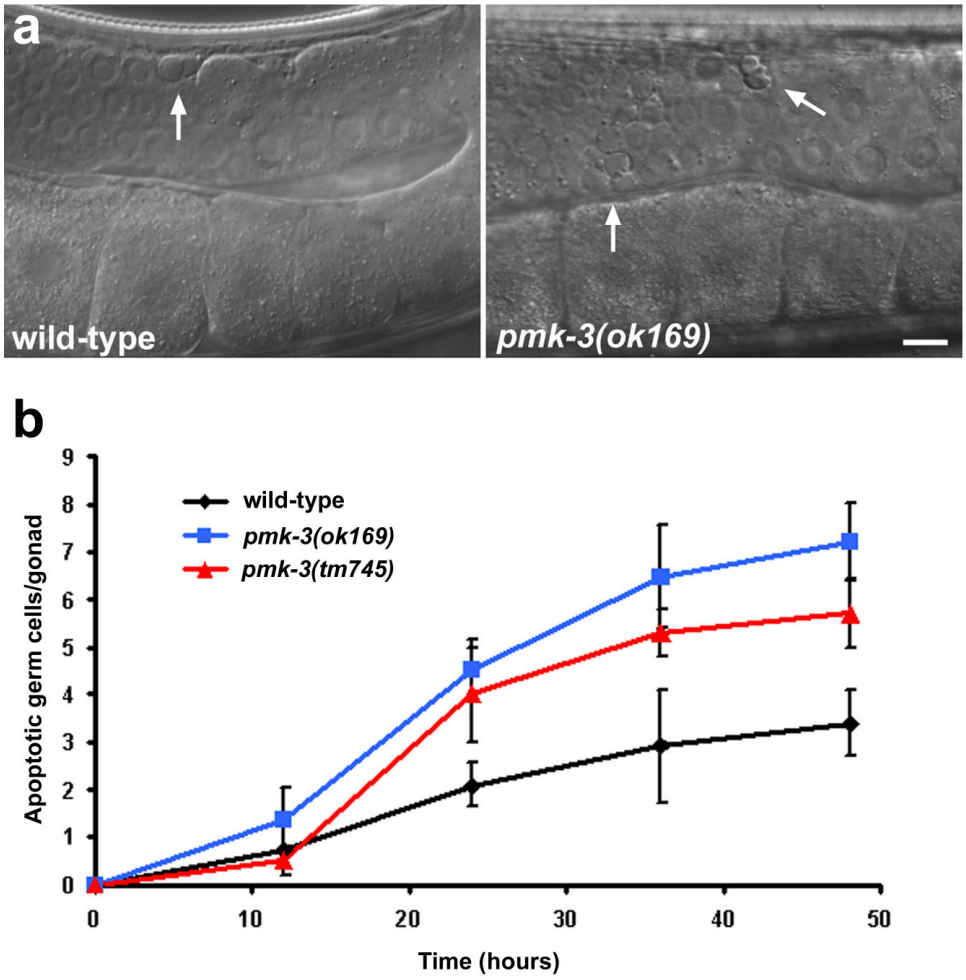

FIGURE 4.2 Loss-of-function mutations in *pmk-3* cause a Gla phenotype

(a) Pictures of gonads from wild-type and *pmk-3(ok169)* worms. DIC pictures of worms grown at 20°C were taken 24 hours post larval stage L4. Apoptotic germ cells can be seen as highly refractile disks (arrows). For all the pictures, anterior is to the left and dorsal to the top. Scale bar, 10 μm.

(b) Time-course analysis of germ cell death in wild-type, *pmk-3(ok169)*, and *pmk-3(tm745)* mutants. Worms were synchronized and scored for germ cell apoptosis by DIC every 12 hours post L4 stage. Data shown represent mean ±s.d. of three experiments (n=20 gonads for each experiment).

FIGURE 4.3 Analysis of the *pmk-3* locus by Southern blotting (next page)

(a) Schematic of the *pmk-3* locus. The *pmk-3* gene (black arrow), the *ok169* deletion, and the probe used for Southern blotting are shown. Also indicated are the *Bam*HI and *Apa*LI restriction sites in this 8 kb fragment of genomic DNA. Note that *ok169* removes one of the *Apa*LI site.

(b) Southern blotting was performed with a *pmk-3* specific probe (see Material and methods) on genomic DNA from wild-type and *pmk-3(ok169)* animals. White asterisks indicate expected restriction products after digestion with *Bam*HI or *Apa*LI. Additional bands can be seen in the *Bam*HI digestion lanes; they likely represent star activity products.

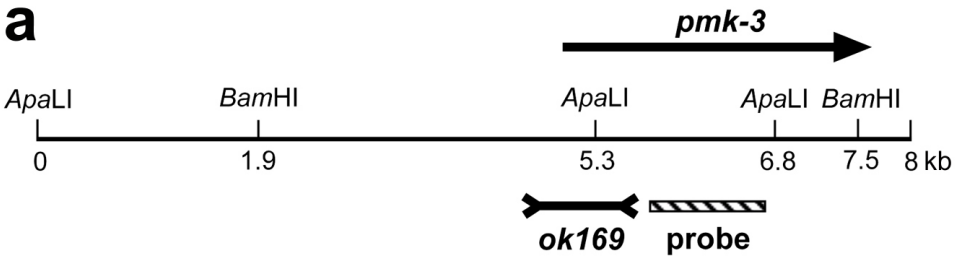

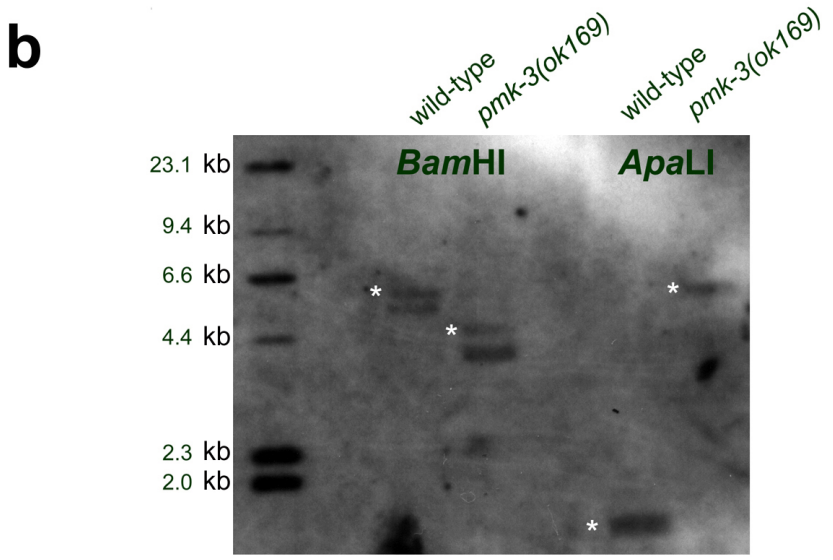

Predicted size after digestion:

*Bam*HI:	wild-type	5.6 kb
	pmk-3(ok169)	4.3 kb
*Apa*LI:	wild-type	1.5 kb
	pmk-3(ok169)	5.5 kb

FIGURE 4.4 *pmk-3* is expressed in the germ line (next page)

pmk-3 mRNA is detectable by RNA *in situ* hybridization at and distal to the bend of the gonad, in the death-sensitive zone. The antisense (AS) and sense (S) probes were synthesized using promoters downstream and upstream of the *pmk-3* cDNA, respectively. Dark purple staining represents specific signal, whereas weaker pink staining corresponds to background. For all gonads, the distal ends are on the left of the figure and the bends are on the right; proximal arms are not shown. Scale bar, 25 μm.

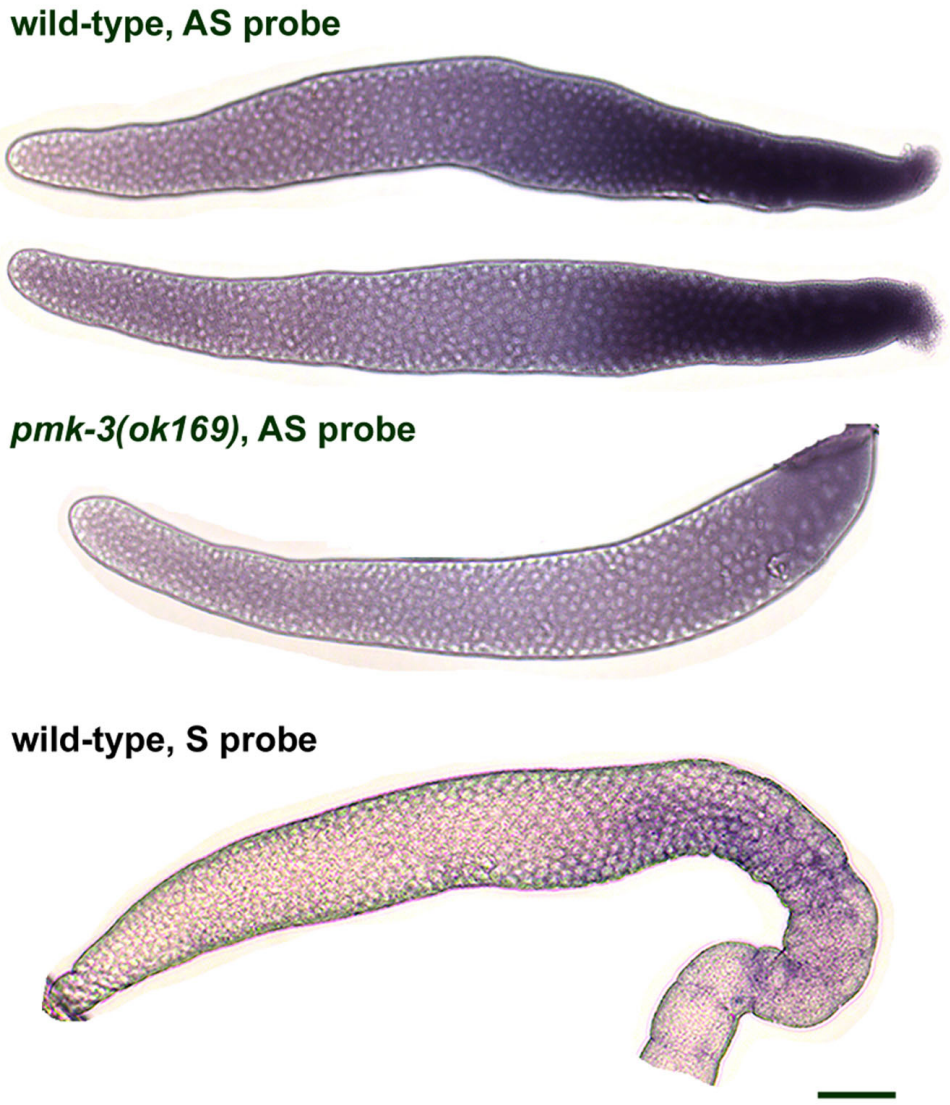
wild-type, AS probe
pmk-3(ok169), AS probe
wild-type, S probe

FIGURE 4.5 *pmk-3* over-expression rescues the *pmk-3(ok169)* Gla phenotype (next page)

(a) Time-course analysis of germ cell death in wild-type, *pmk-3(ok169)*, *pmk-3(ok169); opIs137*, and *pmk-3(ok169); opIs138* animals. *opIs137* and *opIs138* are two independent lines carrying the same transgene: $P_{pie\text{-}1}$*::gfp::pmk-3*. Worms were synchronized and scored for germ cell apoptosis by DIC every 12 hours post L4 stage. Data shown represent mean ±s.d. of two experiments (n=20 gonads for each experiment).

(b) GFP::PMK-3 is nuclear. Gonad of a *pmk-3(ok169); opIs138* transgenic worm seen by Normarski optics (top panel) and with a GFP filter (bottom panel). Scale bar, 10 μm.

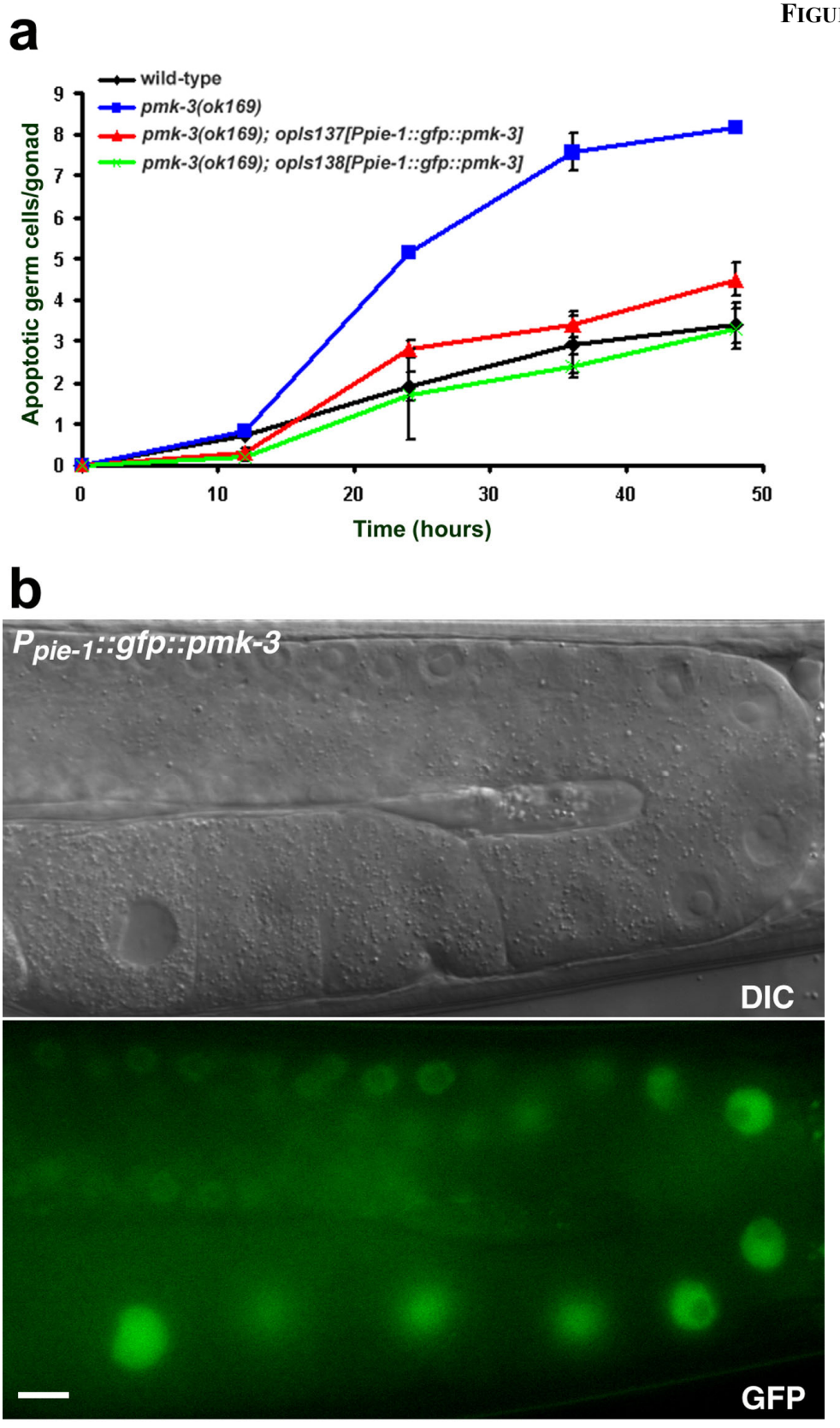
a
wild-type
pmk-3(ok169)
pmk-3(ok169); opIs137[Ppie-1::gfp::pmk-3]
pmk-3(ok169); opIs138[Ppie-1::gfp::pmk-3]
Apoptotic germ cells/gonad
0
1
2
3
4
5
6
7
8
9
0
10
20
30
40
50
Time (hours)
b
Ppie-1::gfp::pmk-3
DIC
GFP

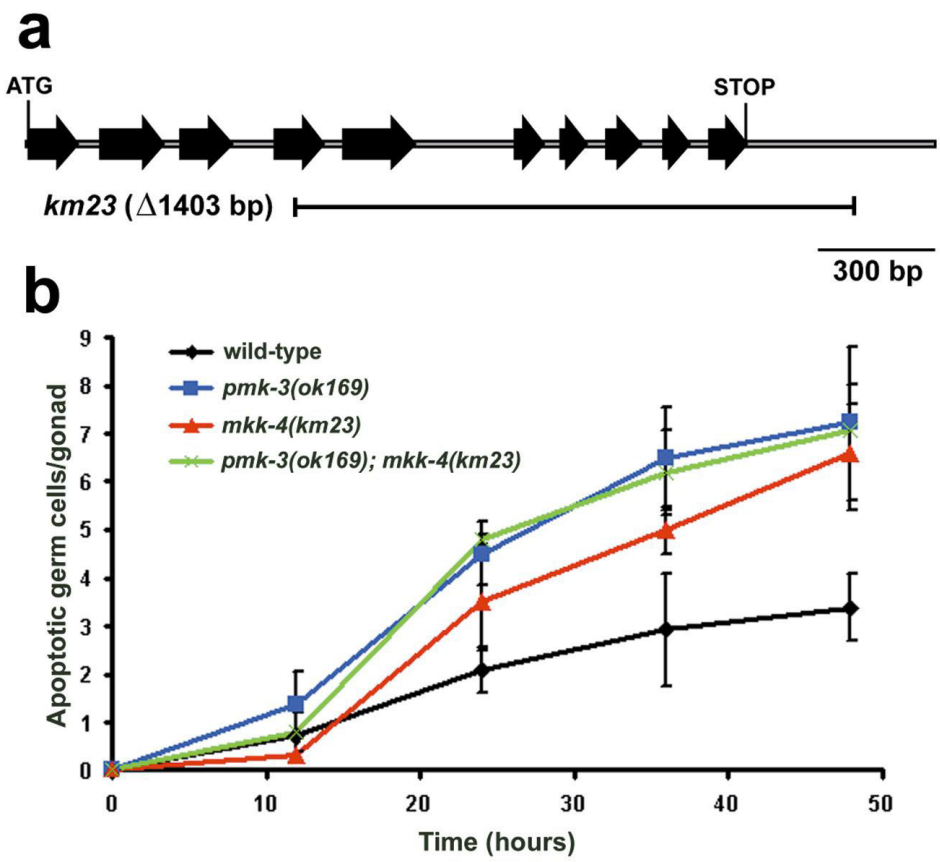

FIGURE 4.6 *mkk-4(km23)* mutants have a Gla phenotype

(a) Genomic structure of the *mkk-4* locus. The *mkk-4* gene has ten exons and encodes a protein of 363 amino acids. The *km23* deletion removes part of exon 4, exons 5-to-10, and part of the 3'UTR of *mkk-4*.

(b) Loss of *mkk-4* function causes a Gla phenotype, and *mkk-4* is in the same genetic pathway than *pmk-3*. Time-course analysis of germ cell death in wild-type, *pmk-3(ok169)*, *mkk-4(km23)*, and *pmk-3(ok169); mkk-4(km23)* animals. Note that the strength of the Gla phenotype in the double mutant is not additive compared to the single mutants. Worms were synchronized and scored for germ cell apoptosis by DIC every 12 hours post L4 stage. Data shown represent mean ±s.d. of two experiments (n=20 gonads for each experiment).

FIGURE 4.7 *mtk-1(km33)* mutants have a Gla phenotype (next page)

(a) Genomic structure of the *mtk-1* locus. The *mtk-1* gene has 15 exons and encodes a protein of 1420 amino acids. The *km33* deletion removes exons 6 and 7, and part of exon 8 of *mtk-1*.

(b) Loss of *mtk-1* function causes a Gla phenotype, and *mtk-1* is in the same genetic pathway than *pmk-3*. Time-course analysis of germ cell death in wild-type, *pmk-3(ok169)*, *mtk-1(km33)*, and *mtk-1(km33); pmk-3(ok169)* animals. Note that the strength of the Gla phenotype in the double mutant is not additive compared to the single mutants. Worms were synchronized and scored for germ cell apoptosis by DIC every 12 hours post L4 stage. Data shown represent mean ±s.d. of two experiments (n=20 gonads for each experiment).

(c) *pmk-3*, *mkk-4*, and *mtk-1* are in the same genetic pathway. Time-course analysis of germ cell death in wild-type, *pmk-3(ok169)*, *mtk-1(km33)*, *mkk-4(km23)*, and *mtk-1(km33); pmk-3(ok169); mkk-4(km23)* animals. Note that the strength of the Gla phenotype in the triple mutant is not additive compared to the single mutants. Worms were synchronized and scored for germ cell apoptosis by DIC every 12 hours post L4 stage. Data shown represent mean ±s.d. of three experiments (n=20 gonads for each experiment).

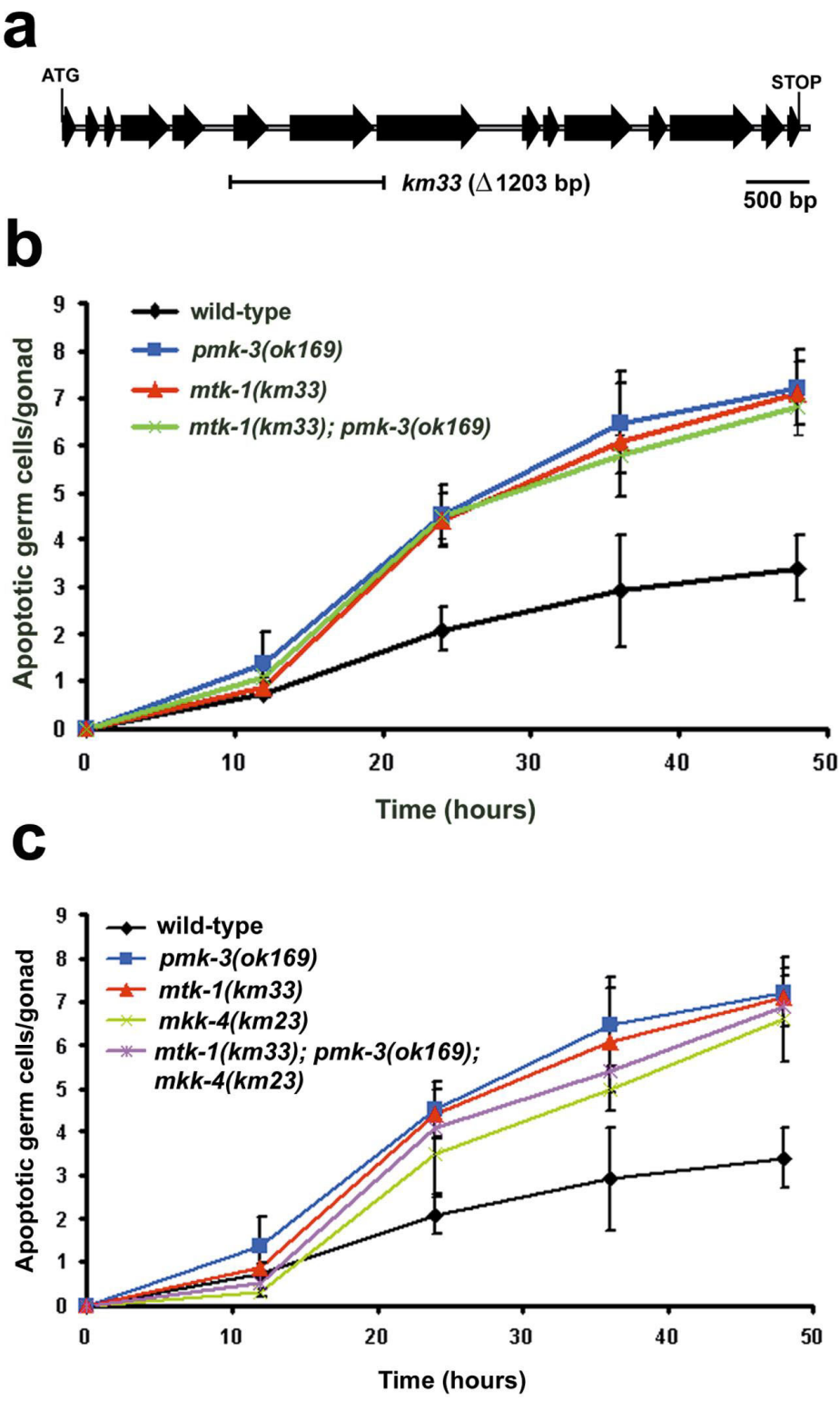
a
ATG
STOP
km33 (Δ1203 bp)
500 bp
b
wild-type
pmk-3(ok169)
mtk-1(km33)
mtk-1(km33); pmk-3(ok169)
Apoptotic germ cells/gonad
Time (hours)
c
wild-type
pmk-3(ok169)
mtk-1(km33)
mkk-4(km23)
mtk-1(km33); pmk-3(ok169); mkk-4(km23)
Apoptotic germ cells/gonad
Time (hours)

FIGURE 4.8 Mutations in the *mef-2* locus cause a Gla phenotype (next page)

(a) Genomic structure of the *mef-2* locus. The *mef-2* gene has five exons and encodes a protein of 340 amino acids. The *gv1* deletion removes exons 2-to-4. The *gv2* deletion removes part of exon 3, exon 4, and part of exon 5.

(b) The *mef-2(gv1)* mutation causes a Gla phenotype, and *mef-2* is in the same genetic pathway than *pmk-3*. Time-course analysis of germ cell death in wild-type, *pmk-3(ok169)*, *mef-2(gv1)*, and *mef-2(gv1); pmk-3(ok169)* animals. Note that the strength of the Gla phenotype in the double mutant is not additive compared to the single mutants. Worms were synchronized and scored for germ cell apoptosis by DIC every 12 hours post L4 stage. Data shown represent mean ±s.d. of two experiments (n=20 gonads for each experiment).

(c) The *mef-2(gv2)* mutation causes a Gla phenotype, and *mef-2* is in the same genetic pathway than *pmk-3*. Time-course analysis of germ cell death in wild-type, *pmk-3(ok169)*, *mef-2(gv2)*, and *mef-2(gv2); pmk-3(ok169)* animals. Note that the strength of the Gla phenotype in the double mutant is not additive compared to the single mutants. Worms were synchronized and scored for germ cell apoptosis by DIC every 12 hours post L4 stage. Data shown represent mean ±s.d. of two experiments (n=20 gonads for each experiment).

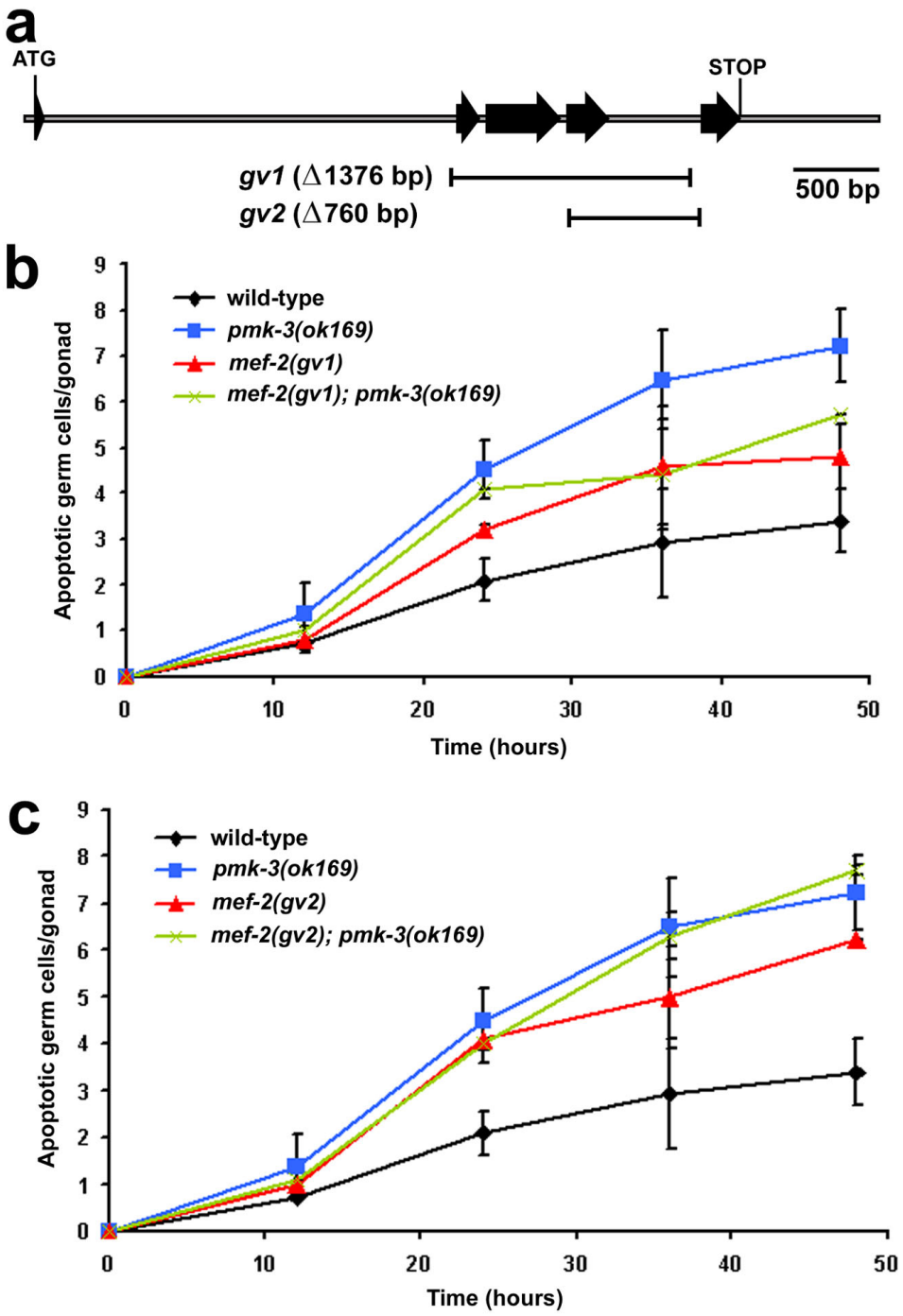
a
ATG
STOP
gv1 (Δ1376 bp)
gv2 (Δ760 bp)
500 bp
b
wild-type
pmk-3(ok169)
mef-2(gv1)
mef-2(gv1); pmk-3(ok169)
Apoptotic germ cells/gonad
Time (hours)
c
wild-type
pmk-3(ok169)
mef-2(gv2)
mef-2(gv2); pmk-3(ok169)
Apoptotic germ cells/gonad
Time (hours)

FIGURE 4.9 Possible role for PMK-1 in the regulation of germline apoptosis (next page)

(a) PMK-1 is hyper-phosphorylated in *pmk-3* (weakly), *gla-1*, and *gla-3* mutants. Immunoblots with anti-phospho p38 MAPK antibody (top panel) and anti-PMK-1 antibody (bottom panel) on protein extracts from *C. elegans* strains with the indicated genotype. PMK-1 has a molecular size of ~44 kDa. The same amount of proteins was loaded in each lane (40 μg), as indicated by the unspecific bands that act as internal loading controls.

(b) *pmk-1(km25)* partially suppresses the Gla phenotype of *gla-1(op234)* and *gla-3(op216)*. Time-course analysis of germ cell death in wild-type, *pmk-1(km25)*, *gla-1(op234)*, *gla-3(op216), gla-1(op234); pmk-1(km25)*, and *gla-3(op216); pmk-1(km25)* animals. Note that *pmk-1(km25)* reduces the Gla phenotype of *gla-1(op234)* and *gla-3(op216)* by about one third. Worms were synchronized and scored for germ cell apoptosis by DIC every 12 hours post L4 stage. Data shown represent mean ±s.d. of two experiments (n=20 gonads for each experiment).

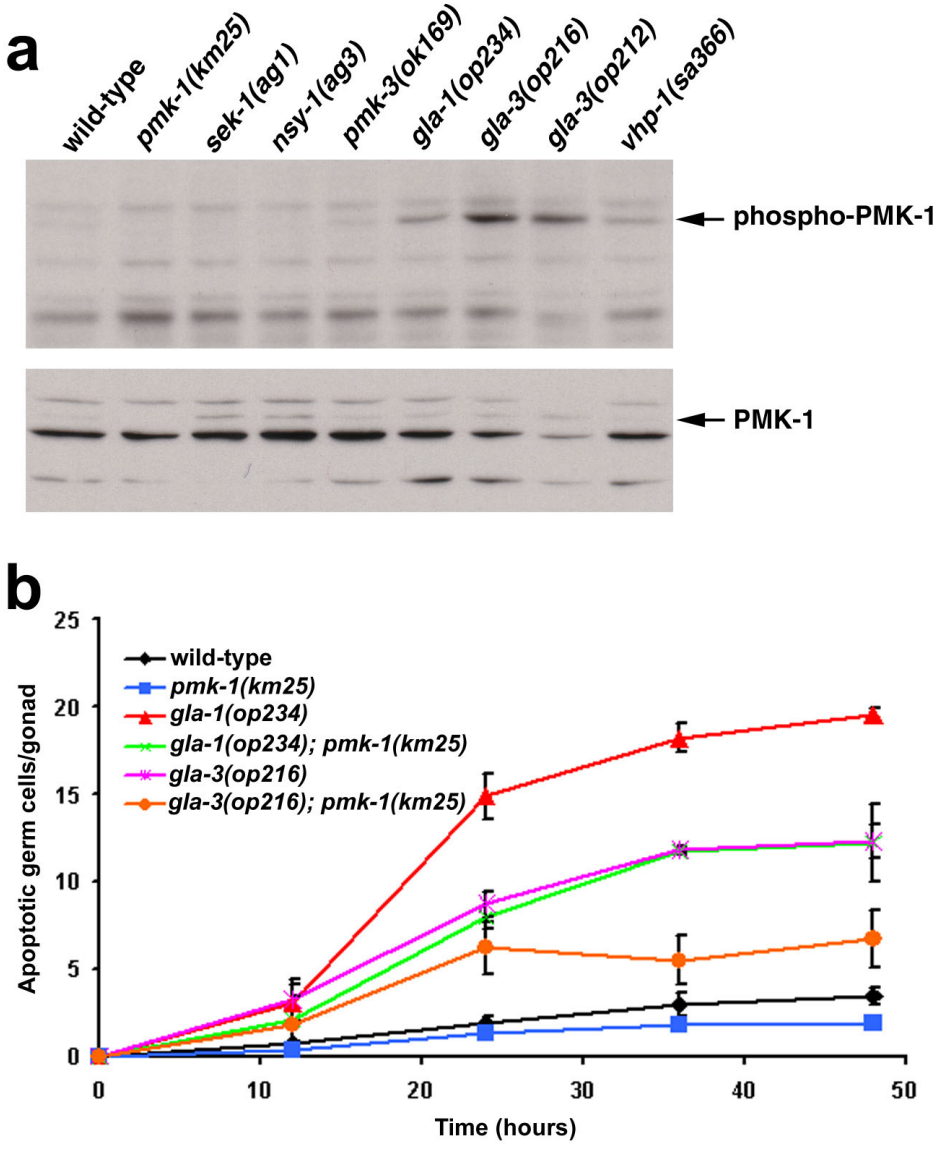
a
wild-type
pmk-1(km25)
sek-1(ag1)
nsy-1(ag3)
pmk-3(ok169)
gla-1(op234)
gla-3(op216)
gla-3(op212)
vhp-1(sa366)
phospho-PMK-1
PMK-1
b
Apoptotic germ cells/gonad
Time (hours)
wild-type
pmk-1(km25)
gla-1(op234)
gla-1(op234); pmk-1(km25)
gla-3(op216)
gla-3(op216); pmk-1(km25)
0
5
10
15
20
25
0
10
20
30
40
50

• CHAPTER 5 •

GENETIC SCREEN FOR GERMLINE-SPECIFIC PRO-APOPTOTIC GENES IN *C. ELEGANS*

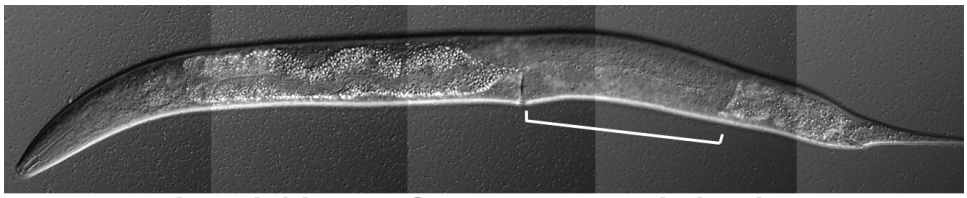

Late L4 larva - Spermatogenesis begins

• CHAPTER 5 •

GENETIC SCREEN FOR GERMLINE-SPECIFIC PRO-APOPTOTIC GENES IN *C. ELEGANS*

5.1 ABSTRACT

gla-1(op234) mutants have increased levels of germ cell apoptotis when compared to wild-type worms. To identify genes that trigger germ cell apoptosis, a *gla-1(op234)* suppressor screen was performed. After screening 21 500 haploid genomes, 16 mutants were recovered. Many of these mutations were in previously identified genes, including four alleles of *ced-3*, three alleles of *ced-6*, and one allele of *ced-2*. Two novel genetic suppressors, *op385* and *op387*, were further characterized. Epistasis analysis implicates *op385* and *op387* in the regulation of the physiological germ cell death pathway: they act upstream of the bcl-2 homologue *ced-9*, and independently of the DNA damage pathway. *op385* and *op387* map to the middle of chromosome V and the right arm of chromosome X, respectively. Using SNP mapping, I narrowed down *op387* to a 85 kb interval, containing 14 predicted genes.

5.2 INTRODUCTION

Physiological germ cell death is the only well-characterized apoptotic pathway in *C. elegans* that is not triggered through transcriptional up-regulation of the pro-apoptotic gene *egl-1* (Gumienny et al., 1999). As such, its study represents an interesting paradigm to identify novel, and potentially conserved, regulators of apoptosis. In this chapter, I describe a forward genetic screen that I performed to find genes that specifically control germ cell death, i.e. genes that play an *egl-1*-like role in the *C. elegans* germ line. To identify such genes, I screened for mutations that could suppress the increased germline apoptosis (Gla) phenotype of *gla-1(op234)*. As discussed in chapter 2, *gla-1* encodes a CPEB protein that might be involved in translational repression and mRNA localization during oogenesis. The *op234* allele, which consists of a point mutation in the very conserved zinc finger, causes a ~eight-fold increase in the level of germ cell death (Chapter 2, Figures 2.2b and 2.2c). Importantly, the Gla phenotype of *gla-1(lf)* animals is independent of the p53 homologue *cep-1* (Lettre et al., 2004). Therefore, this suppressor

screen should not identify genes required for the activation of the apoptotic cascade upon DNA damage.

While the screen aimed at discovering pro-apoptotic genes required for physiological germ cell death, at least five classes of suppressors could in principle be isolated in this genetic screen: (1) genes essential for all apoptotic deaths in the worm (e.g. *ced-3* or *ced-4*), (2) genes involved in engulfment, because non-engulfed corpses do not stain with acridine orange (AO) (see below), (3) genes involved in germ cell development (e.g. mutations that cause sterility), (4) genes that specifically suppress *gla-1(lf)*-induced germ cell death, and (5) genes essential for the physiological germ cell death pathway. The results presented here show that I isolated mutants from classes 1, 2, and 5.

5.3 RESULTS

5.3.1 Methodology and rationale

I carried out an F_2 screen in which parental *gla-1(op234)* worms were mutagenized as young adults with ethyl-nitroso-urea (ENU) (De Stasio and Dorman, 2001), allowed to self-fertilize for two generations, and then screened F_2 adults using AO to identify worms with no or less germline apoptosis (i.e. AO-negative) (Figure 5.1). AO is a vital dye that specifically stains engulfed apoptotic corpses in the *C. elegans* germ line. I chose to mutagenize *gla-1(lf)* mutants instead of wild-type worms because the level of 'physiological' cell death in the germ line of wild-type animals is not readily detectable by AO. Indeed, it is easier to screen for non-Gla mutants among a population of *gla-1(lf)* animals, than among a population of wild-type animals, which only have two or three corpses per gonad.

With this genetic screen, I hoped to find pro-apoptotic genes that specifically regulate germline apoptosis. On the assumption that mutations that will inactivate these genes should reduce the level of apoptosis in the germ line of *gla-1(op234)* mutants, I expected my screen to yield mostly recessive loss-of-function mutations.

5.3.2 Outcome of the screen

I screened 21 500 haploid genomes, and isolated 16 independent mutants (Table 5.1). Of these 16 mutants, four (*op367*, *op368*, *op380*, and *op382*) have a Ced phenotype, that

is extra cells in the anterior pharynx. I performed complementation tests between these four mutants and the strong *ced-3(n717)* mutation: they all failed to complement *ced-3(n717)*, and are therefore all new *ced-3* alleles.

I also isolated four mutants (*op360*, *op369*, *op371*, and *op386*) defective in the engulfment of apoptotic cells. These mutants still have an elevated level of germline apoptosis, but the corpses do not stain with AO because they are not engulfed. Stephanie Züllig performed complementation tests on *op360*, *op371*, and *op386*, and showed that they are new alleles of *ced-6*. Lukas Neukomm sequenced and characterized the *ced-6* locus in these mutants and identified the molecular lesions: *op360* is a A-to-T transversion in the 3' splice site of intron 2, and *op371* and *op380* are both T-to-C transitions in exon 3 that change serine at position 163 into a proline (Figure 5.2a). Characterization of these new *ced-6* alleles in 4-fold embryos revealed that they are all weaker than the canonical *ced-6(n1813)* allele (Figure 5.2b). Doris Klingele performed complementation tests with *op369*, and showed that it is a new allele of *ced-2*. The *ced-2* locus in *op369* animals has not been sequenced yet.

Of the eight remaining mutants, two, *op385* and *op387*, were chosen for further analysis (Figure 5.3). The other six were discarded because they could not be backcrossed, or their penetrance at suppressing the Gla phenotype of *gla-1(op234)* was low.

5.3.3 op385 and op387 block gla-1(op234)-induced germline apoptosis

op385 and *op387* were backcrossed three and five times, respectively, to *gla-1(op234)* mutants before further characterization. Genetic experiments showed that these two mutations are recessive.

The backcrossed strains still have reduced levels of germ cell death (Figures 5.3 and 5.4), but also other pleiotropic phenotypes. *gla-1(op234); op385* animals have a reduced brood size compared to wild-type or *gla-1(op234)* animals, and some worms also have an abnormal germline morphology. In these animals, the gonads appear smaller, filled with vesicles, and their bend does not reach the extremities of the worm. *gla-1(op234); op387* mutants have a normal looking germ line, and the suppression of the Gla phenotype is almost completely penetrant (Figures 5.3 and 5.4). However, this strain has a small brood

size, take 12 hours longer to grow to adulthood, and the worms appear thinner than wild-type animals. The growth delay was taken into account for the time-course analysis presented in Figure 5.4.

5.3.3 Epistasis analysis with other Gla mutants

To check whether *op385* and *op387* are specific suppressors of *gla-1(op234)*-induced germ cell death or if they can also suppress the phenotype of other Gla mutants, I built double mutants with *gla-3(op216)* and the conditional allele *ced-9(n1653)*. *gla-3* encodes a TIS11-like protein involved in meiotic progression (E. Kritikou, personal communication), while *ced-9* is the *C. elegans* bcl-2 homologue. We have shown that like *gla-1*, *gla-3(RNAi)* induces apoptosis in a p53-independent manner (Lettre et al., 2004); it is therefore tempting to speculate that this gene might regulate one of the pathways that contribute to physiological germ cell death. We would expect a general suppressor of apoptosis, or a mutation affecting germ cell development, to block both *gla-3(op216)*- and *ced-9(n1653)*-induced germ cell death. In contrast, a mutation in a specific regulator of physiological germ cell death should suppress *gla-3(op216)*, but not *ced-9(n1653)*, which acts downstream in the apoptotic cascade.

As shown in Figure 5.5, *op385* and *op387* suppress *gla-3(op216)*-induced germ cell death. However, they both fail to significantly suppress the Gla phenotype caused by a temperature-sensitive mutation in *ced-9*. Although there are differences in the level of germline apoptosis between *ced-9(n1653)* worms and the double mutants *ced-9(n1653); op385* or *ced-9(n1653); op387*, these differences might be due to the pleiotropic phenotypes discussed above. Taken together, these results show that *op385* and *op387* can suppress the Gla phenotype of two genes (*gla-1* and *gla-3*) likely involved in the physiological germ cell death pathway, and they suggest that *op385* and *op387* act upstream of the core apoptotic machinery in the germ line of *C. elegans*.

5.3.4 op385 and op387 do not block irradiation-induced germline apoptosis

As mentioned earlier, it should not have been possible in this screen to isolate positive regulators of the DNA damage response in *C. elegans* because *gla-1(op234)* causes apoptosis independently of the main players in this pathway (e.g. CEP-1, HUS-1).

However, to confirm this hypothesis, I irradiated *op385* and *op387* single mutants and looked at the apoptotic response (Figure 5.6). I irradiated worms 24 hours post larval stage L4 with two different doses of X-rays (60 and 120 Gy), and monitored apoptosis six and 24 hours after the irradiation. As positive control, I used wild-type animals, and as negative control, I used the *cep-1(gk138)* strain, which has a putative null mutation in the worm p53 homologue.

As expected, *op385* and *op387* mutants respond to DNA damage, as an increase in the level of germ cell death can be observed after irradiation; in contrast, no response is observed in *cep-1(gk138)* animals (Figure 5.6). However, the responses in the two *gla-1(op234)* suppressors are not as strong as in the wild-type strain N2, especially the response in *op385* worms 24 hours post-irradiation. Again, it is possible that the other phenotypes (germline morphology, growth delay, etc.) associated with *op385* and *op387* are responsible for these 'weaker' responses.

5.3.5 Two-factor mapping of op385 and op387

I used classical mapping with genetic markers to locate *op385* and *op387* on a chromosome. Basically, *gla-1(op234); op385* or *gla-1(op234); op387* strains were crossed into the *dpy-5(e61) gla-1(op234); rol-6(e187); unc-32(e189)* or *gla-1(op234); unc-5(e53); dpy-11(e224); lon-2(e678)* mapping strains. In the F_2 generation, non-Gla animals were picked based on the absence of AO staining, and the segregating markers were scored in the F_3 generation. The results are summarized in Table 5.2. Clearly, *op385* maps to the center of chromosome V as no Dpy-11 animals were observed out of 34 F_2 animals analyzed (68 chromosomes). The mapping results for *op387* are less evident, but nevertheless convincing: *op387* maps on linkage group X because only one third of the F_2 non-Gla animals, instead of the predicted two-third, threw Lon-2 progenies. These data place *op387* about 17 cM from *lon-2*, which is at position -6.8 cM on chromosome X.

5.3.6 Three-factor mapping of op385

The two-factor mapping data put *op385* in the middle of chromsome V, very close to the gene *dpy-11*. To determine on which side of *dpy-11 op385* is located, I crossed *gla-1(op234); op385* males into *gla-1(op234); unc-62(e644) dpy-11(e224)* or *gla-1(op234);*

dpy-11(e224) unc-76(e911) hermaphrodites. In both cases, I singled out, in the F_2 generation, Dpy non-Unc and Unc non-Dpy recombinants, and analyzed by AO staining the segregation of *op385* in the F_3 generation (Table 5.3a). The results of these genetic crosses put *op385* between *dpy-11* and *unc-76*. Note that one of the Unc-62 non-Dpy-11 recombinants segregates a Gla phenotype (Table 5.3a), suggesting that *op385* is on the left of *dpy-11*. However, because the results with the *dpy-11 unc-76* mapping strain are very convincing (Table 5.3a), I suspect this animal to be a double recombinant and maintain my conclusion that *op385* is between *dpy-11* and *unc-76*, at position ~+1.4 cM on chromosome V.

At this point, I stopped mapping *op385*. This decision was motivated by two reasons: (1) I was worried that the abnormal germline morphology of *op385* mutants was indirectly causing the suppression of germ cell death, and (2) I wanted to invest more time in the mapping of the more promising suppressor *op387* (see below). Although the strains are now available to begin single nucleotide polymorphism (SNP) mapping with *op385*, I would not recommend it until a detailed phenotypic characterization (morphology, embryonic lethality, penetrance, temperature-sensitivity) of this mutant is carried out.

5.3.7 Three-factor mapping of op387

Because the two-factor mapping (Table 5.2) did not precisely indicate where *op387* is located on chromosome X, I chose markers that span most of this chromosome. The crosses between *gla-1(op234); op387* males and *gla-1(op234); lon-2(e678) egl-15(n484)* or *gla-1(op234); dpy-6(e14) unc-3(e151)* hermaphrodites put *op387* on the right of *egl-15* (Table 5.3b). However, this work did not allow me to determine a right boundary for an interval encompassing *op387*. To this end, I crossed the suppressor into *gla-1(op234); unc-3(e151) lin-15(n765ts)* animals. All the Lin-15 non-Unc-3 recombinants segregated the non-Gla phenotype, placing *op387* on the left of *lin-15* (Table 5.3b). In conclusion, these genetic crosses located *op387* between *egl-15* and *lin-15*, an interval that corresponds to 20.1 cM.

5.3.8 SNP mapping of op387

The lack of good physical markers on the right arm of chromosome X, and the difficulty to build double mutants on chromosome X (because most hemizygous mutant males do not mate) forced me to choose a very large interval to begin SNP mapping. I built the following strain for SNP mapping: *gla-1(op234); lon-2(e678) op387 lin-15(n309)*. The genetic distance between *lon-2* and *lin-15* is very large (29.8 cM). However, this approach should still be efficient as long as enough recombinants are picked to reach a resolution sufficient to clone *op387*.

To use the polymorphic strain CB4856 from Hawaii in my mapping strategy, I had to first introduce *gla-1(op234)* in this background. Indeed, because I wanted to score the recombinants on the basis of suppression of the Gla phenotype caused by *gla-1(op234)*, I needed all my parental strains to be homozygote for *gla-1(op234)*. I outcrossed *gla-1(op234)* from the original wild-type Bristol background nine times into CB4856. The resulting strain has Hawaii-specific molecular markers on all chromosomes, except on the left arm and middle of chromosome I, where it is still Bristol (*gla-1* is in the middle of chromosome I). However, this should not affect mapping because *op387* is on chromosome X.

I crossed *gla-1(op234)*^{HA} males (that is, *gla-1(op234)* in the CB4856 background) into *gla-1(op234); lon-2(e678) op387 lin-15(n309)* hermaphrodites and singled out, in the F_2 generation, 264 Lon-2 non-Lin-15 recombinants (I did not pick Lin-15 non-Lon-2 animals because *lin-15(n309)* affects gonad morphology). Out of the 264 recombinants, only 23 seggregated *op387* (241 Gla and 23 non-Gla) (Table 5.4). Genotyping all these strains for various molecular markers on chromosome X allowed me to place *op387* between the markers uCE6-1494 on the left and C27C12[2] on the right (Table 5.4). This interval corresponds to 0.14 cM on the genetic map or 85 kb on the physical map, and is predicted to contain 14 genes. There are mutations available for three of the genes in this interval: *unc-3*, *atf-5* and *mbk-1*, but none of them can suppress *gla-1(RNAi)*-induced germ cell apoptosis.

5.3.9 Attempt to phenocopy op387 by RNAi feeding

Having narrowed down *op387* to a reasonably small interval, I decided to try to phenocopy *op387* by RNAi feeding, using clones from the Ahringer library (Kamath et

al., 2003). I performed RNAi at 20°C in a *gla-1(op234)* or a *gla-1(op234); rrf-3(pk1426)* background (*rrf-3* is hypersensitive to RNAi) on 10 of the 14 predicted genes in the interval (Table 5.5). I screened the P_0 generation by DIC microscopy for a reduction in the number of apoptotic corpses caused by *gla-1(op234)*. Unfortunately, I did not identify a RNAi clone that reduced significantly the level of germline apoptosis in *gla-1(op234)*. Negative results with RNAi must always be taken with a grain of salt as it is possible that RNAi knockdown, i.e. not a complete loss-of-function, is not sufficient to reproduce the phenotype. Also, because RNAi is gene-specific, it is possible that inactivation of the locus defined by *op387* does not work. Finally, it remains possible that *op387* inactivates one of the four genes not tested. To conclude, I have been unable to clone *op387* during my doctoral studies. To clone it, I propose to refine the map position using different molecular markers and more recombinants, and to try to rescue the *op387* phenotype with the most promising genes by biolistic transformation.

5.4 DISCUSSION

5.4.1 Overall success of the screen

To identify novel pro-apoptotic genes that specifically act in the *C. elegans* hermaphrodite germ line, I performed a *gla-1(op234)* genetic suppressor screen. *gla-1* encodes a RNA binding protein of the CPEB family, and its inactivation by genetic mutations or RNAi results in p53-independent germ cell apoptosis (Chapter 2). I mutagenized *gla-1(op234)* mutants, and screened the F_2 generation for a loss of AO staining (Figure 5.1). AO is a vital dye that stains engulfed apoptotic germ cells in the germ line of *C. elegans*. After screening 21 500 haploid genomes, I recovered 16 mutants, including four new alleles of *ced-3*, three alleles of *ced-6*, and one allele of *ced-2* (Table 5.1). The fact that *ced-3* alleles and engulfment genes were identified in the screen validates the approach as it was previously known that *ced-3(lf)* mutations suppress *gla-1(op234)*-induced germline apoptosis, and that apoptotic germ cells do not stain with AO in engulfment mutants.

5.4.2 op385 and op387 suppress p53-independent germline apoptosis

Of the eight remaining mutants, I focused my work on *op385* and *op387*, two suppressors that strongly block the Gla phenotype of *gla-1(op234)* worms (Figures 5.3 and 5.4). The next important question was to determine whether *op385* and *op387* are specific to *gla-1(op234)*, or if the can suppress the Gla phenotype of other mutants. I built double mutants with the TIS11-like protein coding gene *gla-3* and the bcl-2 homologue *ced-9*. Both *op385* and *op387* suppress *gla-3(op216)*-induced germ cell apoptosis (Figure 5.5), which is a candidate regulator of the physiological germ cell death pathway. In contrast, they fail to block the Gla phenotype caused by a conditional loss-of-function mutation in *ced-9* (Figure 5.5). This epistasis analysis places *op385* and *op387* upstream of the worm core apoptotic machinery, likely in the physiological germ cell death pathway. Importantly, *op385* and *op387* cannot suppress DNA damage-induced germ cell apoptosis (Figure 5.6), confirming that they specifically act in the p53-independent pathway.

Of course, the next step was to identify the genes affected by *op385* and *op387*. By two- and three-factor mapping, I could place *op385* in the middle of chromosome V, and *op387* on the far end of the right arm of chromosome X. Then, I used SNP mapping to locate *op387* to a 85 kb (0.14 cM) interval, which is predicted to contain 14 genes. *op385* was not mapped further because of the pleiotropic phenotypes associated with this mutation.

Unfortunately, I could not clone *op387*. The fact that I had to choose physical markers really far apart (~30 cM) to carry out SNP mapping turned out to be the limiting factor. Indeed, too much work was required to obtain informative recombinants: at the end, I estimate that only 0.5% of the recombination events between *lon-2* and *lin-15* could have been informative to clone *op387* (*op387* is in a 0.14 cM interval, and the *lon-2 lin-5* interval is 30 cM long).

5.4.3 What kind of genes could op385 and op387 be?

op385 and *op387* can suppress the Gla phenotype of both *gla-1(op234)* and *gla-3(op216)* strains. Because *gla-1* and *gla-3* are thought to act in the same genetic pathway to regulate meiotic progression (G. Lettre, E. Kritikou, and M.O. Hengartner, unpublished), it is possible that *op385* and *op387* affect genes involved in meiosis. For

instance, *op385* and *op387* could reduce the period of time germ cells spend in the pachytene stage of meiosis I, where germ cells normally undergo apoptosis. If this hypothesis is correct, these suppressors should not be able to block germ cell apoptosis caused by mutations in genes not involved in meiosis, such as *pmk-3* (Chapter 4). Assuming that *op385* and/or *op387* can suppress the Gla phenotype of *pmk-3(lf)* mutants, these loci would become prime candidate regulators of the physiological germ cell death pathway. Building the double mutants *pmk-3(lf); op385* and *pmk-3(lf); op387* should be easy, and the results from this epistasis study very interesting.

Another possibility is that *op385* and *op387* define genes whose transcripts are bound by the RNA binding protein GLA-1. Indeed, maybe the CPEB protein GLA-1 represses translation of the pro-apoptotic genes affected by *op385* and *op387*. In this case, the interaction between GLA-1 and the *op385* or *op387* RNAs could be influenced by GLA-3, hence explaining the epistasis observed. Biochemical experiments to co-purify the RNAs bound to GLA-1, as described in Chapter 2, should address this issue.

Finally, *op385* and *op387* could disrupt genes involved in pro-apoptotic MAPK cascades. Indeed, at the end of Chapter 4, I presented evidences that a mutation in the p38 MAPK gene *pmk-1* partially suppress *gla-1(op234)*-induced germ cell death (Figure 4.9). Maybe there are other kinases (*C. elegans* has two JNK-like homologues: JNK-1 and KGB-1) that also positively regulate physiological germ cell death.

To better understand how this locus might regulate physiological germ cell death, it is imperative to clone *op387*. Also, identifying the molecular nature of *op387* should shed light onto the developmental signals or stimuli that activate the physiological germ cell death pathway. More genetic mapping, RNAi knockdowns, and rescue experiments need to be carried out to clone *op387*, but I think that the specificity of the *op387* phenotype justifies the investment of more energy into this project.

5.5 MATERIALS AND METHODS

5.5.1 Nematode strains and culture

Standard procedures for nematode culture and genetic manipulation were followed with growth at 20°C, unless otherwise noted (Brenner, 1974; Gumienny et al., 1999; Sulston and Hodgkin, 1988). The wild-type N2 Bristol strain was used. *C. elegans* gene mutations relevant to this study are as followed: LGI: *dpy-5(e61), gla-1(op234), gla-3(op216), cep-1(gk138);* LGII: *rrf-3(pk1426), rol-6(e187);* LGIII: *ced-6(n1813), ced-6(op360), ced-6(op371), ced-6(op386), unc-32(e189), ced-9(n1653ts);* LGIV: *ced-2(e1752), ced-2(op369), unc-5(e53), ced-3(n717), ced-3(op367), ced-3(op368), ced-3(op380), ced-3(op382);* LGV: *unc-62(e644), dpy-11(e224), op385, unc-76(e911),* LGX: *lon-2(e678), dpy-6(e14), egl-15(n484), unc-3(e151)*, *atf-5(ok576)*, *mbk-1(pk1389), op387, lin-15(n309), lin-15(n765ts).* Phenotypes are described either by Riddle (Riddle et al., 1997), or in this thesis. The polymorphic strain CB4856 was used for single nucleotide polymorphism (SNP) mapping as described by Plasterk and co-workers (Wicks et al., 2001).

5.5.2 Light and fluorescent microscopy

Microscopic analysis of cells was done using standard live-animal techniques: worms were mounted on 4% agarose pad and anesthetized with 30 mM NaN_3 in M9 buffer. Observations were done using a Leica DM RXA2 microscope fitted with Nomarski optics. Images were captured with a ORCA-ER digital CCD camera (Hamamatsu) and processed with OpenLab software. Fluorescence stereomicroscopy was done with a Leica MZ FLIII or a Zeiss Stemi SV11 M^2BIO stereomicroscope.

5.5.3 Mutagenesis and gla-1(op234) suppressor screen

Mutagenesis was performed as described by De Stasio and Dorman (De Stasio and Dorman, 2001). Briefly, young adult *gla-1(op234)* worms were mutagenized with 0.6 mM *N*-ethyl-*N*-nitrosourea (ENU) in M9 buffer for 4 hours. Worms were washed four times with M9 buffer, and allowed to recover overnight at 15°C. Four P_0s were transferred to 10 cm NGM classic plates, and allowed to lay eggs for 8 hours at 20°C, then removed. Three days later, F_1s were removed. Three days later, F_2s were stained

with an acridine orange (AO) solution (Molecular Probes; 0.02 mg/ml in M9 buffer), and screened by fluorescent microscopy for absence of AO staining as described by Lettre et al. (Lettre et al., 2004). AO-negative F_2s were singled out, and their progeny was scored for germline apoptosis (Gla phenotype) and extra cells in the anterior pharynx (Ced phenotype) (Hengartner et al., 1992) by differential interference contrast (DIC) microscopy. For the Ced phenotype, only the cells in the dorsal sector of the pro- and metacorpus of the pharynx, as well as the cells in the metacorpus of both subventral sectors of the pharynx, were scored.

5.5.4 Polymerase chain reaction (PCR)

PCR was performed using Biotaq DNA polymerase (Bioline), *Pfu Turbo* DNA polymerase (Stratagene), or the Expand High Fidelity PCR system (Roche) according to the manufacturers' protocols.

5.6 REFERENCES

Brenner, S. (1974). The genetics of *Caenorhabditis elegans*. Genetics *77*, 71-94.

De Stasio, E. A., and Dorman, S. (2001). Optimization of ENU mutagenesis of *Caenorhabditis elegans*. Mutat Res *495*, 81-88.

Gumienny, T. L., Lambie, E., Hartwieg, E., Horvitz, H. R., and Hengartner, M. O. (1999). Genetic control of programmed cell death in the *Caenorhabditis elegans* hermaphrodite germline. Development *126*, 1011-1022.

Hengartner, M. O., Ellis, R. E., and Horvitz, H. R. (1992). *Caenorhabditis elegans* gene *ced-9* protects cells from programmed cell death. Nature *356*, 494-499.

Kamath, R. S., Fraser, A. G., Dong, Y., Poulin, G., Durbin, R., Gotta, M., Kanapin, A., Le Bot, N., Moreno, S., Sohrmann, M.*, et al.* (2003). Systematic functional analysis of the *Caenorhabditis elegans* genome using RNAi. Nature *421*, 231-237.

Lettre, G., Kritikou, E. A., Jaeggi, M., Calixto, A., Fraser, A. G., Kamath, R. S., Ahringer, J., and Hengartner, M. O. (2004). Genome-wide RNAi identifies p53-dependent and -independent regulators of germ cell apoptosis in *C. elegans*. Cell Death Differ *11*, 1198-1203.

Riddle, D. L., Blumenthal, T., Meyer, B. J., and Priess, J. R. (1997). *C. elegans II*. Cold Spring Harbor Laboratory Press, Cold Spring Harbor, NY.

Sulston, J. E., and Hodgkin, J. (1988). Methods. In *The nematode Caenorhabditis elegans*. Cold Spring Harbor Laboratory, Cold Spring Harbor, NY, 587-606.

Wicks, S. R., Yeh, R. T., Gish, W. R., Waterston, R. H., and Plasterk, R. H. (2001). Rapid gene mapping in *Caenorhabditis elegans* using a high density polymorphism map. Nat Genet *28*, 160-164.

TABLE 5.1 Outcome of the *gla-1(op234)* suppressor screen

Genotype	Germ cell death[1]	Ced[2]	Phenotypes
wild-type	2.1±0.5	0	
ced-3(n717)	0	8.0±1.1	Ced
gla-1(op234)	14.9±1.3	0	Gla
gla-1(op234); ced-3(n717)	0	7.5±1.4	Gla, Ced
gla-1(op234); op358	0.5±1.0	0.9±0.7	
gla-1(op234); op359	0.2±0.4	0.3±0.7	
gla-1(op234); op360	>20	0	Engulfment, *ced-6*
gla-1(op234); op367	0	3.4±2.5	Ced, *ced-3*
gla-1(op234); op368	0	2.9±2.3	Ced, Unc, *ced-3*
gla-1(op234); op369	>20	0.1±0.2	Engulfment, *ced-2*
gla-1(op234); op370	0.6±0.4	0.3±0.5	
gla-1(op234); op371	>20	0	Engulfment, *ced-6*
gla-1(op234); op376	2.5±1.3	0.2±0.4	
gla-1(op234); op380	0.7±1.6	4.5±1.9	Ced, *ced-3*
gla-1(op234); op382	0.1±0.3	4.5±1.5	Ced, *ced-3*
gla-1(op234); op384	0.3±0.5	0.3±0.5	
gla-1(op234); op385	3.4±0.7	0.1±0.4	
gla-1(op234); op386	>20	0	Engulfment, *ced-6*
gla-1(op234); op387	1.3±0.9	0.3±0.8	
gla-1(op234); op388	1.7±1.0	0.3±0.5	

[1]Mean number of apoptotic germ cells ±s.d. per gonad. Corpses were counted by DIC microscopy three days post-L1 stage (n=15). [2]Mean number of extra cells ±s.d. in the anterior pharynx. Only cells in the dorsal sector of the pro- and metacarpus of the pharynx, and cells in both subventral sectors of the metacorpus of the pharynx were counted by DIC (n=10).

TABLE 5.2 Two-factor mapping of *gla-1(op234)* suppressors

Genotype	Mapping to linkage groups[1]					
	dpy-5 I	*rol-6* II	*unc-32* III	*unc-5* IV	*dpy-11* V	*lon-2* X
gla-1(op234); op385	n.d.	n.d.	n.d.	21/34	**0/34**	18/34
gla-1(op234); op387	19/32	20/32	20/32	19/29	17/29	**10/29**

[1]Fractions represent number of non-Gla worms that segregate the chromosomal marker, over the total number of non-Gla worms tested. For all these crosses, the strains were homozygote for *gla-1(op234)*. Chromosomal linkage for *op385* to linkage groups I, II, and III was not determined because of the very strong linkage to chromosome V. n.d., not determined.

TABLE 5.3a Three-factor mapping for *op385*

Physical markers[1]	F_2 recombinants	Segregation of *op385* (non-Gla phenotype)
unc-62 V (-5.2 cM) & *dpy-11* V (0 cM)	9 Dpy-11 non-Unc-62 →	0/9 non-Gla
	10 Unc-62 non-Dpy-11 →	1/10 Gla, 9/10 non-Gla
dpy-11 V (0 cM) & *unc-76* V (+7.3 cM)	10 Dpy-11 non-Unc-76 →	8/10 Gla, 2/10 non-Gla
	10 Unc-76 non-Dpy-11 →	2/10 Gla, 8/10 non-Gla

TABLE 5.3b Three-factor mapping for *op387*

Physical markers[1]	F_2 recombinants	Segregation of *op387* (non-Gla phenotype)
lon-2 X (-6.8 cM) & *egl-15* X (+2.9 cM)	15 Lon-2 non-Egl-15 →	15/15 non-Gla
	15 Egl-15 non-Lon-2 →	0/15 non-Gla
dpy-6 X (0 cM) & *unc-3* X (+21.3 cM)	19 Dpy-6 non-Unc-3 →	19/19 non-Gla
	25 Unc-3 non-Dpy-6 →	0/25 non-Gla
unc-3 X (+21.3 cM) & *lin-15* X (+23.0 cM)	10 Lin-15 non-Unc-3 →	10/10 non-Gla
	3 Unc-3 non-Lin-15 →	0/3 non-Gla

[1]For all these crosses, the strains were homozygote for *gla-1(op234)*. The F_2 recombinants were first homozygosed, and then scored for the Gla phenotype using acridine orange staining. *lin-15(lf)* mutant animals are multivulva.

TABLE 5.4 SNP mapping for *op387*

Markers	*lon-2*	*pkP6166*	uCE6-1494	*pkP6117*	C27C12[2]	uCE6-1502	uCE6-1503	F20D1[3]	*pkP6167*	*lin-15*
Genetic map	-6.8	+16.8	+21.3	+21.5	+21.5	+21.5	+21.5	+21.6	+22.0	+23.0
Physical map	4.7	14.4	14.8	14.9	14.9	14.9	14.9	15.0	15.1	15.7
Gla	241/241	15/241	**2/241**	0/241	0/241	0/241	0/241	0/241	0/241	0/241
non-Gla	0/23	0/23	0/23	0/23	**1/23**	2/23	4/23	5/23	16/23	23/23

Locations on the genetic and physical map are given in cM and Mb, respectively. The mapping cross was: *gla-1(op234)*^{HA} X *gla-1(op234); lon-2(e678) op387 lin-15(n309)*. Only the Lon-2 non-Lin-15 recombinants were genotyped and scored for the Gla phenotype. Numbers represent the fraction of worms that has conserved the wild-type (N2) allele for the Gla recombinants, and the CB4856 (Hawaii) allele for the non-Gla recombinants. See text for details.

TABLE 5.5 Candidate genes for *op387*

Gene	RNAi	Description[1]
Y16B4A.2	N	Serine carboxypeptidase
Y16B4A.1	Y	*unc-3*, transcription factor
F42D1.2	N	Tyrosine aminotransferase
F42D1.3	Y	Rhodopsin-like GPCR superfamily
F42D1.t1	N	tRNA cysteine
T04C10.4	Y	*atf-5*, bZIP transcription factor
T04C10.3	N	
T04C10.2	Y	*epn-1*, epsin N-terminal homology, ubiquitin interacting motif
T04C10.1	Y	*mbk-1*, serine/threonine protein kinase
C27C12.7	Y	*dpf-2*, lipase, peptidase
C27C12.2	Y	Zn-finger, C2H2 type
C27C12.5	Y	Na^+ channel, amiloride-sensitive
C27C12.1	Y	
C27C12.4	Y	

[1]As annotated in wormbase. For the RNAi column, 'Y' indicates that RNAi knockdown of the gene was performed at 20°C in a *gla-1(op234)* background (P_o generation). 'N' indicates that the corresponding clone was not present in the Ahringer feeding library. RNAi clones have not been sequenced yet.

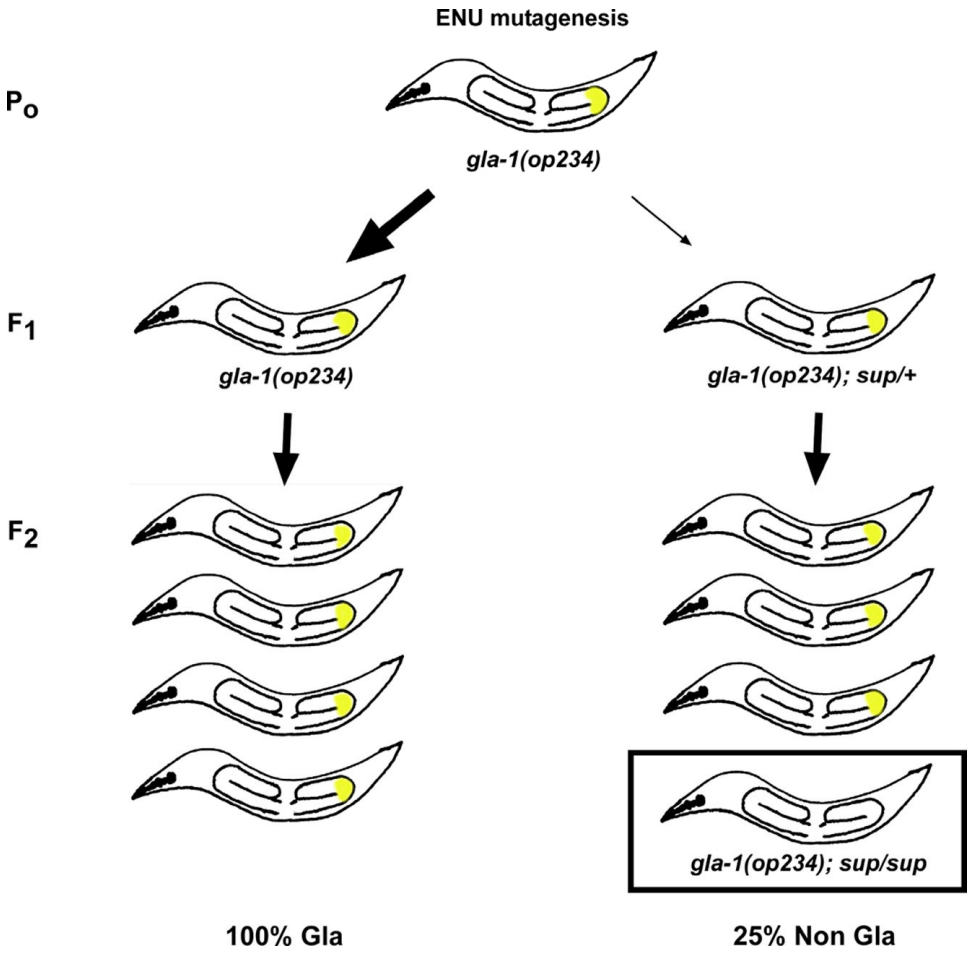

FIGURE 5.1 Outline of the *gla-1(op234)* suppressor screen

Young adult *gla-1(op234)* hermaphrodites were mutagenized with 0.6 mM ENU and allow to self-fertilize for two generations. The F_2 generation was screened by fluorescence microscopy for absence of acridine orange staining. 21 500 haploid genomes were screened and 16 mutants isolated.

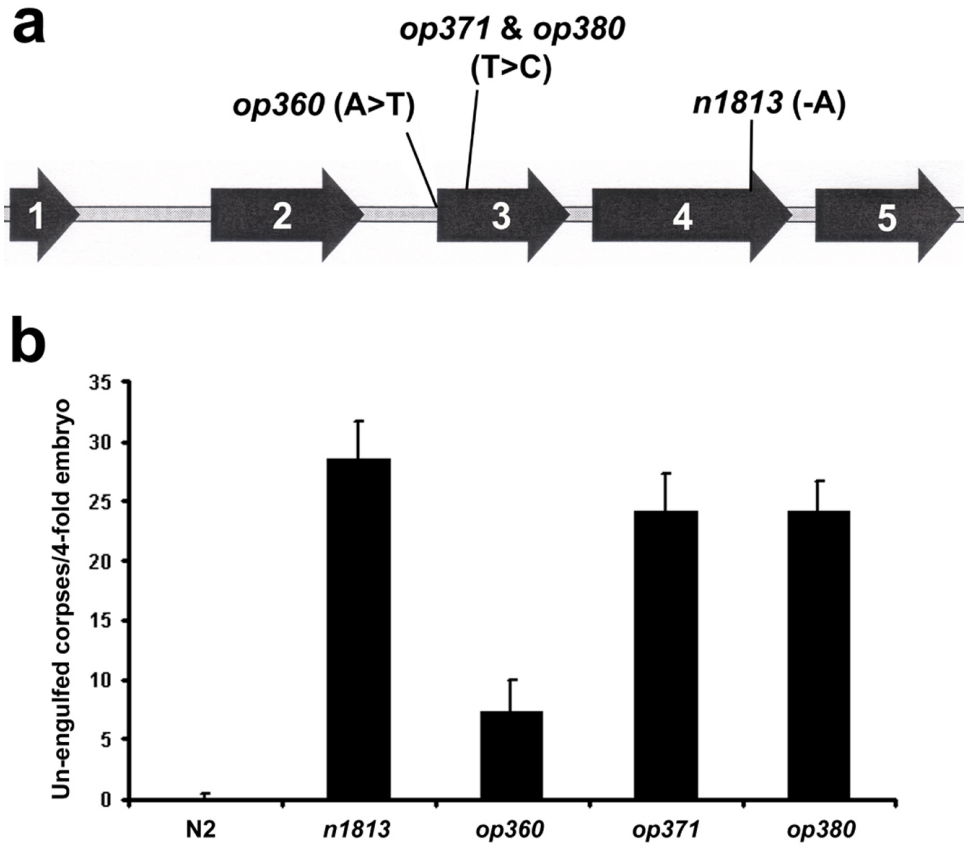

FIGURE 5.2 *ced-6* alelles were found in the *gla-1(op234)* suppressor screen

(a) Genomic structure of the *ced-6* locus. The canonical allele *n1813* is a one base pair deletion that introduces an early stop codon. *op360* is a A-to-T mutation in the 3' splice site of intron 2, and *op371* and *op380* are T-to-C mutations in exon 3 that cause S163P.

(b) Engulfment defect in the new *ced-6* mutants. 4-fold embryos were scored. Data shown are mean ±s.d. (n=20).

FIGURE 5.3 Phenotypic characterization of two *gla-1(op234)* suppressors: *op385* and *op387* (next page)

Pictures of gonads from wild-type and *gla-1(op234)* worms, as well as from two of the *gla-1(op234)* suppressors identified in the forward genetic screen: *gla-1(op234); op385* and *gla-1(op234); op387*. DIC pictures of worms grown at 20°C were taken 24 hours post larval stage L4. Apoptotic germ cells can be seen as highly refractile disks (arrows). Note the almost complete absence of apoptotic corpses in the gonad of *gla-1(op234); op385* and *gla-1(op234); op387* compared to *gla-1(op234)*. For all the pictures, anterior is to the left and dorsal to the top. Scale bar, 25 μm.

FIGURE 5.3

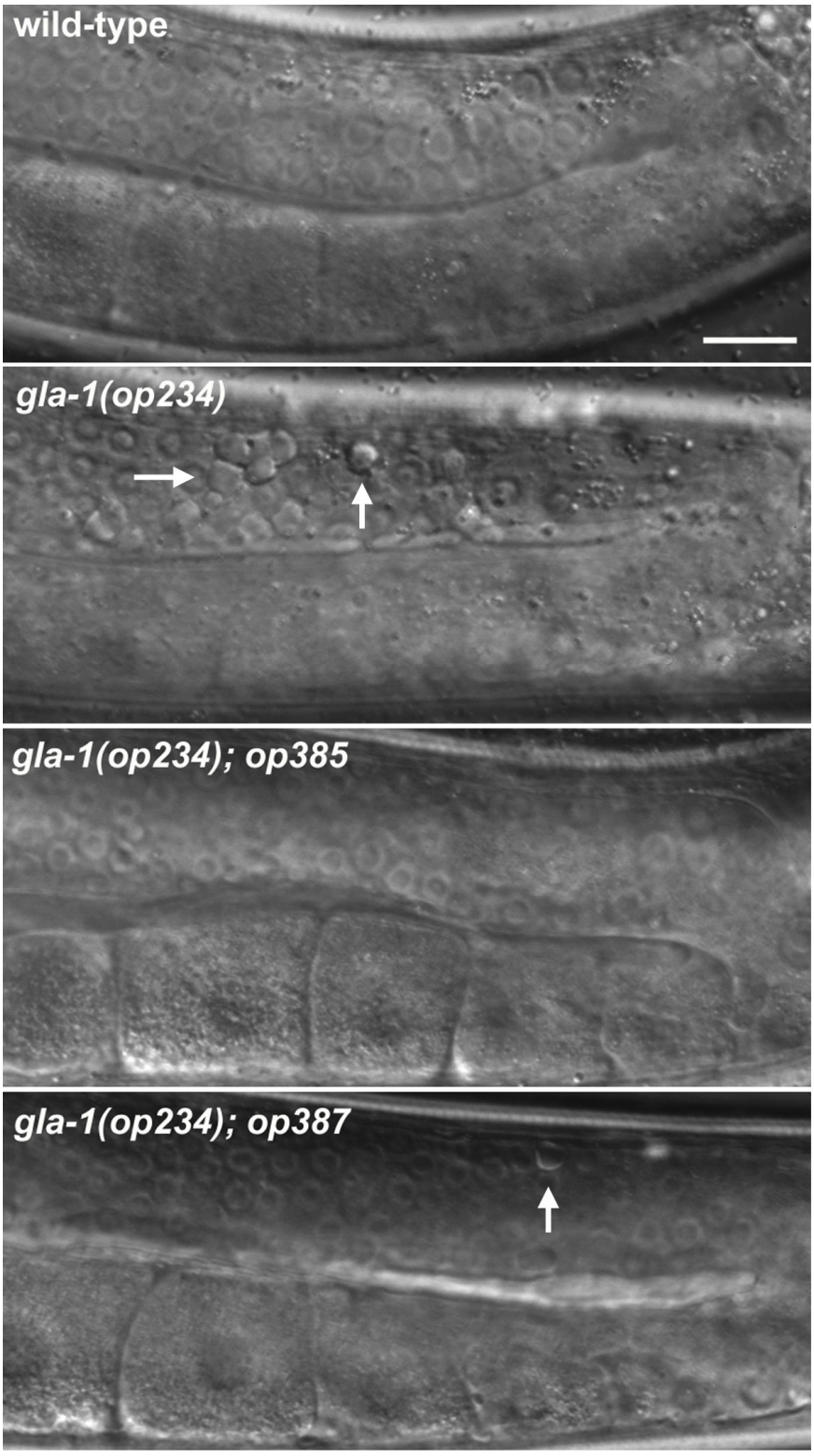

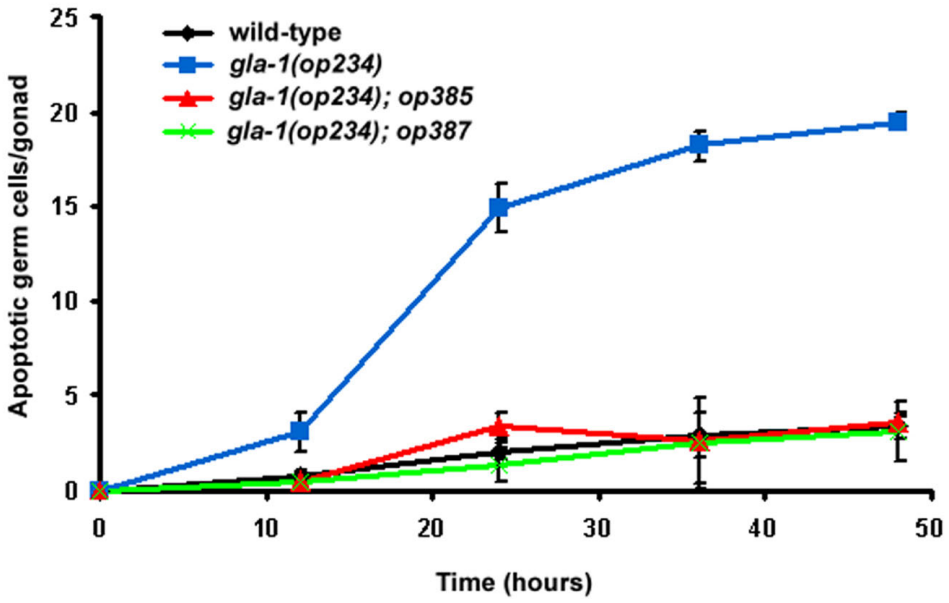

FIGURE 5.4 *op385* and *op387* suppress *gla-1(op234)*-induced germline apoptosis

Time-course analysis of germ cell death in wild-type, *gla-1(op234)*, *gla-1(op234); op385*, and *gla-1(op234); op387* mutants. Worms were synchronized and scored for germ cell apoptosis by DIC every 12 hours post L4 stage. Data shown represent mean ±s.d. of two experiments (n=20 gonads for each experiment).

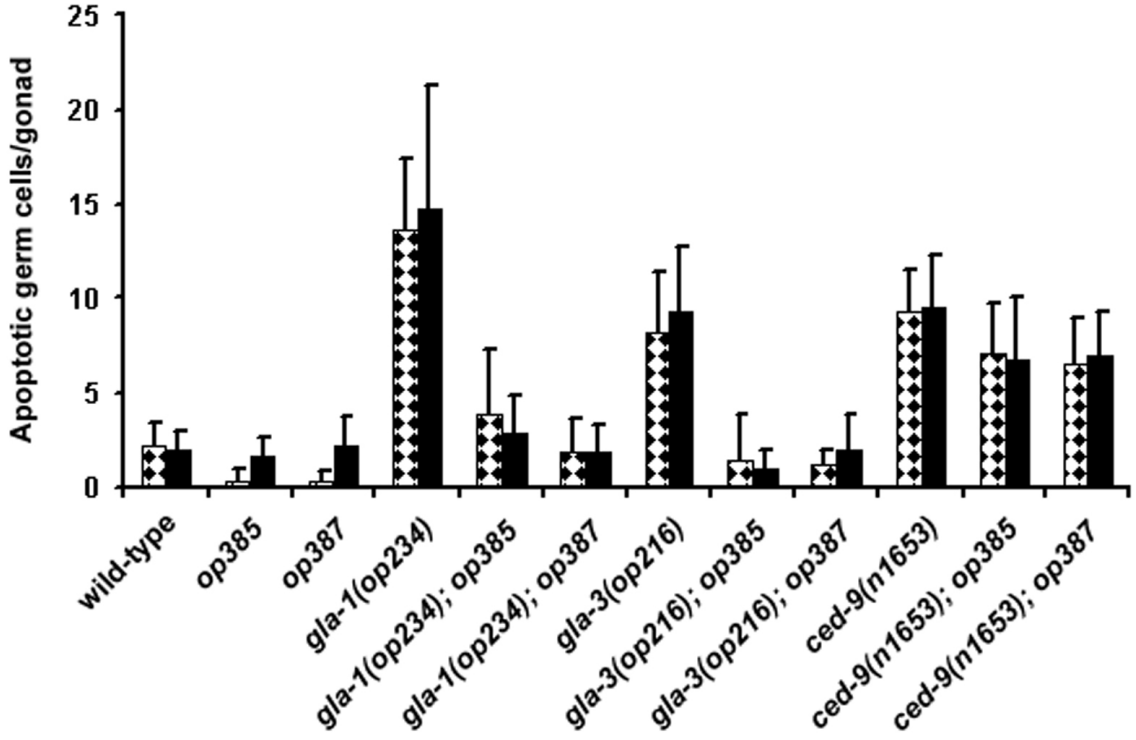

FIGURE 5.5 Epistasis analysis with *op385* and *op387*

op385 and *op387* mutants can suppress the Gla phenotype caused by loss-of-function mutations in *gla-1* or *gla-3*, but not *ced-9*. Worms were synchronized and scored for germ cell apoptosis by DIC 24 hours post L4 stage. Data shown represent mean ±s.d. of two experiments (n=20 gonads for each experiment).

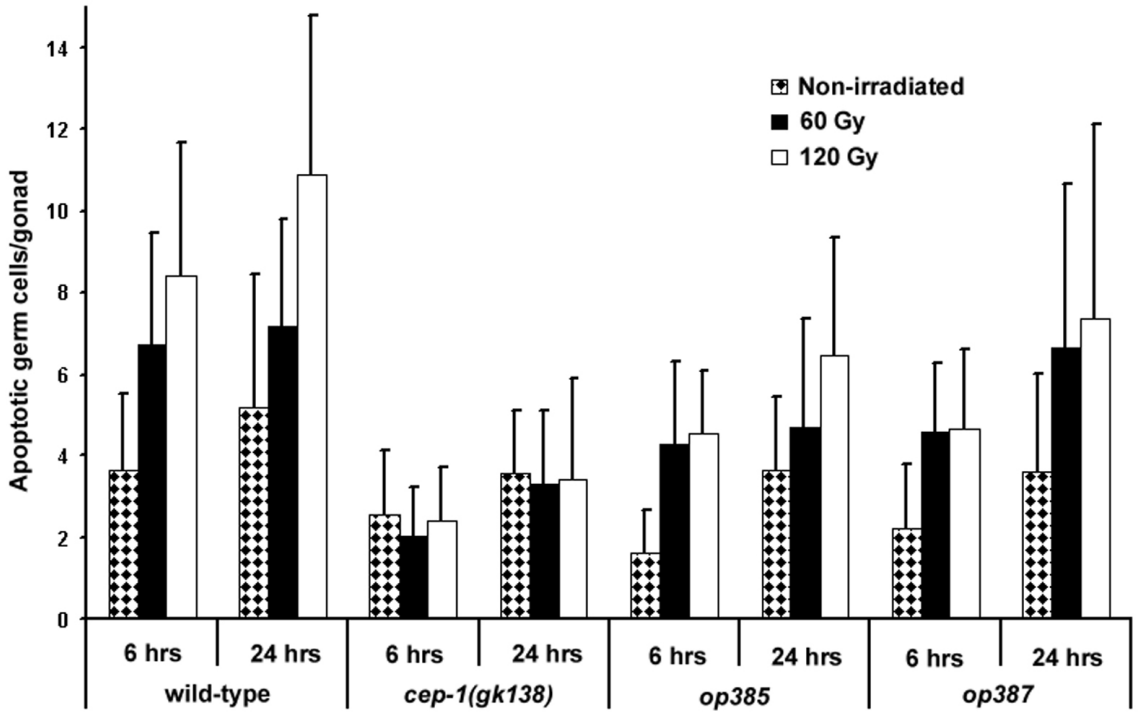

FIGURE 5.6 DNA damage response in *op385* and *op387* single mutants

Wild-type (positive control), *cep-1(gk138)* (negative control), *op385*, and *op387* mutant L4 larvae were irradiated with 60 and 120 Gy of X-rays. The apoptotic response was analysed six and 24 hours after irradiation. Apoptotic corpses were scored via direct observation using DIC microscopy. Data shown represent mean ±s.d. of one experiment (n=20 gonads).

• CHAPTER 6 •

PERSPECTIVES

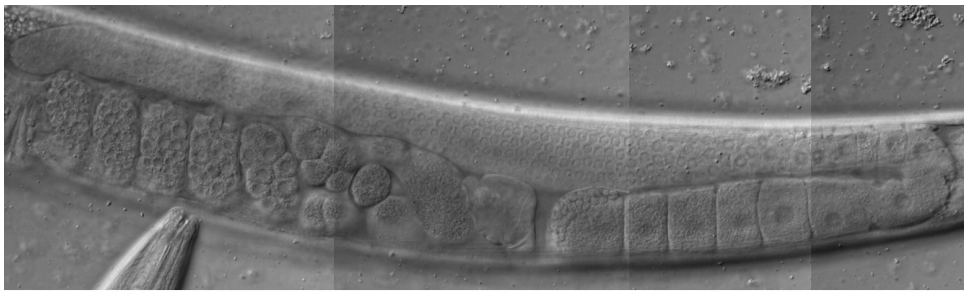

C. elegans adult hermaphrodite germ line

• CHAPTER 6 •

PERSPECTIVES

Professor Yuri Lazebnik, one of my instructors in Cold Spring Harbor laboratory, once wrote about apoptosis research 'that the more facts we learn the less we understand the process we study' (Lazebnik, 2002). Sadly, it seems to me that this philosophical thought also applies to my doctoral project. However, it remains possible that future work, based on the discoveries presented in this PhD dissertation, will yield a more comprehensive view of apoptosis regulation during metazoan development.

6.1 THREE YEARS LATER: AN OUTLOOK

The main objective of my thesis project was to discover the pathways that regulate physiological germ cell apoptosis in *C. elegans* hermaphrodite. To achieve this goal, I identified and characterized mutants with more germline apoptosis (Chapters 2 and 4), performed a genome-wide RNAi screen (Chapter 3), as well as a *gla-1(op234)* modifier genetic screen (Chapter 5). Although these approaches did not help me to pinpoint the stimuli or developmental cues that activate (or block) physiological germ cell death, they provided us with a list of more than twenty genes (or mutants) to investigate further, all of them being possible regulators of germline apoptosis in *C. elegans*.

gla genes cause increased germline apoptosis when inactivated by genetic mutations or RNAi; these deaths can be p53-dependent or p53-independent. The RNAi screen described in Chapter 3 led to the identification of several gene knockdowns that require the p53 homologue CEP-1 to induce apoptosis. Although interesting because they might be involved in the maintenance of genome stability or p53 activation, it is unlikely that studying the p53-dependent class of genes will shed light on the regulation of physiological germ cell death.

To my knowledge, there are less than ten genes that can produce a p53-independent Gla phenotype upon inactivation. Most of them (*gla-1/cpb-3*, *gla-3*, *cgh-1*, *daz-1*, *teg-1*) can be linked to proper RNA processing during oogenesis. Because the regulation of RNA localization, stability, and translation is essential for oocyte maturation in most (all?) sexual species, I strongly believe that further study of these *C. elegans* genes will

provide extremely interesting findings concerning germ cell development. However, I doubt that it will lead to the identification of the signaling cascades that contribute to physiological germ cell death. Indeed, the Gla phenotype in these mutants is likely due to the activation of quality-control programs because oogenesis cannot occur nomally; convincing data from the study of the TIS11-like protein GLA-3 support this hypothesis (E. Kritikou, personnal communication).

The p38 MAPK gene *pmk-3* is an exception among all the known *gla* genes that fall in the p53-independent group (Chapter 4). Even though a null mutation in *pmk-3* does not result in a spectacular Gla phenotype – a bare three-fold increase in germ cell deaths compared to wild-type worms – the phenotype is specific to apoptosis. Indeed, extensive studies of *pmk-3(lf)* mutants have not been able to detect any germline phenotype other than the Gla phenotype. This suggests that the main function of PMK-3 in the germ line is to promote germ cell survival. Using a hypothesis-driven approach, I have identified MTK-1 and MKK-4 as the upstream kinases of the pathway, and the transcription factor MEF-2 as a possible mediator of PMK-3's anti-apoptotic activity. Of course, many more experiments are required to definitely understand how this p38 MAPK pathway regulates physiological germ cell death. We need to focus on the genes upstream of MTK-1 to find what triggers the kinase cascade, and on the MEF-2 targets to clarify how PMK-3 blocks apoptosis and/or promote cell survival: a genetic suppressor screen could address the first question, and microarray experiments the second. To my view, *pmk-3* is the only *gla* gene studied now which is susceptible to give us answers concerning the regulation and mechanistic of physiological germline apoptosis; as such, I consider its study a very promising project which deserves more interest.

6.2 Physiological Germ Cell Death: Past, Present, and Future

Since the first description of physiological germline apoptosis (Gumienny et al., 1999), the Hengartner laboratory has spent time and resources trying to understand what regulates this cell death pathway. The truth is that we are still a long way to answer this question. In the last few years, it has become apparent that some of the germ cell deaths that occur 'physiologically' in wild-type worms are due to genetic defects sensed by the DNA damage pathway. This is reflected by the fact that various mutants (*cep-1(lf)*, *hus-*

1(lf), *ced-9(gf)*, etc.) defective in apoptotic responses to genotoxic treatments have less germline apoptosis that wild-type worms in a normal 'un-stimulated' situation (Lettre et al., 2004). This is not a surprising result since the elimination of impaired oocytes by apoptosis is a process conserved throughout evolution (Tilly, 2001). Therefore, it seems reasonable to believe that ~30% of physiological germ cell deaths are actually due to endogenous damage (i.e. meiotic pairing or recombination anomalies). So, how do we explain the remaining 70%?

Two other hypotheses have been proposed to explain oocyte apoptosis: competition for growth/survival factors, or the nurse cell behavior (Tilly, 2001). Unfortunately, there are no data to support or disprove neither of these two models in *C. elegans*. We know three pathways that are essential for germline apoptosis: GLP-1/Notch, Ras/MAPK, and the core apoptotic machinery. The latter requirement is obvious: in the absence of the adaptor CED-4 and the caspase CED-3, germline apoptosis cannot occur. The GLP-1/Notch signaling pathway regulates the proliferative versus meiotic entry decision of germ cells in the *C. elegans* hermaphrodite gonad. Mutations that activate the pathway prevent germ cells to enter meiosis; these mutants have tumorous germ lines, and these tumors do not contain apoptotic germ cells. Therefore, germ cells must enter meiosis to undergo apoptosis. During meiotic progression, germ cells arrest at the pachytene stage of prophase I; only when the Ras/MAPK pathway is activated can germ cells progress through pachytene and carry on development. Inactivation of Ras/MAPK by mutations block meiotic progression, and germline apoptosis. In conclusion, germ cells must not only enter meiosis, but also escape the pachytene arrest checkpoint, to die by apoptosis. We know that over-activation of Ras/MAPK can lead to increased p53-independent germ cell death (E. Kritikou, personal communication). However, it remains to be determined whether physiological germ cell death is due to the activation of MAPK above a critical threshold in some cells. And if this is the case, we need to investigate what regulates MAPK activation in the germ line. All these observations draw a clear link between proper germ cell development and apoptotic death, but do not explicitly address the biological significance of physiological germline apoptosis in *C. elegans*.

Could transcriptional up-regulation of *ced-4* and *ced-3* causes physiological germ cell death? This model would have the advantage to easily explain why *egl-1(lf)* and *ced-9(gf)*

mutations do not block physiological germline apoptosis, since CED-4 and CED-3 act downstream of EGL-1 and CED-9 in the apoptotic cascade. *A priori*, there is no argument against such a model, although transcriptional regulation of caspase expression seems an unusual way to control apoptotsis. In fact, in an attempt to test this hypothesis, I tried to create transgenic lines with reporter constructs for *ced-4* and *ced-3*. Unfortunately, I have been unable to identify the regulatory sequences required for *ced-4* or *ced-3* transcription, and therefore those experiments were never perfomed. However, my failed attempt should not ruled out this quite exciting possibility. I can easily imagine a model where a signaling cascade (Ras/MAPK?) activates a transcription factor essential for the expression of *ced-4* and/or *ced-3* in the germ line.

My experience in studying germ cell death in *C. elegans* leads me to propose one genetic screen, long and painful, to identify genes responsible for physiological germ cell death: a Nomarski-based screen for suppressors of germline apoptosis in a *cep-1(lf); ced-6(lf)* mutant background. I would use a parental strain with a loss-of-function mutation in *cep-1* such that all germ cell deaths arise independently of the p53 pathway, and a mutation in an engulfment gene to increase the number of observable apoptotic germ cells. Because un-engulfed corpses do not stain with acridine orange, Normarski microscopy would be required for screening. To me, it now seems a better strategy to use an engulfment mutant background rather than mutations in other *gla* genes, such as *gla-1* or *gla-3*, in the parental strain because in the engulfment mutant, the increased number of apoptotic germ cells is not caused by developmental defects during oogenesis. This screen should specifically target genes involved in the physiological germ cell death pathway. A similar approach, without the *cep-1* mutation, was used in Barbara Conradt's laboratory (Dartmouth College) to identify novel regulators of germ cell apoptosis, but no results have so far been published.

6.3 DEVELOPMENTAL APOPTOSIS IN *C. ELEGANS*

Already in 1951, Glücksmann recognized the importance of programmed cell death during metazoan development (Glücksmann, 1951). He divided developmental apoptosis in three categories: (1) phylogenetic apoptosis, i.e. the elimination of embryonic cells or structures of an evolutionary ancestor that are no longer needed in the adult, such as the

tadpole's tail, (2) morphogenetic apoptosis, which acts as a type of organ sculpting, for instance to eliminate the webbing between digits, and (3) histogenic apoptosis, which removes cells following tissue maturation or remodelling, such as neuronal death when neurons fail to establish synaptic connections with their targets.

In *C. elegans*, none of these three forms of apoptosis can explain why, out of the 1090 somatic cells that are born in a hermaphrodite, 131 undergo apoptosis. Of course, apoptosis in the worm can be used to eliminate useless cells, such as the hermaphrodite-specific neurons (HSNs) in males (HSNs are required for egg-laying, a useless task for males). However, apoptosis does not seem to play an important role during *C. elegans* development: the fitness of *ced-3* null mutants is comparable to wild-type worms in physiological conditions, and these mutants do not have aberrant organs or behaviors. On an evolution point of view, this observation does not make sense: why would a species spend some much energy to maintain genes involved in a dispensable process?

One possibility is that apoptosis is actually important for *C. elegans* development, but we have just been unable to obtain mutants with no cell death at all. Indeed, strains with the strongest mutations in *ced-3* or *ced-4* still have some apoptotic deaths (Shaham et al., 1999). The *C. elegans* genome has three genes, other than *ced-3*, that encode putative caspases; it is possible that these proteins play minor roles during programmed cell death in the worm (Shaham, 1998). My favorite explanation is that development is not the main purpose of apoptosis in the worm. Indeed, it is known that *ced-3* and *ced-4* mutants are hyper-susceptible to *Salmonella typhimurium* infections (Aballay and Ausubel, 2001). *C. elegans* is a soil nematode, likely to encounter pathogens in its native environment. It is unknown how the apoptotic machinery protects *C. elegans* against infections, but it could well be that the main function of apoptosis in worms is in innate immunity. Maybe programmed cell death during *C. elegans* development is a by-product of the role of apoptosis in innate immunity, and that the worm is just too simple to re-wire genetic networks that are useless, but at least not detrimental.

However, having said that one has to recognize that the main reason why *C. elegans* has become such a powerful system to study apoptosis is because apoptosis is not essential for its development. Just for this reason, it is hard to argue that apoptosis is an unimportant process in *C. elegans*…

6.4 Forward vs. Reverse Genetic Screens in *C. elegans*

During my doctoral studies, I performed one forward (Chapter 5) and one reverse genetic screen (Chapter 3). Looking back at the outcome of those screens, it is hard to argue which one is better. Of course, the RNAi screen yielded several genes, but genetic characterization of these RNAi candidates was proven difficult. The bottom line is that genetic mutants are required to convincingly show that genes uncovered by RNAi are involved in a specific biological process. And this brings us to the classical genetic screen, where mutants can be 'easily' isolated and extensively characterized. But then, intense effort is required, and not always successful, to clone the genes. Clearly, both approaches are compatible and complementary, with strengths and weaknesses. I can hardly imagine a *C. elegans* laboratory that would, in this post-genomic era, refuse to use both of these two methods to study any aspect of biology.

6.5 Concluding Remarks

The past of apoptosis research in *C. elegans* has been glorious. It was recognized in 2002 when the Karolinska Institut awarded Sydney Brenner, H. Robert Horvitz, and John E. Sulston the Nobel Prize in Physiology or Medicine for their work on organ development and programmed cell death. Certainly, genetic screens in *C. elegans* will identify other genes involved in apoptosis. However, I am skeptical regarding the importance of the new discoveries and doubt that genes as important as *ced-3* or *ced-9* will be cloned. This is emphasized by the fact that most of the worm apoptotic genes identified recently have either a minor role during apoptosis (e.g. *nex-1*, *cps-6*, *crn-1*), or are supported by controversial evidences (e.g. *icd-1*, *psr-1*, *wah-1*). It is possible that the scientific community has identified most of the very important apoptotic genes (not only in *C. elegans*, but in all species), and that the genes that remain to be cloned will have species-, tissue-, or even cell-specific effects.

There has always been intense competition among apoptologists to discover the next 'big thing'. Now that the mouse and human genomes are sequenced, and that loss-of-function phenotypes can easily be obtained in mammalian cells by RNAi, competition will even get worse. I sometimes wonder how long will apoptosis research in *C. elegans*

thrive in such an environment? For sure, we have to stop repeating what has already been discovered in other systems. *C. elegans* is a powerful 'forward' genetic model organism: work must be focus on the identification of novel genes, and not the characterization of homologues of genes from other species. The recent history of *C. elegans* research tells us that the worm has been formidable to discover new pathways (e.g. apoptosis) or phenomenon (e.g. RNAi), but not to explore already characterized genes from other species. Moreover, there are certainly enough genes in the *C. elegans* genome without assigned functions to occupy many graduate students for several years. Let's wait to see how the future of apoptosis research will treat the worm…

6.6 REFERENCES

Aballay, A., and Ausubel, F. M. (2001). Programmed cell death mediated by *ced-3* and *ced-4* protects *Caenorhabditis elegans* from *Salmonella typhimurium*-mediated killing. Proc Natl Acad Sci U S A *98*, 2735-2739.

Glücksmann, A. (1951). Cell deaths in normal vertebrate ontogeny. Bio Rev *26*, 59-86.

Gumienny, T. L., Lambie, E., Hartwieg, E., Horvitz, H. R., and Hengartner, M. O. (1999). Genetic control of programmed cell death in the *Caenorhabditis elegans* hermaphrodite germline. Development *126*, 1011-1022.

Lazebnik, Y. (2002). Can a biologist fix a radio?--Or, what I learned while studying apoptosis. Cancer Cell *2*, 179-182.

Lettre, G., Kritikou, E. A., Jaeggi, M., Calixto, A., Fraser, A. G., Kamath, R. S., Ahringer, J., and Hengartner, M. O. (2004). Genome-wide RNAi identifies p53-dependent and -independent regulators of germ cell apoptosis in *C. elegans*. Cell Death Differ *11*, 1198-1203.

Shaham, S. (1998). Identification of multiple *Caenorhabditis elegans* caspases and their potential roles in proteolytic cascades. J Biol Chem *273*, 35109-35117.

Shaham, S., Reddien, P. W., Davies, B., and Horvitz, H. R. (1999). Mutational analysis of the *Caenorhabditis elegans* cell-death gene *ced-3*. Genetics *153*, 1655-1671.

Tilly, J. L. (2001). Commuting the death sentence: how oocytes strive to survive. Nat Rev Mol Cell Biol *2*, 838-848.

GUILLAUME LETTRE

CONTACT ADDRESS

Institute of Molecular Biology, University of Zurich
Winterthurerstrasse 190, 8057 Zurich, Switzerland
Telephone ++41-1-635-3114
Fax ++41-1-635-6864
Email guillaume.lettre@molbio.unizh.ch

PERSONAL INFORMATION

Date of birth	May 12 1978
Citizenship	Canadian
Languages	English and French
Marital status	Single

EDUCATION

2001-2005 University of Zurich — Zurich, Switzerland
PhD in molecular biology
Doctoral studies in Professor Michael Hengartner's laboratory. Thesis title: Genetic regulation of apoptosis in the germ line of *C. elegans*. Expertise developed in genetics, molecular biology, bioinformatics, and functional genomics (RNAi screen). Teaching assistant for practical courses in molecular biology.

2000-2001 Watson School of Biological Sciences — New York, USA
Cold Spring Harbor Laboratory
MSc in biological sciences
Topics covered include cancer biology and genomics. Special course on scientific exposition and ethics. Three-months (part-time) teaching experience.

1997-2000 Université de Sherbrooke — Québec, Canada
BSc in biotechnology
Focus on biochemistry and molecular biology.

PUBLICATION

Guillaume Lettre, Ekaterini A Kritikou, Martin Jaeggi, Andrea Calixto, Andrew G Fraser, Ravi S Kamath, Julie Ahringer and Michael O Hengartner (2004) Genome-wide RNAi identifies p53-dependent and -independent regulators of germ cell apoptosis in *C. elegans*. Cell Death Differ. 2004 November; 11(11): 1198-1203.

RECENT AWARDS

2004 'Kuratorium der Julius Klaus-Stiftung' Fellowship

	To attend the 'Working with the human genome sequence' course at The Wellcome Trust Sanger Institute (U.K.).
2002	'Fonds Québécois de la Recherche sur la Nature et les Technologies' Doctoral Studies Scholarship Award granted based on the highest level of achievement.
2001	National Sciences and Engineering Research Council of Canada (NSERC) Postgraduate Scholarship This award recognizes academic excellence, research ability and potential, and leadership and communication skills.

INTERESTS

Scientific	• Classical genetics, that is, the beauty and power of the phenotype-genotype approach. • Study of complex genetic paradigms in developmental biology. • The post-human genome sequencing project revolution in human genetics, and its implications for our society. • New technologies (*e.g.* functional genomics) developed to analyze the enormous amount of DNA sequences available.
Others	Ice hockey, climbing, modern history

FAX ++41-1-635-6864 • E-MAIL guillaume.lettre@molbio.unizh.ch
WINTERTHURERSTRASSE 190 • ZURICH, SWITZERLAND • PHONE ++41-1-635-3114

Supplementary Table I : Primer list

Guillaume Lettre's primers - BOX 1

PRIMER NAME	SEQUENCE	PURPOSE	LOCATION
			BOX 1
T21C12(12057)_Fwd	ACAAATCCAAGCGTCTGCC	SNP	1
T21C12(12057)_Rev	GAAAACCGTCAAATTGCTGG	SNP	2
K11D9(29813)_Fwd	CACGGAAATAGACGACACTCAC	SNP	3
K11D9(29813)_Rev	TTCAGTGGAAAAGTTCGACGTC	SNP	4
T28D6(5428)_Fwd	TTTCGTGTACGAACGTCTCC	SNP	5
T28D6(5428)_Rev	CATTTCTCCCACTCTTGCTG	SNP	6
Y47D3B(87052)_Fwd	TGTGCCTACGTGGATTAATTG	SNP	7
Y47D3B(87052)_Rev	AAATTGGACGGAGCTTGG	SNP	8
Y41C4A(128611)_Fwd	ATTTTTGTGAATTCCAGGGC	SNP	9
Y41C4A(128611)_Rev	TTTCAGCCAAAAAGCTCTGA	SNP	10
Y56A3A(149135)_Fwd	TCAACTACGACGACGCTGAC	SNP	11
Y56A3A(149135)_Rev	CGGTGTTTTCAGACAATTTCG	SNP	12
ced9LB/Asc/Not_S	GCGTGGGCGCGCCATGGGCGGCCGCACACGC TGCACGGCGGAC	To lazyboy ced-9 (add NotI site N-ter)	13
ced9LB/Fse_AS	CGCAGGCCGGCCTTACTTCAAGCTGAACATC	"	14
ced9_cDNA_S_468	TGGAAATGCACAGACAGATC	To sequence ced-9 from position 468 (cDNA)	19
eft-3 prom. Seq LB S	TTGGCCAAAGGACCCAAAGG	To sequence pBMB.LBeft-3 lazyboy cassette from eft-3 promoter	15
poly-A seq LB AS	GAGGCACGGGCGCGAGATGG	To sequence pBMB.LBeft-3 lazyboy cassette from poly-A sequence	16
Y47D3B(67807)MaeIII_ Fwd	CTCATGCTGTGCACAAACAACAATC	SNP	17
Y47D3B(67807)MaeIII_ Rev	GCAGCGTATCAAGCTTACATGTACT	SNP	18
W09D10(7357)BstBI_F wd	TCTGGTGGAAGTGTTAATTGGAATG	SNP	20
W09D10(7357)BstBI_R ev	TTTATGGTTGTTCGCAATGGAAAGG	SNP	21
Y48A6C(3473)BspMI_F wd	ATTCGGTATTCCGATCAATTTTACC	SNP	22
Y48A6C(3473)BspMI_ Rev	TTGACCGAAACCTGTTAGAAATGAC	SNP	23
5'GFPYFPNotI	ATGGGCGGCCGCAGTAAAGGAGAAGAA	To create GFP & YFP NotI cassette - YFP did not work!	24
3'GFP-NotI	TGTGCGGCCGCCCTTGTATGGCCGGCTAG	"	25
C09D4_37465'	TGACTCTGCATGATAGAACATCGTC	SNP	27
C09D4_37463'	TCTGTCTCGGAAACTGGTATGTTTT	SNP	28
F18C122332235	TTTTCCTTTGTTGCAGTTTTCCATG	SNP (did not work - use other primers)	35
F18C122332233	AAAATTGAGCCATTTAAAGCGATCC	SNP (did not work - use other primers)	36
K02B12152185	AAAACAGAAATTTGAAGGGATGGAG	SNP	37
K02B12152183	TCAAATTTGGCACGTCATCAGTTTT	SNP	38
K04F10196185	CTTTACCAGTGATCGGGATTCCATT	SNP	29
K04F10196183	CCCGACATCACTATAACTACCTCCG	SNP	30
F21C3183375'	ACCTGCAATATGTGTATATGGAATC	SNP (did not work - use other primers)	31
F21C3183373'	TCGTACAATTCCTCTAGAGTTGTGT	SNP (did not work - use other primers)	32
T23G1190645'	ATGACACAAATAACAACAAACTGGC	SNP (did not work - use other primers)	33
T23G1190643'	TTGAGTCACTGGATGTTTCTTCGAA	SNP (did not work - use other primers)	34
F21C3(18337)MwoI_Fw d	AGCAGATTGAGGCTGAAATATGGTG	SNP	39

F21C3(18337)MwoI_Rev	TCAAGTCGAGCAGCACCAGTTATTG	SNP	40
T23G11(9064)DdeI_Fwd	CGTATACATCTCTGCGTGGCTCTTC	SNP	41
T23G11(9064)DdeI_Rev	CTTCGAATCCATATCGATGCGACGG	SNP	42
F18C12(23323)AclI_Fwd	TTGAATCACCGCCAACATGAGAAC	SNP	43
F18C12(23323)AclI_Rev	GCCAGTGTCCCGATAGAAAACACC	SNP	44
F46F11(29076)NlaIII_Fwd	AGTAGTTGGTATTCACCGAAATCAG	SNP	45
F46F11(29076)NlaIII_Rev	GTGAGTATGCCTTTAAAGAGTACTG	SNP	46
C04F1(3815)MaeIII_Fwd	GTTCTTCTCATTGTTTTCTTCTGGG	SNP	47
C04F1(3815)MaeIII_Rev	CTATAGATGCTAGACAACAAGACGC	SNP	48
C34G6(15466)BstBI_Fwd	CTCTGAATTTTTCTGTAAAGGCACC	SNP	49
C34G6(15466)BstBI_Rev	ATTTCACTTAAAATCAGAAGGCGCC	SNP	50
B0207(42124)SspI_Fwd	AATTGTGAATTCTACAGGAAGGGTG	SNP	51
B0207(42124)SspI_Rev	GTAACGACCCACAAAATCATCCGAG	SNP	52
C06A5(19725)DraI_Fwd	GATTTTTTAAAGGAAACCTCGGAGG	SNP	53
C06A5(19725)DraI_Rev	TCCGTAAAGCAGCTTCAAAATAGGT	SNP	54
T27A3(18348)AlwNI_Fwd	ATAAAGTTATTGCATGTCTACCGGG	SNP	55
T27A3(18348)AlwNI_Rev	TTGAGATCTCAAACTTTTCGTGTGG	SNP	56
B0414_2F	GAATTGAAGAAGACTGTTGGCGG	To sequence exon 4 of gla-1 (where op234 is)	57
B0414_2R	GATACGGCAGGTAGGTCAACCAC	"	58
Y47D3A48624F	TCAGATGTGTAGAACGATCAAGAAG	SNP	59
Y47D3A48624R	ACATCTCTATGCCGAGCACTTATAC	SNP	60
Y47D3A89471F	TGAGTTCTTCGTTCTGGAAAATTAC	SNP	61
Y47D3A89471R	CTGGATCCTTATAAAGGAACATTTC	SNP	62
rab35_ex1_s	TCTTGGGAAATTTGGGTCAAAACTG	To sequence exon 1 of rab-35	63
rab35_ex1_r	CTAAGTTTCTGCTGAATTTTCTGGG	"	64
rab35_ex2-3_f	TCAGCTGAAAAGCTGCTTCTGCTCC	To sequence exons 2 & 3 of rab-35	65
rab35_ex2-3_r	TGTGTTCCTATAATACTGAAAATAG	"	66
rab35_ex4_f	CCCCACCTTTAAGTTAATTGTTGAG	To sequence exon 4 of rab-35	67
rab35_ex4_r	ACACTAAAAAGTTCCGAAAATGATG	"	68
rab35_ex5_f	TAATTTAGGAAGGAGGGGAAAACAG	To sequence exon 5 of rab-35	69
rab35_ex5_r	AAAAGCGTAAGGATTGGAATAATTC	"	70
rab35(ex1)Fwd2	CCCTTAGAAAATTTGATGCCTAACC	To sequence exon 1 of rab-35	71
rab35(ex1)Rev2	AAAACCCCCAATTTCCAGGCTTCTG	"	72
rab35(ex2)Fwd2	CCAAATTTGTCTCTGAAATTCATAG	To sequence exon 2 of rab-35	73
rab35(ex3)Rev2	GTACAATTACATCGACGTATGGCG	To sequence exon 3 of rab-35	74
rab35(ex5)Fwd2	GCAGTCGATCGATTTGGAAATTGGG	To sequence exon 5 of rab-35	75
rab35(ex5)Rev2	TAGGCCACTTTTTGAGCCGTCGTC	"	76

Guillaume Lettre's primers - BOX 2

PRIMER NAME	SEQUENCE	PURPOSE	LOCATION
			BOX 2
F08A8(3890)TaqI_Fwd	ATGACAGGGTTCGATTAATCTCAAG	SNP	A1

F08A8(3890)TaqI_Rev	CTTCTCGTCTCACATGCTGGAATTC	SNP	A2
Y26D4A(7397)AatII_Fwd	GCGACGCAATTCTTCCTATGCAAGG	SNP	A3
Y26D4A(7397)AatII_Rev	CTTGGCGCCAAAATTGGTCAGTTGG	SNP	A4
ZK1053(4253)MwoI_Fwd	CAGAAATATCCTAACAGTTTTGGGG	SNP	A5
ZK1053(4253)MwoI_Rev	TGCGTGTTTGAAATGCATCATCTTG	SNP	A6
pkP1135-MaeI_Fwd	CTCTTCTTCTCCCTTTGACTCATCC	SNP	A7
pkP1135-MaeI_Rev	GACGGTGAAGAGAAATCAAATTTGG	SNP	A8
Y87G2A(21607)MnlI_Fwd	ACTACACACATTTTGAGCCTCAACC	SNP	A9
Y87G2A(21607)MnlI_Rev	GTGCAAAAAGTTTTTGGGTCGATTC	SNP	A10
Y47D3A(126441)Seq_Fwd	GTGAAAGTTAATGGGCCGTAAATAG	SNP	B1
Y47D3A(126441)Seq_Rev	CACGTTCTTAACCATGCGAAATTAG	SNP	B2
Y47D3A.26_Fwd	CTTGAAATTGACTCGTTGAATGAGG	SNP	B3
Y47D3A.26_Rev	TGAATAACTCCTACCGATTTCTGTC	SNP	B4
M13_Reverse	CAGGAAACAGCTATGAC	Colony PCR - TOPO cloning	B5
M13(-20)_Forward	GTAAAACGACGGCCAG	Colony PCR - TOPO cloning	B6
pREP1_MCS	TTTCAATCTCATTCTCACTT	To sequence the insert of the pREP vectors	B7
ced3_5'NdeI	TTGTTAAATCATATGATGCGTCAAGATAG	To clone ced-3 in frame in the pREP vectors	B8
ced3_3'XhoI	TTATGATGAGGCACATTCCACG	"	B9
Y47D3A.28_Fwd	GACGGCCAACGATGCAGTAATTTTG	SNP	B10
Y47D3A.28_Rev	CATGTCACCGCGTTGAACACACCTG	SNP	C1
ced3_5'SalI	AATCATATGTCGACTATGATGCGTCAACATAG	To clone ced-3 in frame in the pREP vectors	C2
ced3_3'SalI	CGTCTCGATTGTCCCATCCACG	To clone ced-3 in frame in the pREP vectors	C3
T28D6.6_Fwd	GCCAAAATTCAACTGCTCGATTTAC	SNP	C4
T28D6.6_Rev	CCTGATTATCATAACGAGACCGCTG	SNP	C5
Y47D3A.gg_Fwd	CTGTATTTTTCCAATTTTGGCTG	SNP	C6
Y47D3A.gg_Rev	CTCACTAATCCTGATGGTTCTGG	SNP	C7
opP113(Y18D10A)BstUI_Fwd	GCTGCGCTTGTGTCGATTTACG	SNP	C8
opP113(Y18D10A)BstUI_Rev	GGGGGCGATCGAATTTGTGAAC	SNP	C9
F22G12(21724)BbsI_Fwd	TTTTGAGTGATTTTCTGCTTGGCAG	SNP	C10
F22G12(21724)BbsI_Rev	TGGCTGGGAATTTCAATTAACAACC	SNP	D1
Y18D10A.17(ex1-2)Fwd	ATTCTCCTATTCCCGACAATATTGC	To sequence exons 1-2 from gene Y18D10A.17	D2
Y18D10A.17(ex1-2)Rev	GTTGTTGTATCCACGGTTAGCTTGG	To sequence exons 1-2 from gene Y18D10A.17	D3
Y18D10A.17(ex3-4)Fwd	CGTCCAGGACGTGGAGGTTATCAGC	To sequence exons 3-4 from gene Y18D10A.17	D4
Y18D10A.17(ex3-4)Rev	GGGTATGGGGATGTGGGGAGAAAAC	To sequence exons 3-4 from gene Y18D10A.17	D5
oJL102	CAACCTTGACTGTCGAACCACCATAG	Mos mutagenesis	D6
oJL103	TCTGCTAGTTGTTTTTGCGTTTGAG	Mos mutagenesis	D7
oJL104	ACAAAGAGCGAACGCAGACGAGT	Mos mutagenesis	D8
oJL114	AAAGATTCAGAAGGTCGGTAGATGGG	Mos mutagenesis	D9
oJL115	GCTCAATTCGCGCCAAACTATG	Mos mutagenesis	D10
oJL116	GAACGAGAGGCAGATGGAGAGG	Mos mutagenesis	E1
IPCR1a	GACCTTGTGAAGTGTCAACCTTGACTG	Mos mutagenesis	E2
IPCR1b	GACAATCGATAAATATTTACGTTTGCGAGAC	Mos mutagenesis	E3

IPCR2b	CATCTATATGTTCGAACCGACATTCCC	Mos mutagenesis	E4
teg-1(ex1-2)Fwd	CCAGGCTGAGATCGATTTTCCTCCG	To sequence exons 1-2 of teg-1	E5
teg-1(ex1-2)Rev	CTCATTTTCCGCGCATAATCCCAAC	To sequence exons 1-2 of teg-1	E6
teg-1(ex3)Fwd	ATTGAGCGTAGCATGAATTTTCTGG	To sequence exon 3 of teg-1	E7
teg-1(ex3)Rev	AAATTTCCGGTAAACCGACAATTGC	To sequence exon 3 of teg-1	E8
teg-1(ex4)Fwd	TCCTCTGAAATCAGTAAAAATTGGG	To sequence exon 4 of teg-1	E9
teg-1(ex4)Rev	TTGGTGAAAAACATCAAAAATAGCG	To sequence exon 4 of teg-1	E10
teg-1(ex5-6)Fwd	GAGATAGAGAGTGAAAACGAGATTC	To sequence exons 5-6 of teg-1	F1
teg-1(ex5-6)Rev	TTCAGTCAAGACAAAGTCAAAATGC	To sequence exons 5-6 of teg-1	F2
teg-1_Gateway_Fwd	GGGGACAAGTTTGTACAAAAAAGCAGGCTTGC CGAAACGCGCCGTTTCTTTCGCC	Creation of a Gateway teg-1 genomic DNA cassette	F3
teg-1_Gateway_Rev	GGGGACCACTTTGTACAAGAAAGCTGGGTTTA CAAATAAAGCTCGAAATCAATTCTGGC	Creation of a Gateway teg-1 genomic DNA cassette	F4
MFG-E8_AscI(5')	TACAGGCGCGCCATGCAGGTCTCCCGTGTG	To lazyboy MFG-E8. Add AscI at 5' end	F5
MFG-E8_NotI_FseI(3')	CTTAGGCCGGCCTTAATTAATTAGCGGCCGCC ACAGCCCAGCAGCTCCAG	To lazyboy MFG-E8. Add NotI & FseI at 3' end	F6
MFG-E8(449-468)	CACAGCTGGGCATGGAAGGG	To sequence MFG-E8. Numbers correspond to cDNA	F7
teg-1_5'_3'UTR	TATATATAGCGGCCGCTGATGTTGGGTTGCAG AAGCCTGG	To create a NotI teg-1 cassette (promoter-teg-1-3'UTR)	F8
teg-1_3'_promoter	AATTTAATGCGGCCGCCTGAAAATTGAACAATT TGTGGAAAATTTCAGCG	To create a NotI teg-1 cassette (promoter-teg-1-3'UTR)	F9
MFG-E8(979-)	CAGATGTCAGCCTCCAGCAG	To sequence MFG-E8 from bp 979 of cDNA	F10
pkP2116.IIR(DraI)Fwd	TCAATTTCTTTCCCATTTTCCTCCC	BSA, Chromosome II, right arm	G1
pkP2116.IIR(DraI)Rev	TTCAAAAACCCAGACACTGGATCGC	BSA, Chromosome II, right arm	G2
Y92C3A.IIIL(13164)AatII_Fwd	CCTAAGCCAAACTTTCCGTCTAAAC	BSA, Chromosome III, left arm	G3
Y92C3A.IIIL(13164)AatII_Rev	GCCACACGGCCTGAATTATCAATAC	BSA, Chromosome III, left arm	G4
gla-1(WT)Fwd	CCTCGAAAGTACATGCTGTATGGTATG	To genotype gla-1(op234). WT band of 530 bp.	G5
gla-1(WT)Rev	TGTTGGCGGAGTCGAAAACTCTGTG	To genotype gla-1(op234). WT band of 530 bp.	G6
gla-1(op234)Fwd	GAAACAGTGTGCTGACTGCGAATTAT	To genotype gla-1(op234). Mutant band of 374 bp.	G7
gla-1(op234)Rev	AGGTACAAATCATTCCATGGGTTACC	To genotype gla-1(op234). Mutant band of 374 bp.	G8
CNX-1.1(FWD)	AGGTAACCATGGTGAACCGGAAATG	To find deletion in cnx-1 mutants	G9
CNX-1.1(REV)	CTTGACCTTCCTCAAACTTGATGTC	To find deletion in cnx-1 mutants	G10
CNX-1.2(FWD)	TGATGCGAATACTTTCGTTGTTCAG	To find deletion in cnx-1 mutants	H1
CNX-1.2(REV)	TAGGTTTTATAGGCATTCGGTGAAG	To find deletion in cnx-1 mutants	H2
Y26D4.2_Fwd	TCTTCTCCTGATGACTCTGTGTTTG	New SNP around op199	H3
Y26D4.2_Rev	TTAACCGGACACAACTGGAAGACAG	New SNP around op199	H4
C17H1.5(Intron2)Fwd	TGTTTCACAGCCCCACAACATCAGC	New SNP around op199	H5
C17H1.5(Intron2)Rev	TTTGCACGTTGCAGCTCAACTTTTC	New SNP around op199	H6
F17B5.2_Fwd	GAAGCCTCGAACCTGATGGATCTTC	New SNP around op199	H7
F17B5.2_Rev	ACTGCGCCACTTGACCATTTTCAGG	New SNP around op199	H8
ZK1225.1_Fwd	AGACCGTGCTCAACGAAGTTGGATC	New SNP around op199	H9
ZK1225.1_Rev	CCTGGAAATCATTCAAGAGCAGTTG	New SNP around op199	H10
K10G9.3_Promoter_Fwd	TACAGGCGCGCCGATTTTTATTAATACGTGGTG TCAGGC	To amplify and AscI C21ORF80 promoter	I1
K10G9.3_Promoter_Rev	TACAGGCGCGCCCTGGAAAATCGAGAGATTTT GAGG	To amplify and AscI C21ORF80 promoter	I2
K10G9.3_3'UTR_Fwd	TACAGGCCGGCCATTATTTTTTGTATAATATATT ACGGATCTC	To amplify and FseI C21ORF80 3'UTR	I3
K10G9.3_3'UTR_Rev	TACAGGCCGGCCACTTTTTATGTGATTCACAAG TGATTAG	To amplify and FseI C21ORF80 3'UTR	I4
K10G9.3_Gene_Fwd	TACAGGCGCGCCATGGGCGGCCGCCATTTCTT TCCAATTCAATTACTGG	To amplify and lazyboy C21ORF80 gene	I5
K10G9.3_Gene_Rev	TACAGGCCGGCCTTAATAAACTATTTTCCATTT GGCCG	To amplify and lazyboy C21ORF80 gene	I6
K10G9.3_Exon1_Rev	TAAATCGCCACATGGCAGAG	To sequence C21ORF80	I7

K10G9.3_Exon2_Fwd	AGAGACGGCTCGCCAAGAC	To sequence C21ORF80	I8
K10G9.3_Exon3_Rev	GACAACTTTATGTTGCTATAAC	To sequence C21ORF80	I9
K10G9.3_Exon4_Rev	ATAATCTCAAAGCAGACTCC	To sequence C21ORF80	I10
F17B5.4_Fwd	TAACGAAGAAAGTTCAGTTTTGTTG	New SNP around op199	J1
F17B5.4_Rev	CAACTGCTATAGAACCTTCGTTTGAG	New SNP around op199	J2
C17H1.4-5_Fwd	CAATGGTTTCAACGAATATGGATGC	New SNP around op199	J3
C17H1.4-5_Rev	TTTTGCACCTATGGAGGGTTTTGTC	New SNP around op199	J4

Guillaume Lettre's primers - BOX 3

PRIMER NAME	SEQUENCE	PURPOSE	LOCATION
			BOX 3
F17B5.1(ex1-2)F	CATTCATTTTTATTGAAGTTTGGGC	To sequence F17B5.1	A1
F17B5.1(ex1-2)R	AATTCGACTCATCGTCTTGATTATCAC	To sequence F17B5.1	A2
F17B5.1(ex3)F	CCATAGAAGTTCAACAATTTCTTGTGG	To sequence F17B5.1	A3
F17B5.1(ex3)R	GTAATGAGCAAATCACTGTAGGCAAG	To sequence F17B5.1	A4
F17B5.1(ex4-5)F	TTGGGATTATTATTGGGATGGTAGG	To sequence F17B5.1	A5
F17B5.1(ex4-5)R	AAATGTGAGAGTCCTGGATAGCAATC	To sequence F17B5.1	A6
F17B5.1(ex6-7)F	ATGAGCAGTAGGAGAAAATCGGATG	To sequence F17B5.1	A7
F17B5.1(ex6-7)R	TGAAAACCAACCTGTCAAGAATCTG	To sequence F17B5.1	A8
F17B5.1(ex8)F	AAGATGAGGTTATAGCTTTGGTTGTTG	To sequence F17B5.1	A9
F17B5.1(ex8)R	TTTCTGTCAAGAATGCAATTTCAGG	To sequence F17B5.1	A10
F17B5.1(SeqEx8)F	AAAACGCAAGAAAGAGTTGG	To sequence F17B5.1	B1
F17B5.1(SeqEx8)R	GCCTAGCTTTCTCTTCTGCG	To sequence F17B5.1	B2
R05D3.4(ExtLeft)	CATTTCCGTCTCTTGACCGT	To detect ok572	B3
R05D3.4(ExtRight)	CATTTGTCGATTCGCTTCCT	To detect ok572	B4
R05D3.4(IntLeft)	TCTCTCACTCAGGTCTCGCA	To detect ok572	B5
R05D3.4(IntRight)	AATCTTCGATTTCACGTGCC	To detect ok572	B6
pmk-3(ok169)Fwd	CCCATTTTTCACTGCGTCTCAATCG	To detect ok169	B7
pmk-3(ok169)Rev	TCTGCTTCTCCAGGGATTAACGGTG	To detect ok169	B8
pmk-3(WT)Rev	TCGGGGGAAATTAGAGGAGTGTCGG	To detect pmk-3(wt)	B9
C17H1.4(Fwd)	TAGCAATAAATTGCTAACCCAGAGAAT	To find SNP around op199	B10
C17H1.4(Rev)	GTCGAAAAATCACGTGTAAAAGCT	To find SNP around op199	C1
C17H1.8(Fwd)	CAGTATCCCAACCCATGCATATAAC	To find SNP around op199	C2
C17H1.8(Rev)	CGTTGCCTAAAACAAATATGGGTAC	To find SNP around op199	C3
pkP5114(AluI)Rev	TTCAAAACTGGCGTTGACGAAATC	SNP around op385	C4
pkP5114(AluI)Fwd	AGAGAGCGAGATCTTCACAGCAAG	SNP around op385	C5
pkP5063(HinfI)Fwd	ACCACGGCCTTCAAAAGAGTAC	SNP around op385	C6
pkP5063(HinfI)Rev	TTCTGCAAGAGAGTGACAGGTC	SNP around op385	C7
pkP5064(DraI)Fwd	TCTCTTAGATACCCTTTCTGCGCC	SNP around op385	C8
pkP5064(DraI)Rev	CATTCAGCGTTTGGTCTGACGTAG	SNP around op385	C9
pkP5093(BspHI)Fwd	TTTCAGCTAGACCTCCCATGCG	SNP around op385	C10
pkP5093(BspHI)Rev	ATATCAATCACATGATGCCGT	SNP around op385	D1
pkP5124(DraI)Fwd	TTCGGGATCTGTTTGGATTTATAG	SNP around op385	D2
pkP5124(DraI)Rev	GTATTGCAATTGGCTTTCTTGG	SNP around op385	D3
pmk3(1613)Fw	CAAATGATAAAATTGGCACGTGTAC	Probe for pmk-3(ok169)	D4
pmk3(2565)Re	TCCATAATCTCTTTGTTGCTTCAAG	Probe for pmk-3(ok169)	D5
pmk3(WT)Fwd	TTCCTCTTATGGGTCTCGCCATCAG	Primer inside ok169 deletion	D6
pmk-1(AscI)F	TACAGGCGCGCCGGTAACGGAGCCAATGTTTC CACAG	To create lazyboy pmk-1 for RNAi feeding	D7
pmk-1(FseI)R	TACAGGCCGGCCCACCCAACTGACCATACATC AACAG	To create lazyboy pmk-1 for RNAi feeding	D8
pmk(promo.3Kb)Fwd	TACAGGCGCGCCTAACCATCAAAGCAATACTG AGAAG	To create lazyboy pmk promoter (AscI)	D9
pmk(promo.3Kb)Rev	TACAGGCCGGCCAATTTAAATGGGTTCAAGTTA GGGC	To create lazyboy pmk promoter (FseI)	D10
pmk(promook169)Rev	TACAGGCCGGCCCGTTCCTGTATTGATTGATTT TGAG	To create lazyboy pmk promoter (FseI)	E1
K10G9.3(prom)Fwd	TACAGGCGCGCCTTTTTATTAATACGTGGTGTC AGGC	To lazyboy K10G9.3 promoter(AscI)	E2
K10G9.3(prom)Rev	TACAGGCCGGCCTGAAATTTAGAATTCTTAGAG GGGC	To lazyboy K10G9.3 promoter(FseI)	E3

pmk1(QRT)Fwd	ACACGCAGACTGTTGATGTATGGTCA	For Q-RT-PCR with pmk-1	E4
pmk1(QRT)Rev	TGGTGTTCCAGTTACTGACATGATACT	For Q-RT-PCR with pmk-1	E5
pmk2(QRT)Fwd	GCCTCTAGGAGAAGGAGCGTATGG	For Q-RT-PCR with pmk-2	E6
pmk2(QRT)Rev	TGTACTTTGAAATGGGCGAAAGAACT	For Q-RT-PCR with pmk-2	E7
pmk3(QRT)Fwd	GAAGCAACGGGAAACAACGAGAT	For Q-RT-PCR with pmk-3	E8
pmk3(QRT)Rev	GATCATCACAAATTGGAATCGTCGTT	For Q-RT-PCR with pmk-3	E9
Tubulin Fwd	Ask Lili	For Q-RT-PCR with tubulin	E10
Tubulin Rev	Ask Lili	For Q-RT-PCR with tubulin	F1
ActinFwd	GCTGATCGTATGCAGAAGGAAATCAC	For Q-RT-PCR with actin	F2
ActinRev	AGGTGGAGAGGGAAGCGAGGA	For Q-RT-PCR with actin	F3
GAPDHFwd	AAGGGAGGAGCCAAGAAGGTCATC	For Q-RT-PCR with GAPDH	F4
GAPDHRev	TGTGGTCGTTGGCATGATCGTACT	For Q-RT-PCR with GAPDH	F5
pmk-3(Gateway)Fwd	GGGGACAAGTTTGTACAAAAAAGCAGGCTTGA TGGCGTCAGTCCCATCGTCATCTAG	To gateway clone pmk-3 genomic sequence and cDNA	F6
pmk-3(Gateway)Rev	GGGGACCACTTTGTACAAGAAAGCTGGGTTCA GCGATCTGCTTCTCCAGGGATTAAC	To gateway clone pmk-3 genomic sequence and cDNA	F7
pmk-3(intron1)Fwd	AAACCAAATAGGAAACTGGC	To sequence pmk-3	F8
pmk-3(intron3)Fwd	GGAAAATTGCCAAAACTTTAG	To sequence pmk-3	F9
pmk-3(intron5)Fwd	AAGAACATGACTAAAACACG	To sequence pmk-3	F10
PMK(operon)Fwd	TACAGGCGCGCCGTTACTGTAGAAACATAGAG AAACG	To create lazyboy pmk promoter (AscI)	G1
pmk1km25)F	TTTGTGTCCCTAATTCCTTGATCTC	To genotype km25 deletion	G2
pmk1(km25)R	TGAGTCCACGAAGAATTTGATAGAC	To genotype km25 deletion	G3
ced-3(Pro)F	TACAGGCGCGCCTACAACCAAGGCATCGAACT TCACG	To amplify ced-3 promoter(AscI/FseI)	G4
ced-3(Pro)R	TACAGGCCGGCCATCTTCGGCTGATGGTTGAC CTCTC	To amplify ced-3 promoter(AscI/FseI)	G5
ced-4(Pro)F	TACAGGCGCGCCTTAAATGTTTCAGACAATCAT CCAC	To amplify ced-4 promoter(AscI/FseI)	G6
ced-3(Pro)R	TACAGGCCGGCCAGAGCATCTGAAAAATCTTC TTG	To amplify ced-4 promoter(AscI/FseI)	G7
ced-3(Pro)R	TACAGGCGCGCCGTAGTGGTTTTGTACTGATTT CC	To amplify ced-9 promoter(AscI/FseI)	G8
ced-3(Pro)R	TACAGGCCGGCCTGACTCTCCGATGGACATTC TTC	To amplify ced-9 promoter(AscI/FseI)	G9
dlk1(km12)Fwd	TTTCAGGGAAAATATACTCACTTGG	To genotype km12 deletion	G10
dlk1(km12)Rev	AACTGTTAGGTAAGTTGGAACTTGG	To genotype km12 deletion	H1
mkk4(km23)Fwd	ATCCGAGAAAGGACCAAATATCGTG	To genotype km23 deletion	H2
mkk4(km23)Rev	AATCGGAGGGAAGAGAGAGAGAAAG	To genotype km23 deletion	H3
pkP6133(DdeI)F	GGTTTCGATGACGGTGTGAGAGATG	To SNP map op387 on LGX	H4
pkP6133(DdeI)R	AGGTGAAGCAAGTTTGATTTTCCGG	To SNP map op387 on LGX	H5
pkP6162(SspI)F	AAAGTTTTAGGCTTTTTGGGATCAC	To SNP map op387 on LGX	H6
pkP6162(SspI)R	CAGCCAGTAAATCTGGTGTATTTTG	To SNP map op387 on LGX	H7
pkP6166(SspI)F	GAGTCCAAACAGTTGTGTAATTGAG	To SNP map op387 on LGX	H8
pkP6166(SspI)R	CTATGTTCCAACAACACTTCAACAC	To SNP map op387 on LGX	H9
pkP6167(HinfI)F	TCCTGTAACTATTCACCACTATTTC	To SNP map op387 on LGX	H10
pkP6167(HinfI)R	AGTGATTGAGCTCGTTAAGAAATTG	To SNP map op387 on LGX	I1
pkP6116(BfaI)F	GTCCAACAAAATATAAATTACGGCC	To SNP map op387 on LGX	I2
pkP6116(BfaI)R	ATTTTGCTGAAGGGCTATAATCCAG	To SNP map op387 on LGX	I3
pkP6117(FokI)F	TTCACGATATGTTATTTTGTGTGCG	To SNP map op387 on LGX	I4
pkP6117(FokI)R	AAATAAGGCAAGTTTCAGAGCAATC	To SNP map op387 on LGX	I5
flr-4(ex1-2)F	TGCAATTTTTGCAACACGACTCGTC	To sequence flr-4	I6
flr-4(ex1-2)R	TTTGCCAAAAATGAAAATATCCGGC	To sequence flr-4	I7
flr-4(ex3-6)F	ACAAAACTTTAAAGTATGCACATAC	To sequence flr-4	I8
flr-4(ex3-6)R	AATAACATTTCAATGAACGTACATC	To sequence flr-4	I9
flr-4(ex7-10)F	CGGCAGACATTTGGTAACTGATGAT	To sequence flr-4	I10
flr-4(ex7-10)R	TCTCAGTTTCTCGGTGTTACAAATC	To sequence flr-4	J1
flr-4(ex11-12)F	ATCTAACCCAAATTACGCATTGAAC	To sequence flr-4	J2
flr-4(ex11-12)R	TGGAAGTTCCTGAAGTGAAATTATG	To sequence flr-4	J3
F20D1[3]Fwd	GGCGATGATGTTATCCAACTCTTTG	To SNP map op387 on LGX	J4
F20D1[3]Rev	GTATTGCAGGTAAGCTTATGGTCTG	To SNP map op387 on LGX	J5

Guillaume Lettre's primers - BOX 4

PRIMER NAME	SEQUENCE	PURPOSE	LOCATION
			BOX 4
mak2(km24)Fwd	TGTGAGTTTTTTAGAACTACTTGGC	To genotype km24 deletion	A1
mak2(km24)Rev	TTTGAAATAAAGAGGAACCTGTAGC	To genotype km24 deletion	A2
mtk1(km33)Fwd	CATGAACCTATGTTTAGCCTTTAAC	To genotype km33 deletion	A3
mtk1(km33)Rev	CGAAAACAATACATGATGGTTATGG	To genotype km33 deletion	A4
gck2(km29)Fwd	GCTGAAAGTGATCCAAGAACAAAAG	To genotype km29 deletion	A5
gck2(km29)Rev	ATGTTTTTGCACCGTAACTCACGAG	To genotype km29 deletion	A6
F20D1.9(fwd)	GCAAGGAAAGAAAAACGAACTGGTG	To sequence F20D1.9	A7
F20D1.9(rev)	GAAGGATAGGCATCAAAGATGGGTG	To sequence F20D1.9	A8
F20D1.9(int)	CATAATTTACTTTTCCGCCG	To sequence F20D1.9	A9
C18B12[1]Fwd	AAGACAATGAAACTTTAGCGGTCAG	SNP around op387	A10
C18B12[1]Rev	AACGTATTCGACTTTCCTGATCTCC	SNP around op387	B1
H03G16[1]Fwd	TTGAAAGTTCTTCAACTCACCGTTC	SNP around op387	B2
H03G16[1]Rev	TTAGTACCGCATATTCCCAAACTTC	SNP around op387	B3
pmk-3(cDNA)CorRe	CTATCAATCTTCCAATAAATGACTT	To correct stop codon in pmk-3 cDNA	B4
pmk-3(cDNA)CorFwd	AAGTCATTTATTGGAAGATTGATAG	To correct stop codon in pmk-3 cDNA	B5
pmk3(QRT)F-N	CAATAAAGAAGATGCGAGAACCGTTCT	To measure pmk-3 transcript level	B6
pmk3(QRT)R-N	AGGTGTGTAGATGTCAAGAGCACAGATG	To measure pmk-3 transcript level	B7
hda4(ok518)F	CGAAAAAGCCTTGTGAGAGAAGATC	To genotype ok518 deletion	B8
hda4(ok518)R	AGGTAATGATTCGAGAGCAACTGAG	To genotype ok518 deletion	B9
mef2(gv)Fwd	CCTTAATTAATTAATGCTGCTGCTC	To genotype gv1 and gv2 alleles	B10
mef2(gv)Rev	TAATGCAAAATTACGGTAAACGGTC	To genotype gv1 and gv2 alleles	C1
mef2(pro)F/A	TACAGGCGCGCCTAAGTTTTTTCAGAGAGCAA GCAAC	To amplify and lazyboy mef-2 promoter	C2
mef2(pro)R/F	TACAGGCCGGCCCTCCATACCGCAATAATCATT AATC	To amplify and lazyboy mef-2 promoter	C3
mef-2(Gateway)F	GGGGACAAGTTTGTACAAAAAAGCAGGCTtgatg ggtcgcaagaaaattcaaatcac	To gateway clone mef-2(cDNA)	C4
mef-2(Gateway)R	GGGGACCACTTTGTACAAGAAAGCTGGGTTCA AGTCAATTGCTGTGGTCTCCACTC	To gateway clone mef-2(cDNA)	C5
mef2(Gat.DN)Rev	GGGG AC CAC TTT GTA CAA GAA AGC TGG GTT CAT TCA TCA TCC GAA TTT CCG CCT CCC	To create mef2 dominant negative	C6
mef2-VP16-Rev	GACATCGGTCGGGGGGGCTGGTCCAGGGCTT TCATC	To create mef2 activated form	C7
mef2-VP16-Fwd	GATGAAAGCCCTGGACCAGCCCCCCCGACCGA TGTC	To create mef2 activated form	C8
VP16(Gateway)Rev	GGGG AC CAC TTT GTA CAA GAA AGC TGG GTC TAC CCA CCG TAC TCG TCA ATT CC	To create mef2 activated form	C9
uCE6-1494F	CACCAATAAAGTTGCTCCAGAGATC	SNP around op387	C10
uCE6-1494R	TGAACACATGTTCAAGCTTTTAGTC	SNP around op387	D1
epn1-1(F)	TCTATGTTTTAGCCACACCATTCAG	To sequence epn-1 (T04C10.2)	D2
epn1-1(R)	TTTATATCTTACCAAGAGACGCGTC	To sequence epn-1 (T04C10.2)	D3
epn1-2(F)	ACAAATTCAAGCAAAACAATCCAGG	To sequence epn-1 (T04C10.2)	D4
epn1-2(R)	ACCATTTGTGGAGTTGTTAGTGTTG	To sequence epn-1 (T04C10.2)	D5
epn1-3(F)	CAACTACTCCATCAACAATGCCAAC	To sequence epn-1 (T04C10.2)	D6
epn1-3(R)	GGGAAAAACGTGGTGAGTGTATATG	To sequence epn-1 (T04C10.2)	D7
uCE6-1503F	GGCGGATACGAAAAATAACAATGTC	SNP around op387	D8
uCE6-1503R	TGTAATTACGTGCGCACAAATACTG	SNP around op387	D9
uCE6-1502F	TAGGAATCAATCATGTTTGGAGAAG	SNP around op387	D10
uCE6-1502R	AATCTTTGTATTCACCGACTTCGTG	SNP around op387	E1
C27C12[2]F	TGGTCACAGATTATCGGAGCAAGTG	SNP around op387	E2
C27C12[2]R	CTTACCATATTGCGCTGGGTTGTTC	SNP around op387	E3

Supplementary Table II : Plasmid list

Guillaume Lettre's plasmids - BOX 1

PLASMID NAME	DESCRIPTION	LOCATION
		BOX 1
pPD128.110	L4440 RNAi feeding vector with gfp insert (Fire kit)	1
pGL-1	Lazyboyed ced-9 cDNA cloned (AscI/FseI) into pBMB.LB_eft-3	2
pGL-2	pBMB.LB_eft-3 cut with NotI, then fill-in, creates FseI site	3
pGL-3	Lazyboyed ced-9 cDNA cloned (AscI/FseI) into pRH10	4
pGL-4	GFP cassette flanked by NotI sites, cloned into pCR2.1-TOPO	5
L4440.LB_ced9	RNAi feeding vector with lazyboyed full-length ced-9 cDNA (AscI/FseI)	6
pREP1	Fission yeast vector	7
pREP41	Fission yeast vector	8
pREP81	Fission yeast vector	9
pBS1761	TAP-TAG vector (from Cellzone)	10
pBS1479	TAP-TAG vector (from Cellzone)	11
pDX-2	ced-3 cDNA with FLAG epitope (from Horvitz lab)	12
pY47D3A.12	RNAi feeding vector against corresponding gene (from Vidal lab)	13
pY47D3A.13	RNAi feeding vector against corresponding gene (from Vidal lab)	14
pY47D3A.16	RNAi feeding vector against corresponding gene (from Vidal lab)	15
pY47D3A.21	RNAi feeding vector against corresponding gene (from Vidal lab)	16
pY47D3A.30	RNAi feeding vector against corresponding gene (from Vidal lab)	17
pTOPO_ced3	ced-3 cDNA flanked by SalI sites, cloned into pCR2.1_TOPO	18
pREP1_ced-3	Fission yeast vector, inducible over-expression of ced-3 (cloned SalI)	19
pREP41_ced-3	Fission yeast vector, inducible over-expression of ced-4 (cloned SalI)	20
pMFG-E8	MFG-E8 cDNA (from Nagata lab)	21
pMFG-E8_D89E	MFG-E8 cDNA with point mutation (from Nagata lab)	22
pPDMM016	unc-119 rescuing construct (Fire kit)	23
pLB.lim7_MFGE8	MFG-E8 cDNA driven by lim-7 promoter (AscI/FseI)	24
pTOPO_teg1	teg-1 genomic fragment cloned into pCR2.1_TOPO (with Gateway site)	25
pDONR_teg1	teg-1 genomic fragment Gateway cloned into pDONR201	26
pID3.O1B_teg1	Ppie-1::gfp::teg-1, unc-119(+)	27
pRF4	rol-6(su1006), co-injection marker	28
pTOPO_teg1(FL)	teg-1 promoter, CDS, and 3'UTR, cloned into pCR2.1_TOPO (AscI/FseI)	29
pPDMM016_teg1(FL)	teg-1 promoter, CDS, and 3'UTR, cloned into pPDMM016	30
pL4440.LB	RNAi feeding vector with lazyboyed sites	31
pTOPO_K10G9.3	K10G9.3 gene with lazyboy sites cloned into pCR2.1_TOPO	32
pL4440.LB_K10G9.3	RNAi feeding vector with lazyboyed full-length K10G9.3 gene (AscI/FseI)	33
pTOPO_K10G9.3(3'UTR)	3'UTR of K10G9.3 cloned into pCR2.1_TOPO (FseI)	34
pTOPO_K10G9.3(gene+3'UTR)	gene and 3'UTR of K10G9.3 cloned into pCR2.1_TOPO (AscI/FseI/FseI)	35
pRH10_K10G9.3(gene)	K10G9.3 gene with lazyboy sites cloned into pRH10 (AscI/NotI/FseI)	36
pRH10_K10G9.3(gene)+GFP	K10G9.3 gene with lazyboy sites +GFP cloned into pRH10 (AscI/NotI/FseI)	37
pHSK10G9.3	Phsp16.41::K10G9.3 (AscI/FseI)	38
pHSGFPK10G9.3	Phsp16.41::GFP::K10G9.3 (AscI/FseI)	39
pL4440_pmk1	RNAi feeding vector agains pmk-1	40
pDK177	RNAi feeding vector agains pmk-1 (from Ausubel lab)	41
pL4440_mkk4	RNAi feeding vector agains mkk-4 (Ahringer library)	42
pL4440_pmk2	RNAi feeding vector agains pmk-2 (Ahringer library)	43
pcmu5-HA #347	pmk-3 cDNA (with mutations) from the Cobb lab	44
p348	pmk-3 cDNA (with mutations) from the Cobb lab	45
pRSET_pmk3 #349	pmk-3 cDNA (with mutations) from the Cobb lab	46
pRSET_pmk2 #350	pmk-2 cDNA from Cobb lab	47
pRSET_pmk1 #351	pmk-1 cDNA from Cobb lab	48

pcmu5-HA #352	pmk-1 cDNA from Cobb lab	49
pRH20_K10G9.3(promoter)	Promoter(K10G9.3)::2XNLS::GFP (AscI/FseI), unc-119(+)	50
pRH20_pmk(promoter)	Promoter(pmk3Kb)(AscI/FseI)::2XNLS::GFP, unc-119(+)	51
pRH20_pmk(promoter-ok169)	Promoter(pmk-ok169)(AscI/FseI)::2XNLS::GFP, unc-119(+)	52
pTOPO_pmk3(gene)	Full-length pmk-3 gene with Gateway sites cloned into pCR2.1_TOPO	53
pDONR_pmk3(gene)	Full-length pmk-3 gene cloned into pDONR201 (Gateway)	54
pID2.02_pmk3	Ppie-1::pmk-3(gene), unc-119(+) (Gateway)	55
pID3.01B_pmk3	Ppie-1::gfp::pmk-3(gene), unc-119(+) (Gateway)	56
pDONR 201	Entry Vector for Gateway cloning (Invitrogen)	57
pID2.02	Destination vector for Gateway cloning (Seydoux lab) Pie-1 promoter	58
pID3.01B	Destination vector for Gateway cloning (Seydoux lab) Pie-1 promoter +GFP	59
pRH20	From Randy's collection, To clone AscI/FseI promoter in front 2XNLS::GFP	60
pBMBeft3.LB	From Jason's collection, eft-3 promoter, AscI/FseI sites, unc-119(+)	61
pGL-5	GFP::ced-9(cDNA) (AscI/NotI/FseI) cloned into pRH10	62
pGL-6	GFP::ced-9(cDNA) (AscI/NotI/FseI) cloned into pBMBeft3.LB	63
pBluescript SK(-)	Original vector from Stratagene	64
pTOPO_pmk3(cDNA)	pmk-3 cDNA with Gateway sites cloned into pRC2.1_TOPO	65
pBS_pmk3	pmk-3 cDNA cloned into pBluescript SK(-) as a EcoRI fragment	66
pRH20_ced3(pro)	3 kb upstream of ced-3 cloned into pRH20 as a AscI/FseI fragment	67
pRH20_ced4(pro)	3 kb upstream of ced-4 cloned into pRH20 as a AscI/FseI fragment	68
pRH20_ced9(pro)	3 kb upstream of ced-9 cloned into pRH20 as a AscI/FseI fragment	69
pTOPO_pmk3(new cDNA)	pmk-3 cDNA with Gateway sites cloned into pRC2.1_TOPO (NO MUTATIONS)	70
pTOPO_mef2(cDNA)	pmk-3 cDNA with Gateway sites cloned into pRC2.1_TOPO	71
pTOPO_mef2(promoter)	3 kb upstream and first exon of mef-2 cloned into pCR2.1_TOPO	72
pRH20_mef2(promoter)	mef-2 promoter cloned into pRH20 as a AscI/FseI fragment	73

Guillaume Lettre's plasmids - BOX 2

PLASMID NAME	DESCRIPTION	LOCATION
		BOX 2
pTOPO_mef2DN	312 first bp of mef-2 cDNA, with Gateway sites, cloned into pCR2.1_TOPO	A1
pTOPO_mef2ActFo	321 first bp of mef-2 cDNA fused to 237 bp of VP16, with Gateway sites, cloned into pCR2.1_TOPO	A2
pDONR_mef2(cDNA)	mef-2 cDNA Gateway cloned into pDONR 201	A3
pDONR_mef2DN	mef-2 dominant negative Gateway cloned into pDONR 201	A4
pDONR_mef2ActFo	mef-2 activated form Gateway cloned into pDONR 201	A5
pID3.01B_mef2(cDNA)	Ppie-1::gfp::mef2(cDNA), unc-119(+)	A6
pID3.01B_mef2DN	Ppie-1::gfp::mef2DN, unc-119(+)	A7
pID3.01B_mef2ActFo	Ppie-1::gfp::mef2ActFo, unc-119(+)	A8